

Optimal control for wave energy converters:  
Non-linear model predictive control approach

---

Juan Luis GUERRERO FERNÁNDEZ

*9th December 2022*

Version: Final





---

# Optimal control for wave energy converters: Non-linear model predictive control approach

---

by

Juan Luis GUERRERO FERNÁNDEZ

A dissertation submitted to

The University of Sheffield



in partial fulfillment of the requirements for the degree of

**Doctor of Philosophy**

9th December 2022

**Juan Luis GUERRERO FERNÁNDEZ**

*Optimal control for wave energy converters:*

*Non-linear model predictive control approach*

Ph.D. Dissertation, 9th December 2022

Supervisor: Dr J. Anthony Rossiter

**The University of Sheffield**

Department of Automatic Control and Systems Engineering

Amy Johnson Building

Portobello Street

Sheffield, S1 3JD



” *Think globally,  
Act locally.*

– Lloyd N. Trefethen –



To the co-authors of this work:

Elba, Liam, Julián and Emma  $\mapsto$  My family,

for their unconditional love and support.





# Acknowledgement

First and foremost, I would like to thank the Costa Rican Ministry of Science, Innovation, Technology and Telecommunications (Ministerio de Ciencia, Innovación, Tecnología y Telecomunicaciones, MICITT) and Costa Rica Institute of Technology (Tecnológico de Costa Rica, TEC) for the financial support I received to carry out this research.

Second, I would like to express my sincere appreciation to my academic advisor, Dr John Anthony Rossiter, for all his help and encouragement during this research. I am grateful for the freedom he granted me to explore my interests while paving the way for my growth as an independent researcher.

I do not want to pass up the opportunity to express my gratitude and acknowledgement to Oscar González Villareal, a former ACSE PhD student and current Research Fellow at Cranfield University, for all his assistance at the beginning of my journey. I can't even begin to count the hours he spent with me teaching me about algorithms and code for real-time iteration nonlinear model predictive control.

Last but not least, I want to thank my family for their unconditional love and support. But in particular to my wife Elba, who has supported me in both good and difficult times, and who has occasionally cared for our children as a single parent so that I could devote myself completely to this work.

Without your help and support, I would not be able to write these lines.

To every one of you, thank you!





# Declaration

I, Juan Luis Guerrero-Fernández, declare that the work presented in this thesis is my own. All material in this thesis which is not of my own work has been properly accredited and referenced.

*Sheffield, 9th December 2022*

---

Juan Luis Guerrero-Fernández



# Abstract

Obtaining cost competitiveness is the major challenge facing ocean wave energy technology. Reducing the structural cost of wave energy converters (WEC) and improving energy capture are two ways to decrease its levelised cost of energy (LCOE). This research aims to contribute to the second route by enhancing energy capture using an advanced control strategy tailored for WEC applications to optimise their power performance.

In this study, a moving window blocking technique is proposed for reducing the size of the optimal control problem (OCP) arising at each time step. Using a Moving Window Blocking (MWB) technique reduces the number of decision variables, thereby reducing the time required to solve each OCP. Through numerical simulations, the advantages of the MWB-model predictive controller are demonstrated.

Moving to advanced energy-maximising control strategies, a non-linear model predictive control (NMPC) approach based on the real-time iteration (RTI) scheme is introduced to maximise the energy recovered from the ocean waves. The proposed controller incorporates the efficiency of the Power Take-Off (PTO) system when solving the optimal control problem at each time step. This controller differentiates from others in that it does not require offline computations to solve the non-linear programming problem that arises from incorporating the PTO's efficiency into the optimal control problem.

Numerical simulations of the proposed RTI-NMPC controller indicate that the RTI-NMPC approach can significantly improve wave energy converter performance. The proposed controller outperformed the other two controllers used for comparison, i.e., a resistive controller and linear MPC while keeping the amount of power "borrowed" from the grid to a bare minimum. The proposed RTI-NMPC strategy is later evaluated using a Kalman filter paired with a random-walk model to estimate the wave excitation force and a linear autoregressive (AR) model to forecast the wave excitation force over the prediction horizon where similar results are obtained.

A further contribution of this research is the derivation of a computationally efficient algorithm  $O(N^2)$  for "only-output" cost functions. For large prediction horizons, the algorithm  $O(N^2)$  significantly reduces the time required to calculate the hessian, which is the primary time driver in solving an optimal control problem numerically.





# Contents

## Chapter 1

<b>Introduction</b> .....	<b>1</b>
1.1 Challenges of Wave Energy Systems .....	3
1.2 Research Aim .....	4
1.3 Research Objectives .....	4
1.4 Research Contributions .....	5
1.5 Dissertation Outline .....	5

## Chapter 2

<b>Wave Energy Converter: Background</b> .....	<b>7</b>
2.1 Wave energy converters: Overview .....	8
2.2 Ocean wave modelling .....	11
2.3 Hydrodynamic modelling .....	16
2.3.1 Point Absorber dynamics .....	17
2.3.2 Fluid dynamics .....	18
2.3.3 Linear Model .....	21
2.3.4 Non-linear extension to the linear model .....	23
2.4 Power take-off systems .....	24
2.4.1 Hydraulic Systems .....	25
2.4.2 Air Turbines .....	26

2.4.3	Hydro Turbines	27
2.4.4	Direct Mechanical Drive Systems	27
2.4.5	Direct Electrical Drive Systems	28

## Chapter 3

### Control Strategies for Wave Energy Converters:

#### *A state-of-the-Art review* .....31

3.1	Primary Controllers: Function	33
3.2	Optimal unconstrained control law: Impedance-matching principle	33
3.3	Classical control strategy	36
3.3.1	Passive Loading Control	37
3.3.2	Reactive Control	38
3.3.3	Latching Control	38
3.3.4	Declutching Control	38
3.4	Modern control strategies	39
3.4.1	Hydrodynamic model	42
3.4.2	Cost function	44
3.4.3	PTO system efficiency	45
3.4.4	Real-time capabilities	47
3.5	Summary	48

## Chapter 4

### Optimal Control for Wave Energy Converters:

#### *Contributions* .....51

4.1	Contributions overview	52
-----	------------------------	----

## Chapter 5

### Summary of Findings and future work ..... 59

5.1	Summary of Findings	60
5.2	Future work	63



<b>References</b>	<b>References</b> ..... <b>65</b>
<b>Appendix A</b>	<b>Manuscript 1</b> ..... <b>83</b>
<b>Appendix B</b>	<b>Manuscript 2</b> ..... <b>91</b>
<b>Appendix C</b>	<b>Manuscript 3</b> ..... <b>107</b>



---

# Introduction

” *There is no wealth but life. Life, including all its powers of love, of joy, and of admiration.*

- John Ruskin -

1.1	Challenges of Wave Energy Systems . . . . .	3
1.2	Research Aim . . . . .	4
1.3	Research Objectives . . . . .	4
1.4	Research Contributions. . . . .	5
1.5	Dissertation Outline . . . . .	5

Over the next several decades, there will be an increase in the number of countries making commitments to attain net-zero emissions. However, even if all of the pledges made by governments are fulfilled, those efforts will not be enough compared with what is required to steer global energy-related carbon dioxide emissions to net-zero by 2050 and give the world a fair chance of keeping the global temperature rise to 1.5 °C [1]. Another global concern is that the current energy demand is met by burning fossil fuels. The International Energy Agency has projected an increase in global energy demand for the next decades [2]. Between the worldwide energy demand and carbon reduction commitments, there is a growing divide between rhetoric and action [3], and achieving carbon neutrality will need a massive reform of the energy sector, involving additional technological and non-technical measures.

Renewable energy forms a vital part of any viable solution to substitute fossil fuels. It has grown exponentially recently, particularly in solar photovoltaic (PV), hydropower, and wind energy. Besides the global interest, renewable energies offer a more diverse energy matrix, guaranteeing the energy supply and reducing the country's fossil-fuel dependence. Furthermore, *ocean wave energy*, a relatively untapped renewable energy resource, has tremendous potential in bridging the gap between the rhetoric of carbon neutrality and growing energy demand, among other renewable energy alternatives.

The theoretical estimate of global wave power is around 32 000 TWh/year [4]. However, the precise figure for the global estimate of wave energy remains a point of contention [4]. In terms of extractable resources, excluding locations with wave power levels less than 5 kW/m, the global gross resource is about 3.0 TW [5], whereas in the coastal areas the average wave power is estimated to be around  $2.11 \pm 0.05$  TW [6].

In comparison to other renewable energy resources, particularly solar photovoltaic and wind energy, wave energy has various advantages: **a)** ocean wave energy is one of the most concentrated renewable energy sources<sup>1</sup>; **b)** wave power has high availability, up to 90 %, compared to wind and solar power, which are typically available at a rate of 20 % to 30 % [8]; **c)** wave energy technology has a negligible environmental impact [9, 10]; **d)** wave energy production may also be used with existing wind or solar power facilities to help smooth power output [11–16]; **e)** wave power is more predictable [17, 18], allowing for greater flexibility in managing and planning regional or national energy systems.

However, despite the immense potential of wave power, the installed capacity of wave energy is only around 2.3 MW [19], and current wave energy projects are primarily focused on research and demonstration with many small-scale devices. Wave energy technology is

---

<sup>1</sup>from 2 kW/m<sup>2</sup> to 3 kW/m<sup>2</sup>, compared to solar energy:  $\approx 0.2$  kW/m<sup>2</sup> or wind energy:  $\approx 0.5$  kW/m<sup>2</sup> [7].



still in its infancy compared to wind or solar, with no fully commercial-scale wave energy converter (WEC) farm in operation, despite developing numerous WEC prototypes and filed patents [20].

---

## 1.1. Challenges of Wave Energy Systems

Despite the apparent benefits of ocean wave energy, large-scale wave energy converters (WECs) implementation has been hindered by several technological and non-technical challenges. Although far from exhaustive, some of the significant difficulties wave energy converters face are:

- a) the conversion of variable oscillatory wave energy input (from low-frequency, i.e., 0.1 Hz oscillating motion and large forces 1 MN) into clean electrical output [21, 22]. This requires highly reliable structures and power take-off (PTO) systems and, consequently, high capital expenditure (CapEx) [22];
- b) due to the nature of the offshore environment where WECs are to be deployed, the operating expenditure (OpEx), which includes the costs for installation, operating, and maintenance, is relatively large [22];
- c) due to the large variability of the wave power resource, there are a large number of WEC concepts with no obvious convergence towards a single design, as it has been observed for other renewable technologies such as wind energy. Consequently, the research and development (R&D) and commercialisation efforts are diluted [23];
- d) WECs should be able to operate (efficiently) on normal sea state conditions but also withstand extreme sea state weather, in which the exerted peak forces can be up to 100 times the average forces [24]. This presents structural engineering challenges, as well as economic challenges. This is because, while the average occurring waves produce the energy output of the WEC, the device must be designed considering structural integrity, survivability and longevity according to the most extreme expected sea conditions [23];
- e) at the moment, WEC technology is considered as not mature, with a high degree of uncertainty and risk that requires significant initial capital. All these factors discourage private investors [22], and

- f) real sea states waves are irregular in nature, which causes another challenge for extracting energy from these waves. The high randomness in amplitude, phase and wave direction makes it challenging to optimise device efficiency over the entire range of excitation frequencies [25].

This work aims to overcome some technical challenges related to maintaining efficiency over the range of working frequencies through advanced control strategies.

---

## 1.2. Research Aim

Based on the challenges mentioned above of wave energy systems and in the literature review presented in Chapter 3, the prime aim of this project has been to improve wave energy extraction from single-body heaving wave energy converters (WEC); to reduce countries' energy matrix's reliance on fossil fuels, to contribute to the supply of (ever-growing) electric energy through the incorporating renewable energy sources, and reach the economically feasible levels for commercially implementation of wave energy converters.

---

## 1.3. Research Objectives

The project's overarching aim will be accomplished through the following list of objectives:

- a) Define a hydrodynamic model of a point absorber wave energy converter for testing and validating proposed control strategies.
- b) Review control strategies proposed to date for the control wave energy converters of the point absorber type to evaluate their properties and possible shortcomings.
- c) Propose and implement in simulations a control strategy able to improve the extracted wave energy from a point absorber WEC, estimating the current excitation wave force and considering prediction for excitation wave force.
- d) Propose and implement in simulations a robust control strategy for wave energy converters capable of coping with uncertainties in the short-term prediction of the incoming excitation wave forces.



---

## 1.4. Research Contributions

The prime contributions gathered throughout the development of this project are summarised below:

- a) The primary contribution of the project is the development and implementation of a detailed Non-linear model predictive control (NMPC) approach based on the real-time iteration (RTI) scheme that considers the power take-off system's efficiency. Computer simulations confirm that the proposed control strategy can significantly improve the performance of the wave energy converter. In addition, the proposed RTI-NMPC can solve the non-linear optimal control problem in real time with sample times of the order of 10 ms.
- b) A further contribution is the proposal and implementation of a model predictive control coupled with a moving blocking approach to reduce the number of decision variables used in the input parameterisation to minimise the time required to solve the optimal control problem at each sampling time.
- c) Finally, a parallel contribution of this project is the derivation of a condensing algorithm  $O(N^2)$  for "output-only" cost functions required to improve computational efficiency.

---

## 1.5. Dissertation Outline

This dissertation is presented as a hybrid between a chapter-wise and a paper-wise dissertation. A brief description of each chapter is given below:

- For the reader who is unfamiliar with the topic of wave energy converter (WEC) systems, Chapter 2 serves as a stand alone introduction to the field. Classification of the devices and the mathematical model for a type of wave energy converter known as point absorbers are provided. The chapter concludes with a review of the power take-off systems typically used in wave energy converters.
- Chapter 3 offers a detailed literature review of the most relevant control strategies in wave energy converter literature.
- Chapter 4 provides an overview of the published paper contributions.

- The dissertation is concluded with Chapter 5 summarising the main findings gathered during the project's development and followed by suggestions on possible directions for future work.
- The Official Version of each manuscript written within this project is included in the appendices. These papers are:
  - Paper 1** Model Predictive Control for Wave Energy Converters: A Moving Window Blocking Approach (Published).
  - Paper 2** Efficiency-aware non-linear model-predictive control with real-time iteration scheme for wave energy converters (Published)
  - Paper 3** Non-linear Model Predictive Control based on Real-Time Iteration Scheme for Wave Energy Converters using WEC-Sim. (Published).





---

## Wave Energy Converter: Background

” *The greatest enemy of knowledge is not ignorance, it is the illusion of knowledge.*

– Daniel J. Boorstin –

2.1	Wave energy converters: Overview . . . . .	8
2.2	Ocean wave modelling . . . . .	11
2.3	Hydrodynamic modelling. . . . .	16
2.3.1	Point Absorber dynamics . . . . .	17
2.3.2	Fluid dynamics. . . . .	18
2.3.3	Linear Model . . . . .	21
2.3.4	Non-linear extension to the linear model . . . . .	23
2.4	Power take-off systems . . . . .	24
2.4.1	Hydraulic Systems . . . . .	25
2.4.2	Air Turbines . . . . .	26
2.4.3	Hydro Turbines. . . . .	27
2.4.4	Direct Mechanical Drive Systems . . . . .	27
2.4.5	Direct Electrical Drive Systems . . . . .	28

## 2.1. Wave energy converters: Overview

The International Renewable Energy Agency, in its 2020 report, *Innovation outlook: Ocean energy technologies* defined wave energy converters as [19]:

*"Wave energy converters are devices that harvest the energy contained in ocean waves and use it to generate electricity. When the wind blows over the ocean, it transmits some of its kinetic energy to the ocean's surface, creating wave energy, a form of energy that contains both kinetic and gravitational potential energy. Wave energy converters can be conceptualised to absorb either the kinetic energy, mainly through moving bodies, the potential energy, through overtopping devices or attenuators or both, through, for example, point absorbers"*

Although this definition implies that the input to the system is ocean energy and the output is electric energy (other uses include desalination and hydrogen production), no information is provided regarding the technologies that may be utilised throughout the energy conversion process. This is because WEC concepts differ, with over a thousand devices reported [8, 26, 27]. As commented in Section 1.1, the large number of concepts makes it challenging to develop a single categorisation method for all potential WEC systems.

Several authors have proposed classifying WECs based on their horizontal extension and orientation, deployment location (water depth), working principles of the primary capture system, and the secondary conversion system (the power take-off (PTO) system) [8, 23, 25, 27-31].

Similar to the classification described in [28] is the classification adopted in this dissertation. This categorisation of WECs is depicted in Figure 2.1.

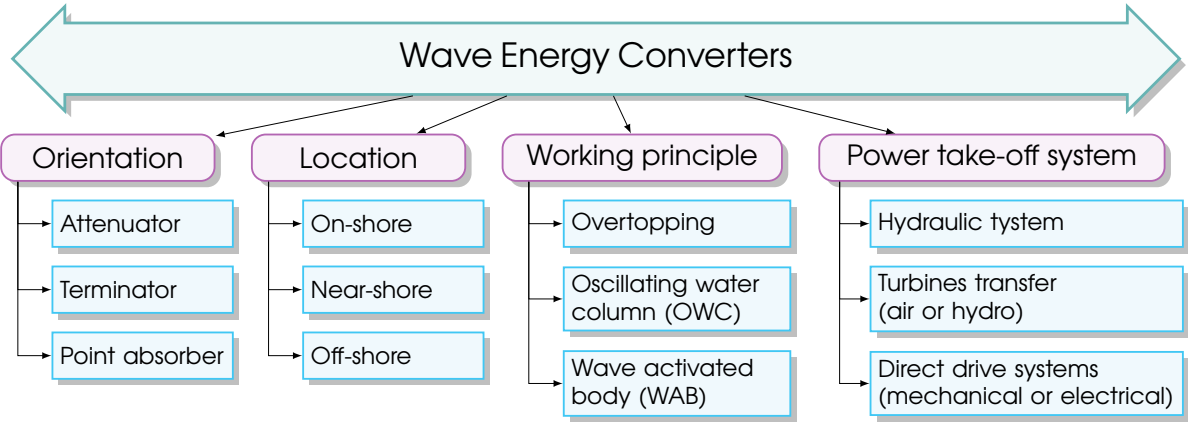


Figure 2.1.: Classification of Wave energy converters

The proposed classification by orientation, location and working principle is briefly commented on in the following lines. Classification by PTO systems is detailed in Section 2.4.

### By orientation:

According to the orientation of the device concerning the incoming ocean wave (see Figure 2.2), WECs can be classified as [8, 30]:

**Attenuator:** this is a floating device, Typically a large structure, that "attenuates" the wave's amplitude. It operates parallel to the predominant wave direction and rides the waves. These devices capture energy from the relative motion of two bodies or more as the wave passes through.

**Terminator:** are similar to attenuators, with their structural orientation perpendicular to the wave propagation direction. Physically intercepting / terminating waves, terminators are generally located near shorelines.

**Point Absorber (PA):** This is one of the most common wave energy converters investigated so far [20]. Compared with the incoming wavelength, PAs are small and can absorb energy from any direction.

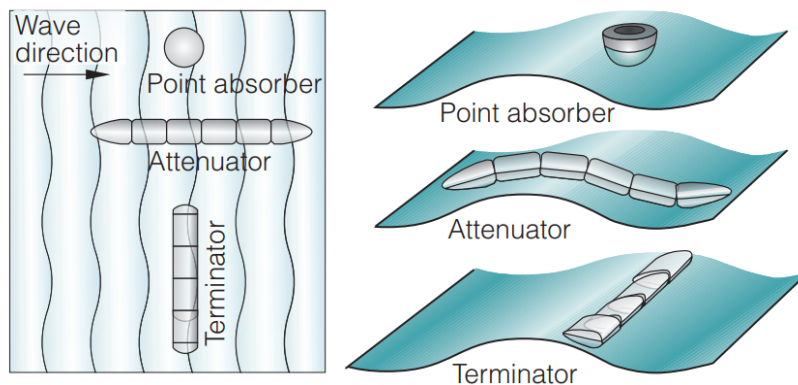


**Figure 2.2.:** Classification of wave energy converters based on the device's orientation concerning the incoming ocean wave. Extracted from [32]

### By location:

Regarding the location, the classification scheme indicates the water depth at which the device is deployed. There are three types of converters within this category: onshore, nearshore and offshore devices. Some of the essential features of each one are [8]:

**Onshore devices:** are situated at the coast and can be installed above the water (in shallow), for example, integrated into a breakwater, dam or cliff. The main advantage of these converters is their easy access for maintenance and installation. In addition, neither anchoring devices nor lengthy sea cables are required to connect the WEC to the grid. On the other side, waves carry less energy to the shoreline due to their interaction with the seafloor (see Figure 2.3). Also, environmental issues could potentially arise due to the reshaping of the seashore [29–31].

**Nearshore devices:** are characterised for being deployed a few hundred metres off the coast in water depths between 10 to 30 metres. To avoid moorings, they often are designed for resting on the seafloor. However, the structure must be able to withstand the forces caused by passing waves. Occasionally they are floating constructions [29–31]. Additionally, nearshore waves tend to be uni-direction (towards the coast), whereas offshore waves tend to be multi-direction, making them more challenging to harvest energy.

**Offshore devices:** or deep water (more than 40 metres) devices are farthest out from the coast and are constructed in floating or submerged structures anchored to the seafloor. However, due to the open sea, the device’s liability and survivability constitute a significant concern, and their structure must be able to withstand extremely heavy loads (usually in the order of 10 times the loads of regular operation). Placing a wave energy converter in deep waters increases the amount of energy that can be harvested since the energy content of waves in deep water is more significant (see Figure ) [24]). Contrary to onshore devices, installation, maintenance and operational cost are higher, and in addition, long, costly marine cables are utilised to transport electricity to the grid [29–31].

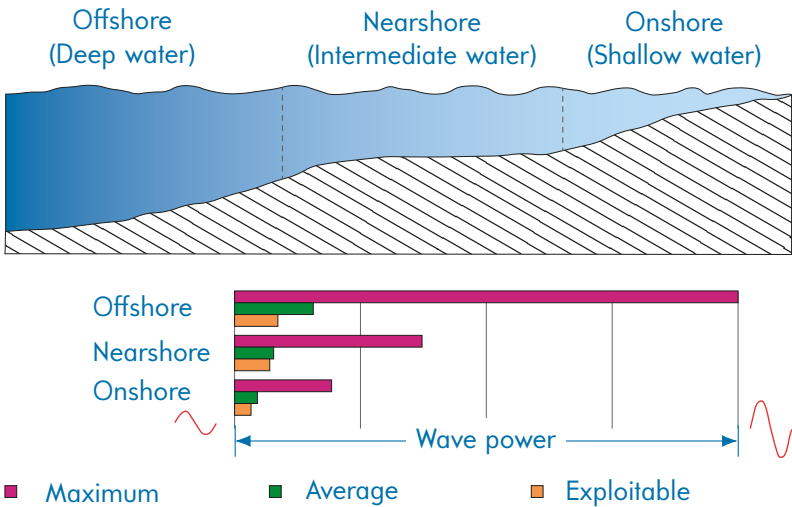


**Figure 2.3.:** Classification of wave energy converters by site of deployment. Redrawn from [33]

## By working principle:

As for the working principle of the primary capture system, WECs can be classified as:

**Oscillating water column (OCW):** the fundamental principle consists of a partly submerged concrete or steel structure. The water free surface inside the structure and the structure's walls generate an air chamber. The immersed section of the WEC is open to the action of ocean waves. The oscillating motion of the internal free surface, produced by the incoming waves, causes the trapped air to flow through a self-rectifying, single-direction air turbine, which drives an electrical generator [23].

**Overtopping:** commonly observed on shore, as part of wave breakers [23]. The reservoir, placed above sea level, is refilled by the incoming ocean waves. Later, the stored water's potential energy is used to drive hydro turbines coupled to electrical generators.

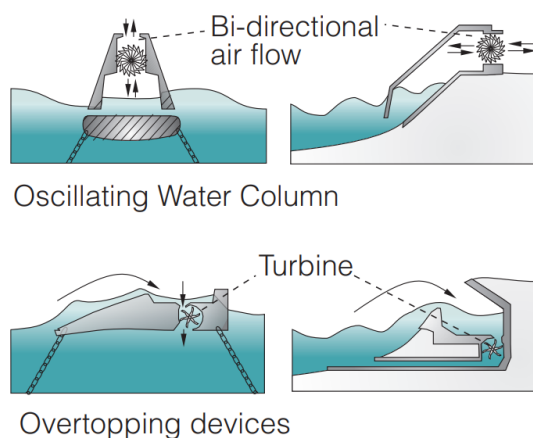


**Figure 2.4.:** Schematic representation of oscillating column water devices and overtopping devices. Extracted from [32]

**Wave-activated body (WAB):** Also referred to by other authors as oscillating body systems [29]. In this group of devices, the absorber is moved by the active interaction with the wave motion. WABs can float on the surface of the ocean or be submerged. Depending on their design, they may have a single or several degrees of freedom concurrently.

Finally, it is important to mention that the aforementioned classification are not mutually exclusive.

---

## 2.2. Ocean wave modelling

Wave energy converters are generally designed to harvest energy from gravity waves. Gravity waves are generated by the wind blowing over the ocean's surface (which is also the

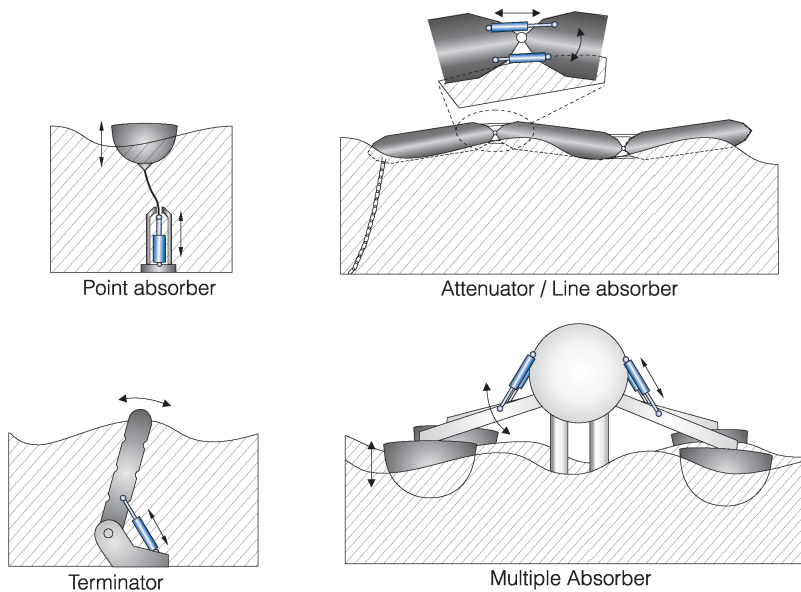


**Figure 2.5.:** Examples of wave-activated body devices with their respective classification based on orientation. Extracted from [34]

result of the differential heating of the ocean surface by solar energy) [35]. It is usual to divide gravity waves into wind waves, generated by local winds, and swell waves, caused by winds that have ceased to blow [35]. The characteristics of the generated waves are determined by the amount of energy transferred, which depends on the wind speed, the duration and the distance covered (fetch) [20]. Figure 2.6 illustrates the origin of ocean waves.

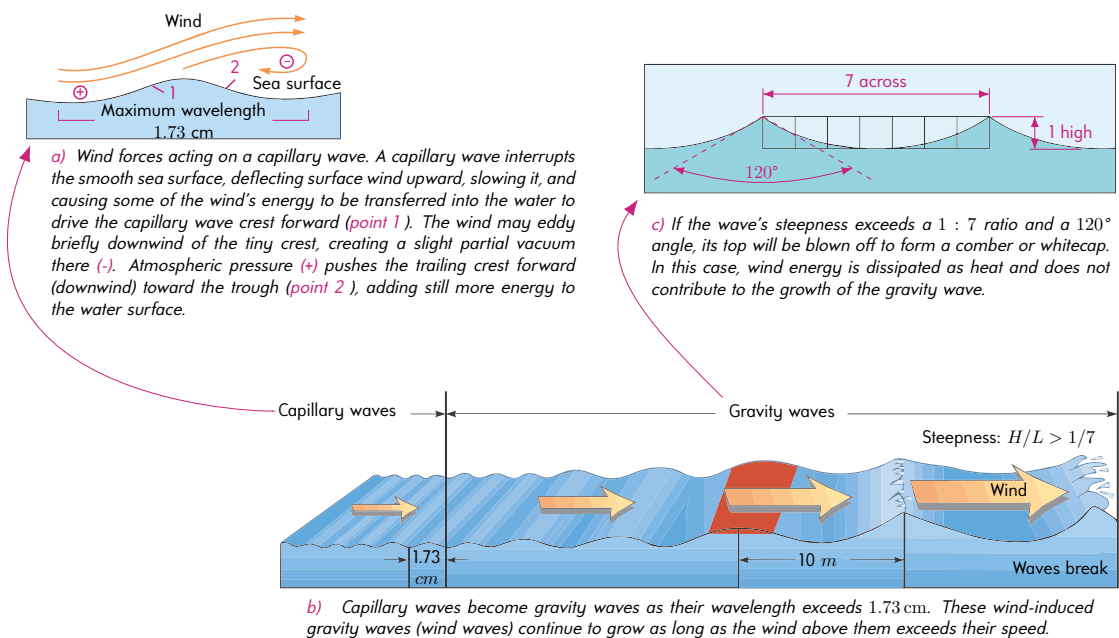


**Figure 2.6.:** Wind waves growth and progression. Redrawn from [36] with the same text as the original source. In the figure, wave speed refers to group velocity.

The mathematical models presented in this section to describe the underlying physic of ocean waves focus on first-order waves, i.e., waves exhibiting *linear* behaviour. This wave



theory is credited to the English mathematician Sir George Biddell Airy and is hence known as Airy’s wave theory [37]. Even though it is restricted to waves with small wave height to wavelength ratios, i.e.,  $H_w/L_w \ll 1$ , Airy’s wave theory offers significant insight into the behaviour of ocean waves and, subsequently, of floating bodies exposed to their influence.

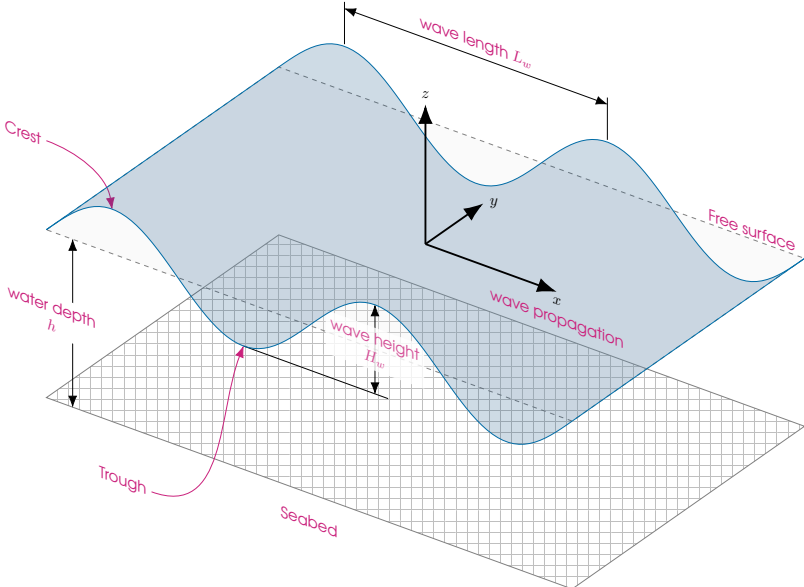


**Figure 2.7.:** Definition of wave parameters over a sinusoidal wave.

**Remark:** In Airy’s wave theory, it is assumed that the function characterising the fluid’s free surface elevation, i.e., the elevation of the free surface from the still water level (SWL), as seen in Figure 2.7, is analytic. This excludes automatically overturning or breaking waves from this model (see Figure 2.8)

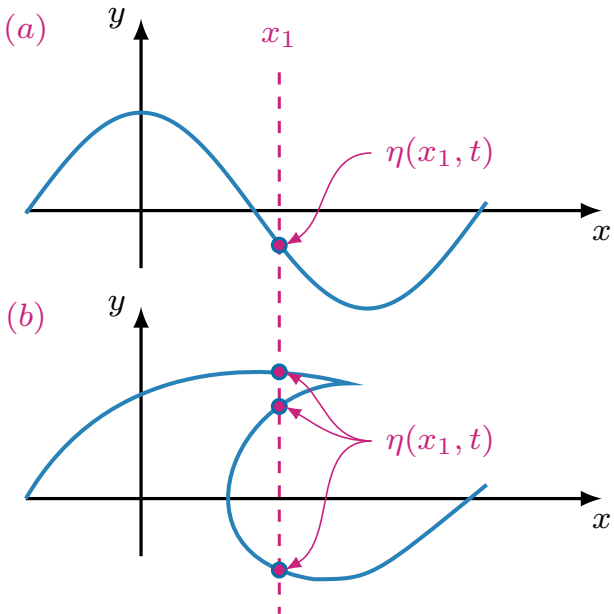


**Figure 2.8.:** (a) Linear waves, (b) Overturning (or breaking) waves. For a specific location, an analytical function determines the free-surface elevation of the wave, as in (a). While breaking waves (b) cannot be described by analytical functions. Redrawn from [37]

## Regular waves

The simplest model to describe the fluid's free surface elevation  $\eta$  at a fixed point in the  $xy$  – plane is by a *single* frequency component  $\omega \in \mathbb{R}^+$ , by which the free surface elevation is represented as:

$$\eta(t) = \frac{H_w}{2} \sin(\omega t + \theta_\omega) \quad (2.1)$$

where  $H_m$  is the wave height (from crest to trough),  $\omega$  stands for the particular frequency being used for the wave in consideration, and  $\theta$  is the phase shift associated with the spatial location.

Even though the simplicity of regular waves effectively misrepresents an actual sea-state, this sort of wave may be used to obtain findings of theoretical interest and gain critical insight into the dynamics of a floating body.

## Irregular waves

Ocean waves are irregular, meaning their frequency and amplitude vary with time. Alternative definitions based on a stochastic description of waves can be used to correct the regular wave model's inaccurate depiction of real ocean waves. The wave amplitude spectrum is commonly used to characterise irregular waves [38]. The *significant wave height*  $H_{m0}$  and the *peak wave period*  $T_p$  are typically the two variables used to define the wave spectrum of a specific sea condition/location.

For a specific irregular wave profile, the peak wave period  $T_p$  is defined as the wave period associated with the most energetic waves, and the significant wave height  $H_{m0}$  is the average wave height of the third-highest waves [39].

Through a frequency representation, these two parameters, i.e.,  $T_p$  and  $H_{m0}$ , along with an underlying assumption of the shape of the power spectral density (PSD)  $S(\omega)$ , stochastically describe the behaviour of ocean waves at a specific place, may qualitatively define the profile of an irregular wave. The spectrum's form is mainly site-dependent and may even vary at the same location [32].

In ocean engineering, several wave spectrums are used to model wave elevations in specific cases. For example, the Pierson–Moskowitz spectrum is typically used to model a fully developed sea (It is when a constant wind has blown for a sufficiently long time over a reasonably long fetch of the ocean); whereas the JONSWAP (Joint North Sea Wave Project) spectra is used in situations where the fetch is limited [28]. Other typical wave spectra include





Bretschneider, Scott, ISSC, Ochi-Hubble bi-modal, TMA and Mitsuyasu [40].

The wave spectrum used in this dissertation is the JONSWAP. The underlying PSD is given as [41]:

$$S(\omega) = \frac{\alpha g^2}{\omega^5} \exp \left[ -\frac{5}{4} \frac{\omega_p^4}{\omega^4} \right] \gamma^a \quad (2.2)$$

where  $\alpha$  is the intensity of the spectra, a constant that relates to the wind speed and fetch length, typical values in the northern north sea are in the range of 0.0081 to 0.01;  $g$  is the acceleration of gravity;  $\omega$  is the wave frequency;  $\omega_p$  is the peak wave-frequency;  $\gamma$  is the peak enhancement factor and  $a$  the exponent of the peak-shape parameter which is computed as [41]:

$$a = \exp \left[ -\frac{(\omega - \omega_p)^2}{2\omega_p^2 \sigma^2} \right] \quad \sigma = \begin{cases} 0.07 & \text{if } \omega \leq \omega_p \\ 0.09 & \text{if } \omega > \omega_p \end{cases}$$

Under the assumption of linear theory, the surface elevation  $\eta(t)$  of any irregular ocean wave may be represented as the superposition of several harmonic waves with varying amplitudes and phases [39]. This can be appreciated in Figure 2.9. The free surface elevation  $\eta(t)$ , which is the interface between the water and the air, is approximated about the still water level (SWL) at a reference location using the following equation [42]:

$$\eta(t) = \sum_{i=1}^{N_c} \eta_i(t) = \sum_{i=1}^{N_c} A_i \sin(\omega_i t + \theta_i), \quad A_i = \frac{H_i}{2} = \sqrt{2 S(\omega_i) \Delta\omega_i} \quad (2.3)$$

where  $N_c$  is the number of regular wave components;  $H_i$ ,  $\omega_i$ ,  $\theta_i$  and  $A_i$  are the wave height, angular frequency, phase and amplitude for the wave component  $i$ ;  $\Delta\omega_i$  is the wave angular frequency interval for component  $i$  and  $S(\omega_i)$  is the wave energy spectrum. Each wave component's wave height and angular frequencies are obtained from a given wave spectrum.

Theoretically, an irregular wave consists of an unlimited number of linear waves, but, in practice, 1000 monochromatic waves are considered good enough to represent an irregular wave [42]. The values assigned to each wave component  $i$  are determined by the representative's wave distribution for the location and sea state in the study.

Figure 2.9 depicts an example of the JONSWAP spectrum for wave height  $H_{m0} = 2$  m and wave period  $T_p = 6$  s on the *Frequency domain* plane. The realisation of sine waves for four specific frequencies is out of the *Frequency domain* plane. On the *Time domain* plane, the approximation of an irregular wave profile realisation is presented. Important to remark that

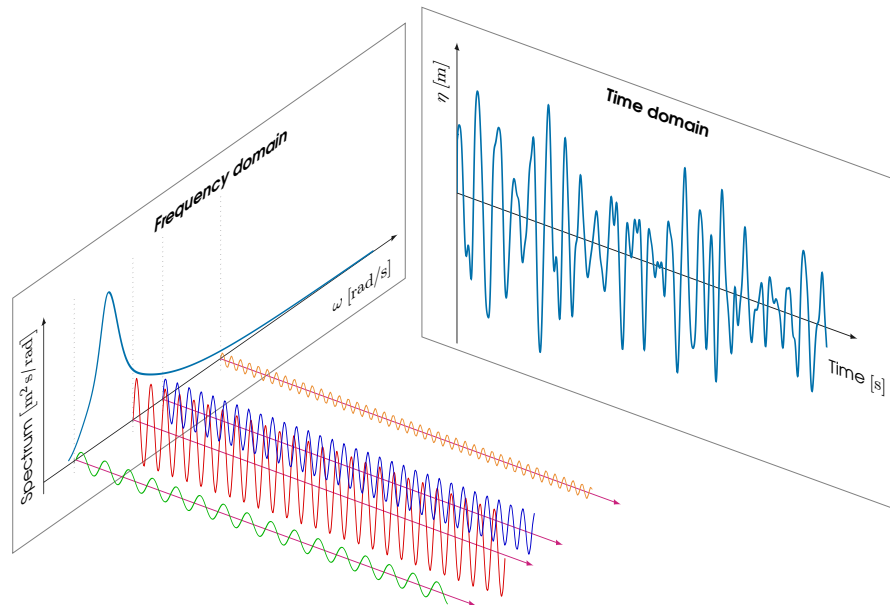


**Figure 2.9.:** *Frequency domain* plane depicts an example of the JONSWAP spectrum for wave height  $H_{m0} = 2$  m, wave period  $T_p = 6$  s. Out of the *Frequency domain* plane are the realisation of sine waves for 4 specific frequencies. On the *Time domain* plane the approximation of an irregular wave profile realisation is presented. Important to remark that the wave profile realisation has been constructed using 500 frequencies and not only the 4 frequencies shown.

the wave profile realisation has been constructed using 500 frequencies and not only the 4 frequencies shown.

---

## 2.3. Hydrodynamic modelling

As commented in Section 1.1, many different wave energy conversion technologies are still being pursued. Currently, oscillating water columns predominate in terms of deployments. Nonetheless, oscillating bodies are expected to play a more significant role based on the projected wave energy capacity [19]. Therefore, the work developed within this project has been focused on the latter, specifically on point absorbers.

Modelling the first stage of the energy conversion chain in wave energy converters is a wave-body interaction topic. It requires knowledge of body dynamics and ocean waves theory. Therefore, before modelling methods for the wave-body interaction are given, body dynamics for the point absorber are presented.

### 2.3.1 Point Absorber dynamics

The interaction between a floating body and seawater allows for six degrees of freedom: three rotations (pitch, roll, and yaw) and three translations (heave, surge and sway). This is depicted in Figure 2.10.

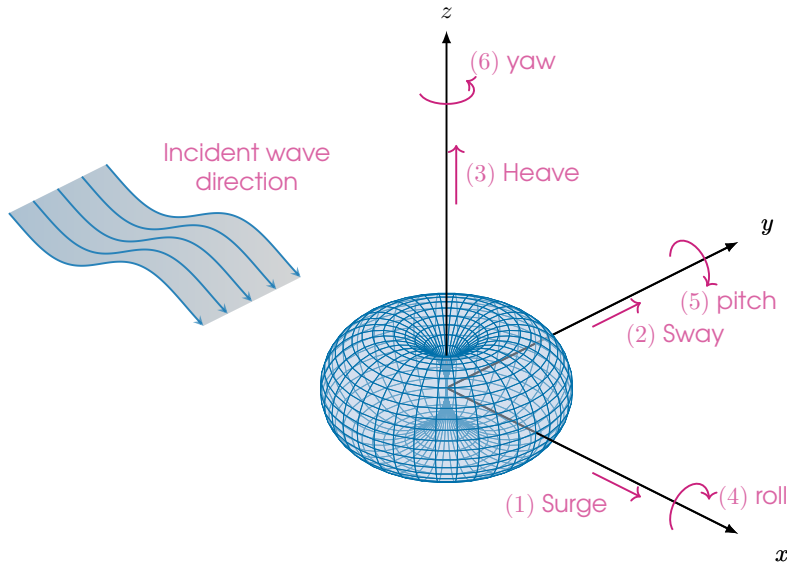


**Figure 2.10.:** Modes of motion for a rigid body: Surge (1), sway (2), heave (3), roll (4), pitch (5) and yaw (6).

Applying Newtons  $2^{nd}$  law to the floater, the motion of a point absorber WEC can be described in general by the following equation:

$$M \ddot{\zeta}(t) = F_h(t) + F_g(t) + F_{pto}(t) + F_{ext}(t) \quad (2.4)$$

where  $M \in \mathbb{R}^{6 \times 6}$  is the generalised inertial matrix,  $\zeta \in \mathbb{R}^6$  is the displacement vector of the floater, relative to its hydrostatic equilibrium position,  $F_h$  is the hydrodynamic force,  $F_g$  is the gravity force,  $F_{pto}(t)$  is the force exerted by the power take-off system (control input, described in section 2.4), and  $F_{ext}$  group all possible external forces. This latter may include, but is not limited to, mooring and other potentially non-linear forces, for example, end-stop forces.

The generalised inertial matrix  $M$  includes the mass of the floater, and the matrix  $I \in \mathbb{R}^{3 \times 3}$  for the corresponding moments of inertia for each rotational mode of the system;  $M$  is computed as:

$$M = (m \otimes \mathbb{I}_3) \oplus I \quad (2.5)$$

where  $m$  is the mass of the floater, and  $\mathbb{I}_3$  is the identity matrix of size 3.

The hydrodynamic force  $F_h$  can be calculated by integrating the pressure  $p(t)$  on the immersed body surface  $S$ , written as:

$$F_h = - \iint_{S(t)} p(t) \mathbf{n} dS \quad (2.6)$$

where  $p(t)$  is the pressure on an element  $dS$  on the buoy wetted surface,  $\mathbf{n}$  is the vector normal to the surface element  $dS$  and  $S$  is the time-varying submerged wetted surface, see Figure 2.11. Thus, the key to hydrodynamic modelling, though a nontrivial task, is to compute the pressure  $p(t)$  in the fluid surrounding the floater.

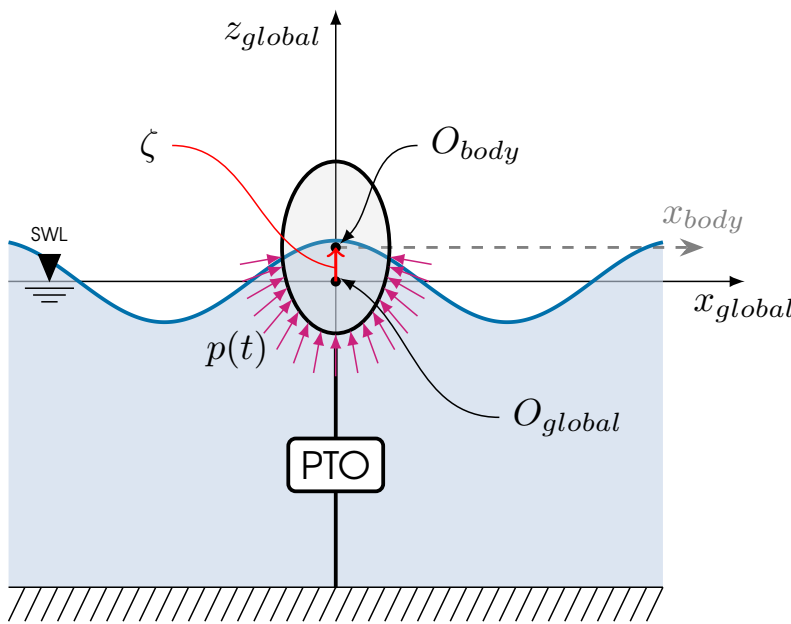


**Figure 2.11.:** Simplified representation of forces acting on a generic wave energy converter with 1-DOF: Heave.

### 2.3.2 Fluid dynamics

The fluid-structure interaction (FSI) can be modelled using the Navier-Stokes equations (NSE). Solving NSE provides a detailed analysis of the FSI. However, NSEs cannot be solved analytically, and computational fluid dynamics (CFD) methods are typically used to provide a numerical solution [22].

Even though CFD provides high-accuracy solutions due to the inclusion of all non-linear effects, its complexity and computational cost are significant limitations. For example, CFD methods require typically between  $1 \times 10^4$  s and  $1 \times 10^5$  s of computation (real) time for 1 s of simulation time [22, 43, 44], depending on the set-up.



It is common to assume an ideal fluid (incompressible, inviscid and irrotational) for a practical and quicker solution. This allows the NSEs to be reduced to the Laplace and Bernoulli equations, which may be solved using potential flow theory (PFT) [45] (see Figure 2.12). With the pressure  $p$  obtained via CFD or PFT methods, the hydrodynamic force in Eq. (2.6) can be computed.

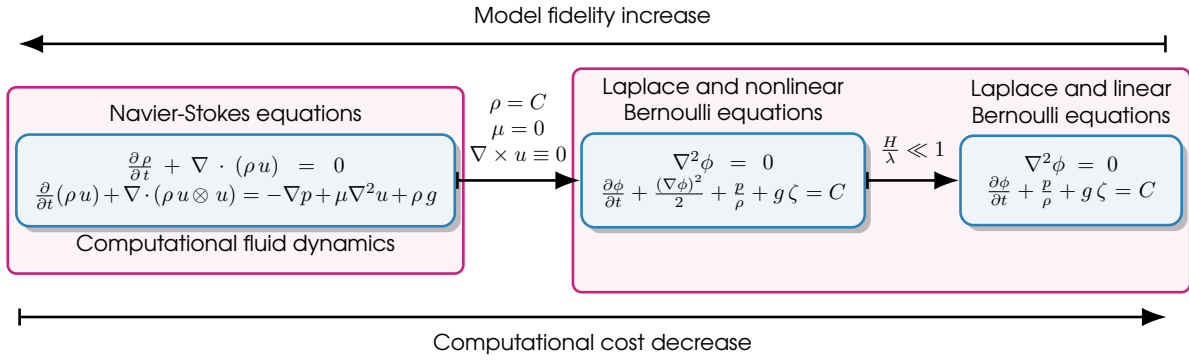


**Figure 2.12.:** Governing equations for CFD and PFT, and their relative accuracy and computation cost between them. Adapted from [22].

Fully non-linear potential flow (FNPF) theory may be utilised to solve the Laplace and non-linear Bernoulli equations and compute the velocity potential function  $\phi$  [46] under the assumption that seawater is ideal. Therefore, the pressure may be determined by

$$p = -\rho g \zeta - \rho \frac{\partial \phi}{\partial t} - \rho \frac{|\nabla \phi|^2}{2} \quad (2.7)$$

where  $\rho$  is the water density,  $g$  is the gravity, and  $\zeta$  is the vertical body displacement.

Additionally, assuming the wave height is much smaller than the wavelength, and the device displacement is small, the Laplace and linear Bernoulli equations can be solved using linear potential flow (LPF) theory. As a result, the total potential flow can be broken down into incident, diffracted and radiated potentials [42], as shown below:

$$\phi = \phi_{inc} + \phi_{diff} + \phi_{rad} \quad (2.8)$$

In general, numerical solutions based on boundary element methods (BEMs) approximate the incident, diffracted and radiated potentials. Standard BEM solvers include WAMIT [47], NEMOH[48], and AQWA [49] in the frequency domain, whilst ACHILD3D [50] solves in the time domain.

By substituting  $\phi_{inc}$ ,  $\phi_{diff}$  and  $\phi_{rad}$  in equations (2.8) and (2.7), and omitting the quadratic term in Eq. (2.7) [22], the pressure  $p$  can be calculated, allowing for the calculation of the hydrodynamic force in Eq. (2.6).

Further development of the preceding equations is based on the presentation given by [43]. From the combination of equations (2.6) - (2.8), the following hydrodynamic forces may be derived:

- $F_{FK, st}(t)$  is the static Froude-Krylov force. This force represents the balance between the gravity force and the force due to the static pressure (Archimedes force):

$$F_{FK, st}(t) = F_g - \iint_{S(t)} \rho g \zeta(t) \mathbf{n} dS \quad (2.9)$$

- $F_{FK, dy}(t)$  is the dynamic Froude-Krylov force:

$$F_{FK, dy}(t) = \iint_{S(t)} \left[ \rho \frac{\partial \phi_{inc}}{\partial t} + \rho \frac{|\nabla \phi_{inc}(t)|^2}{2} \right] \mathbf{n} dS \quad (2.10)$$

- $F_{diff}(t)$  is the diffraction force:

$$F_{diff}(t) = \iint_{S(t)} \left[ \rho \frac{\partial \phi_{diff}}{\partial t} + \rho \frac{|\nabla \phi_{diff}(t)|^2}{2} \right] \mathbf{n} dS \quad (2.11)$$

- $F_{rad}(t)$  is the radiation force

$$F_{rad}(t) = \iint_{S(t)} \left[ \rho \frac{\partial \phi_{rad}}{\partial t} + \rho \frac{|\nabla \phi_{rad}(t)|^2}{2} \right] \mathbf{n} dS \quad (2.12)$$

Using equations (2.9)-(2.12), Eq. (2.4) can then be re-written as:

$$M \ddot{\zeta}(t) = F_{FK, st}(t) + F_{FK, dy}(t) + F_{diff}(t) + F_{rad}(t) + F_{pto}(t) + F_{ext}(t) \quad (2.13)$$

The decomposition of the total potential flow into the incident, diffracted and radiated potentials allow a clear identification of the individual forces' contribution. Figure 2.13 depicts the forces acting on a single-point absorber WECs. Several significant non-linear terms appear when solving Eq. (2.4), among them: pressure forces integrated over the instantaneous body wetted surface (creating geometric non-linearities). In Bernoulli's equation, Eq. (2.7): the quadratic terms and the non-linear incident potential flow. For heaving point absorbers, [51] claims that the quadratic terms in Eq. (2.7) can be neglected to consider only linear waves, which cover the vast majority of waves in the power generation region.



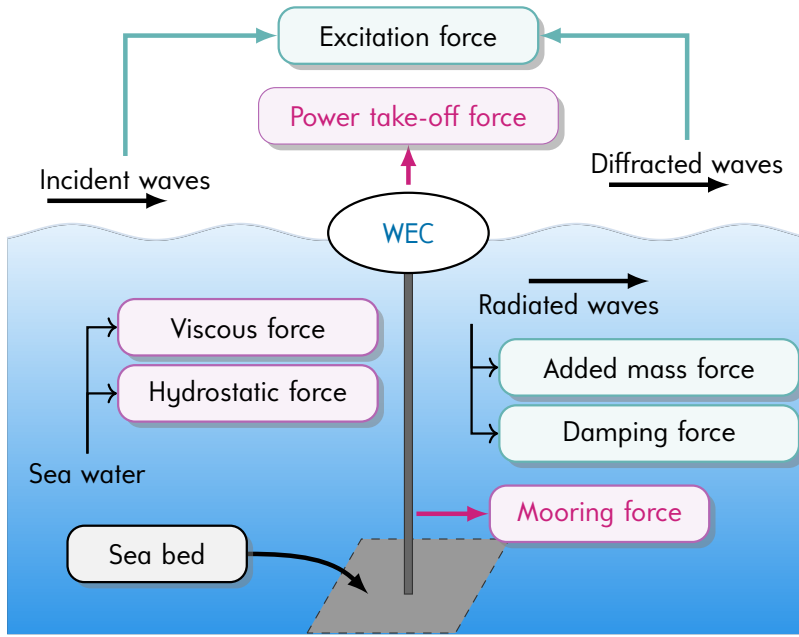


**Figure 2.13.:** Individuals forces acting on a single-point absorber WECs. Adapted from [52]

From Eq. (2.13), several models can be derived, depending on the complexity, computational time and accuracy desired. In the following subsections, as examples, two models are detailed: Linear Model and the Non-linear restoring force model.

### 2.3.3 Linear Model

For linear models, the potential problem is linearised and computed around the equilibrium position. Considering small displacements and mean wetted-surface  $S_m$ , Eq. (2.4) is rewritten as follows:

$$m \ddot{\zeta}(t) = \underbrace{\int_{-\infty}^{\infty} K_{exc}(t - \tau) \eta(\tau) d\tau}_{F_{exc} = F_{FK,dy} + F_{diff}} + \underbrace{-\mu_{\infty} \ddot{\zeta}(t) - \int_{-\infty}^{\infty} K_{rad}(t - \tau) \dot{\zeta}(\tau) d\tau}_{F_{rad}} + \underbrace{-K_h \zeta(t) + F_{pto}(t) + F_{ext}(t)}_{F_{FK,st}}, \quad (2.14)$$

where  $F_{FK,st}$  is described by the linear hydrostatic stiffness  $K_h$ . The dynamic Froude-Krylov ( $F_{FK,dy}$ ) and diffraction forces ( $F_{diff}$ ) are computed together as an excitation force  $F_{exc}$  with a convolution of the excitation impulse response  $K_{exc}$  with the undisturbed free surface elevation  $\eta$  at the centre of the body;  $F_{rad}$  is the radiation force, represented by the sum of the frequency-independent added mass  $\mu_{\infty}$  and the convolution between the radiation impulse response  $K_{rad}$  and the buoy velocity  $\dot{\zeta}$ . The integrodifferential Eq. (2.14) is known

as Cummins' equation [53]. In summary, and with the idea of having a "clean" view of the system's dynamics, Cummins' equation is re-written as:

$$(M + \mu_\infty) \ddot{\zeta}(t) = -K_h \zeta(t) - K_{rad}(t) * \dot{\zeta}(t) + K_{exc}(t) * \eta(t) - F_{pto}(t) + F_{ext}(t), \quad (2.15)$$

where the symbol  $*$  stands for the convolution operator, and the convolution kernels  $K_{exc}$ ,  $K_{rad}$  and the frequency-independent added mass are computed using boundary element methods (BEMs). BEMs are based on the potential theory, in which the potential flow models the velocity flow as the gradient of the velocity potential [54]. Examples for BEMs solvers are given in Section 2.3.2.

The integral term in the  $F_{rad}$  component from Eq. (2.14) is often substituted by a closed-form (finite-order) counterpart [55]. This replacement offers various advantages: first, the integrodifferential Eq. (2.14) is replaced by a higher-order differential equation, simplifying its analysis; second, the resulting finite-order dynamical system is faster to simulate; and third, the closed-form dynamical equation may be utilised as a foundation for model-based control design. Depending on how  $K_{rad}(t)$  or  $K_{rad}(\omega)$  was obtained and the intended (time/frequency domain) application of the finite-order approximation, approximations may be derived in either the time or frequency domain. The approximation may take the form of a state-space model or transfer function, and in general, a linear approximation of  $K_{rad}(t)$  with an order from 4 to 10 is used [55, 56].

**Remark: Excitation force as unmeasured disturbance** Notice the excitation force,  $F_{exc} = \int_{-\infty}^{\infty} K_{exc}(t - \tau) \eta(\tau) d\tau = K_{exc} * \eta$ , where the symbol  $*$  stands for the convolution operator, does not depend on the internal variables describing the system evolution (displacement, velocity or acceleration). Therefore, from the standpoint of system dynamics, the excitation force may be viewed as an external input to the system, and its dependence is limited to the free surface elevation  $\eta$ .

**Remark: Internal stability of Cummins' equation** is guaranteed, in the Lyapunov sense, for any physically meaningful parameters and impulse response function  $K_{rad}(t)$  involved. This claim is supported by the passivity property of radiation effects, as shown in [42].





### 2.3.4 Non-linear extension to the linear model

To enhance the linear model presented in Section 2.3.3, several studies have incorporated additional terms into Cummins' equation. The next paragraphs briefly discuss the two principal non-linear hydrodynamic effects investigated in the WEC control literature, restoring force and viscous force [43].

#### Restoring force

The restoring force term in Cummins' equation (Eq.(2.15)) is based on the assumption of a *constant* cross-sectional area of the floating body concerning the displacement of the body. However, if this is not the case, the relationship between the restoring force and the body displacement is effectively non-linear. If a more accurate description is desired, the static Froude-Krylov force has to be evaluated using the instantaneous wetted surface  $S_w$  [57]. The general procedure to this end is presented below. If  $S_{wp}$  is the water-plane surface whose area is  $A_{wp}$ , a closed surface  $S_c$  can be formed as  $S_c = S_w + S_{wp}$ . Then, the static Froude-Krylov force becomes:

$$F_{FK,st}(t) = F_g - \left( \iint_{S_c} \rho g \zeta(t) \mathbf{n} dS - \iint_{S_{wp}} \rho g \zeta(t) \mathbf{n} dS \right) \quad (2.16)$$

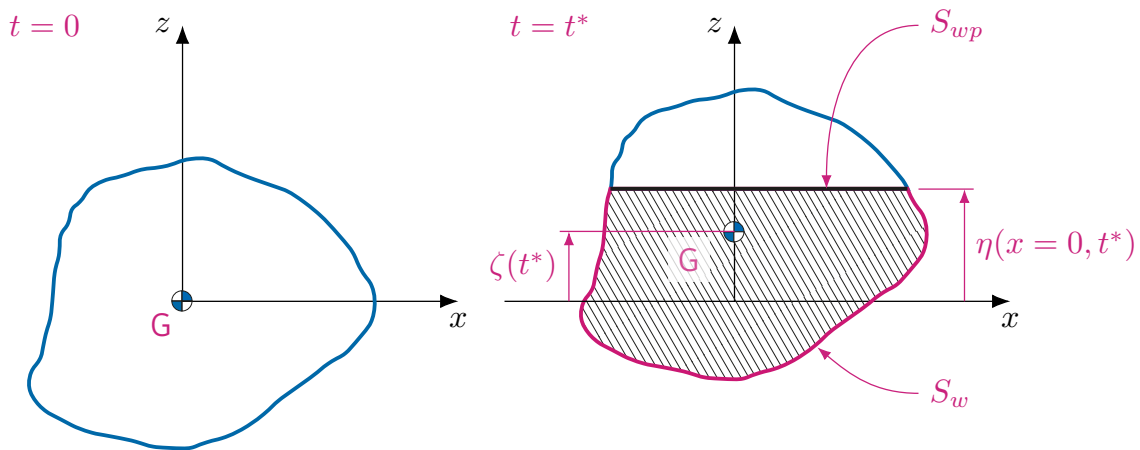


**Figure 2.14.:** Generic heaving device. On the left: the body is at its hydrostatic equilibrium position, with the centre of gravity  $G$  at the still water level (SWL). The free surface elevation  $\eta$  and the device displacement  $\zeta$  after a time  $t^*$  are represented on the right. The submerged volume  $V_{sub}$  is enclosed by the wetted surface  $S_w$  surrounds and the water-plane surface  $S_{wp}$ . Redrawn from [43]

Next, Eq. (2.16) can be simplified by using Gauss's divergence theorem to the integral over the closed surface  $S_c$  [43]. By which, Eq. (2.16) becomes:

$$F_{FK,st}(t) = F_g - (\rho g V_{sub} - \rho g \eta(t) A_{wp}) \hat{\mathbf{k}} \quad (2.17)$$

Here, the submerged volume  $V_{sub}$  is enclosed by the wetted surface  $S_w$  and the water plane surface  $S_{wp}$ ,  $\hat{\mathbf{k}}$  is the unit vector in the  $z$  – direction.

Because the computation of the wetted surface as a function of the vertical displacement of the body is always possible, analytically or numerically, the non-linear restoring force approach applies to any body shape.

## Viscous force

As the fluid is considered inviscid in linear potential flow models, viscous effects are not considered in Cummin's equation, Eq. (2.15). However, omitting these effects may result in inaccurate modelling of the system dynamics, i.e., excessive displacement amplitudes and velocities [58]. The most common way to improve Cummin's equation concerning the viscous effects is by adding terms to account for the viscous force [37]. Viscous forces are linear or quadratic functions of the device's velocity concerning the fluid [58]. In wave energy applications, a quadratic relationship is typically assumed, and viscosity is modelled as an additional Morison-like term, as illustrated in Eq (2.18):

$$F_v(\dot{\zeta}) = \frac{1}{2} \rho C_d A_d \dot{\zeta} |\dot{\zeta}| \quad (2.18)$$

where  $\rho$  is the fluid density,  $C_d$  is the viscous drag coefficient, and  $A_d$  is the characteristic area of the device perpendicular to the flow.

---

## 2.4. Power take-off systems

The Power Take-Off (PTO) system is the mechanism used to transform the energy absorbed by the body into another more useful type of energy, usually electricity [35]. The selection of a PTO system has a significant impact on the overall efficiency of the energy conversion chain but also contributes to the physical properties of the WEC, such as mass, size and dynamics [35].



The wave energy literature has investigated many mechanisms for power take-off systems. Figure presents a schematic classification of the PTO systems found in the WEC literature. The PTO systems considered range from using transmissions based on hydraulics, mechanical gears or magnetic gears to using direct drive solutions. Figure 2.15 presents a schematic classification of the PTO systems found in the WEC literature.

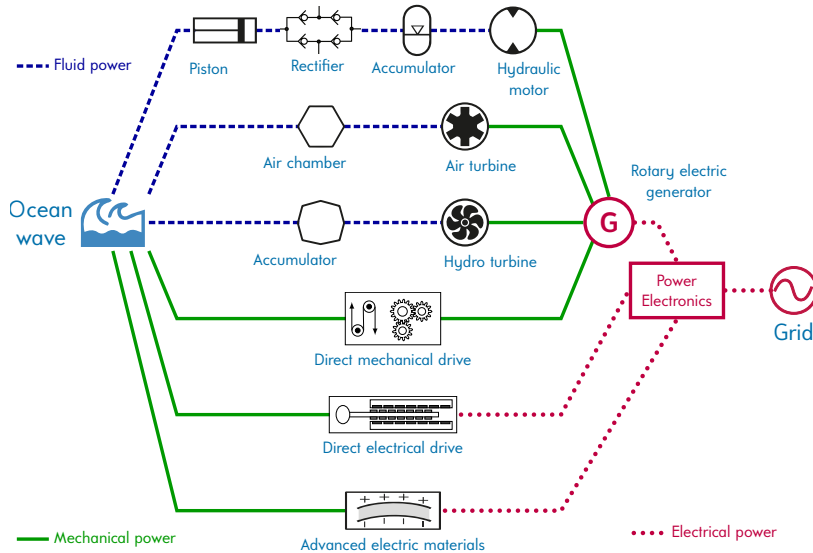


**Figure 2.15.:** General classification of the Power Take-Off systems. Redrawn from [35, 59]

A brief introduction to the classifications given in Figure 2.15 is presented in the following sub-sections.

### 2.4.1 Hydraulic Systems

In the case of wave-activated bodies, such as point absorbers, attenuators and terminators, the energy capture mechanism can not be directly coupled with conventional rotary electrical generators, necessitating an intermediary mechanism.

Hydraulic systems such as PTO-mechanism are commonly encountered in the WECs proposal designs since these types of systems can deal with large forces at low frequencies. In contrast to standard hydraulic systems, the energy flow is reversed in wave energy harvesting, with the absorber oscillating energy into a hydraulic motor that drives an electrical generator [35].

Figure 2.16 depicts a schematic hydraulic circuit used as a PTO system for wave energy converters. As seen in Figure 2.16, the proposed hydraulic solution often incorporates gas accumulators into the circuit, which can store energy over a few wave periods and smooth out the irregular power absorbed from the waves [29].

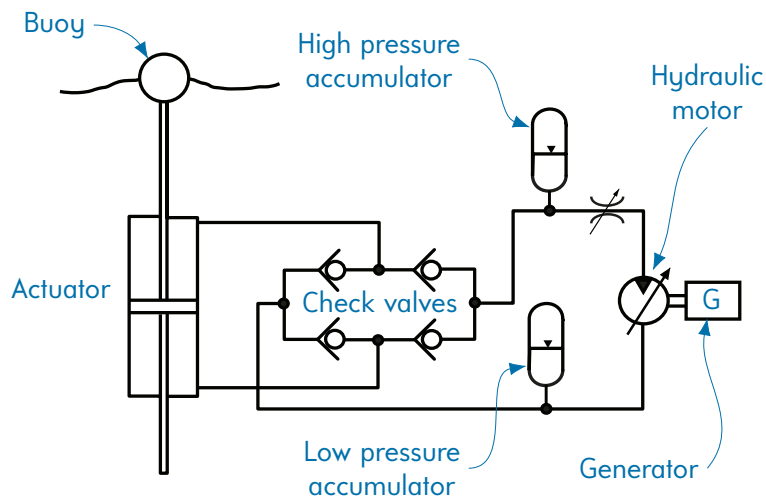


**Figure 2.16.:** Schematic representation of hydraulic power take-off system for WECs. Redrawn from [30]

## 2.4.2 Air Turbines

Air turbines are driven by the flow of air instead of water. This turbine type is primarily employed in the oscillating water column (OWC) WECs [35]. The air turbine located at the top of the OWC structure is driven by the pressure differential caused by the ocean waves within the chamber.

The nature of the flow through the turbine, which is reciprocating, random and highly variable over several time scales ranging from a few seconds to yearly variations, [29] is the main challenge for air turbines.

Since the mid-1970s, many types of self-rectifying turbines have been proposed. New concepts are being explored to create a compelling and reliable air turbine for PTO systems. Most often encountered in the literature on wave energy are [35]:

- Wells type turbines
- Impulse turbines
- Denniss-Auld turbines

Figure 2.17 shows a schematic representation of a self-rectifying Wells turbine, the most common type of air turbine in the OWCs literature.

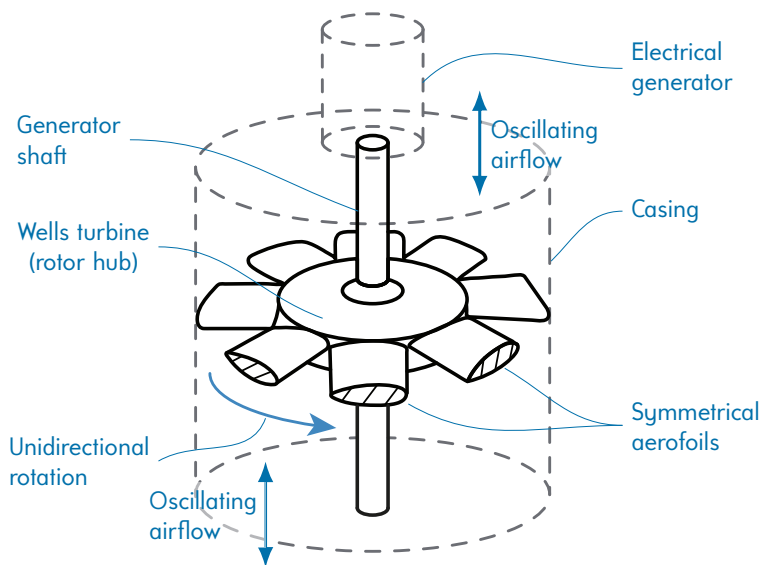


**Figure 2.17.:** Schematic representation of a self-rectifying Wells turbine. Redrawn from [60]

### 2.4.3 Hydro Turbines

Hydro-turbines technology is well established and has been utilised for decades in hydroelectric power plants, often with high efficiencies ( $\eta > 90\%$ ) [35]. Hydro turbines are linked directly to an electrical generator. Typically, hydro-turbines are employed in overtopping WECs and hydraulic power take-off systems using seawater as fluid [8].

One of the key benefits of employing seawater turbines is that no environmental issues are caused by fluid leakage. On the other hand, one of the downsides is that seawater is a fluid with fluctuating composition and typically with uncertain components [30].

Figure 2.18 shows a schematic representation of a Kaplan turbine, often utilised in overtopping devices.

### 2.4.4 Direct Mechanical Drive Systems

The energy captured by the absorber can be transferred directly to a rotating electrical generator through direct mechanical drivers [35]. Frequently, designs include a device for rectifying the bi-directional motion of the absorber to prevent the generator from continually reversing its spin direction. Direct mechanical transmissions include gearboxes, pulleys, cables to ratchets and rack and pinion devices. Figure is a schematic illustration of a direct mechanical drive system.

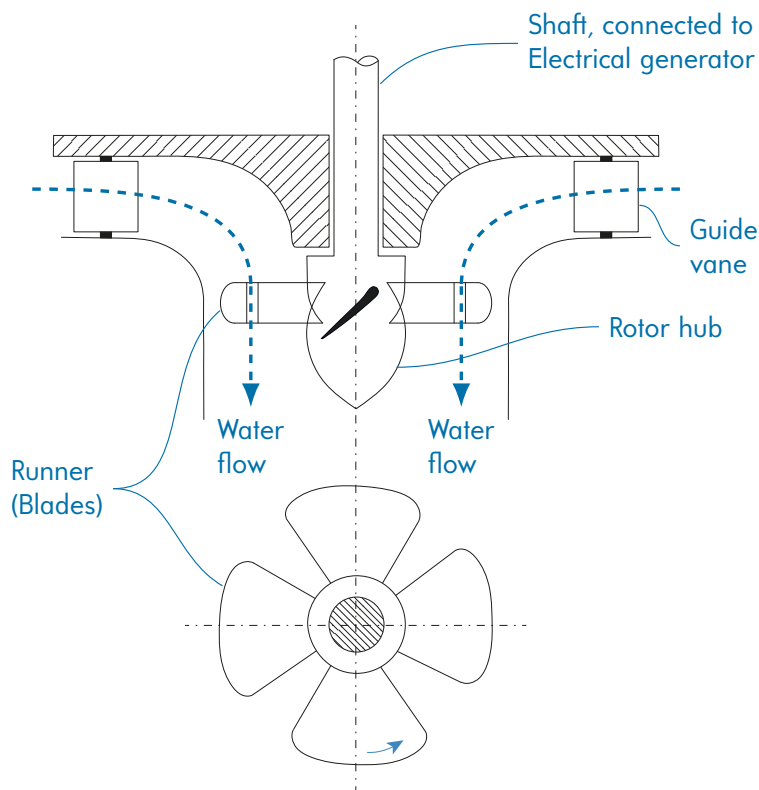


**Figure 2.18.:** Schematic of representation of a Kaplan turbine. On top: cross-section of the turbine; bottom: the runner. Redrawn from [35]

One of the benefits of this type of PTO system is its typically high efficiency, as fewer energy conversion stages are required [35]. On the other hand, one of the issues of direct mechanical drives is the power variations caused by the non-uniform oscillation of the absorber.

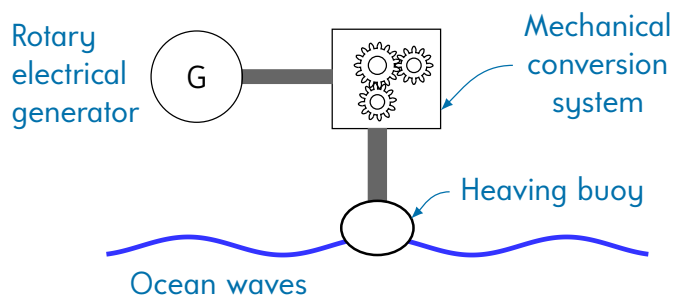


**Figure 2.19.:** Schematic direct mechanical drive PTO system. Adapted from [35]

### 2.4.5 Direct Electrical Drive Systems

The absorber is directly coupled to the linear electrical generator moving part in direct electrical drive PTO systems. The architecture of a permanent magnet linear generator for direct electrical driving systems is shown in Figure 2.20.

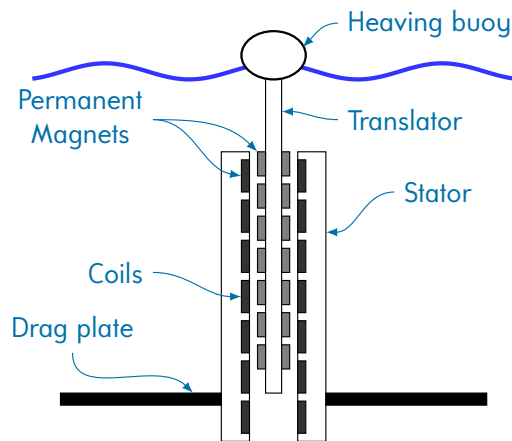


**Figure 2.20.:** Schematic permanent magnet linear generator configuration for direct electrical drive systems. Redrawn from [30]

The basic concept idea of a linear electrical generator is to have a translator (what would be the rotor in a rotary machine) on which magnets with alternating polarity are installed and directly coupled to a heaving buoy, with the stator containing windings installed in a relative stationary framework (connected to a drag plate, large inertia, or fixed to the ocean bed) [30].

The direct electrical drive PTO alternative enables the direct transfer of mechanical energy into electrical energy, making the system highly efficient and more straightforward than hydraulic systems. However, one of the disadvantages of this PTO solution is the necessity for electronics to rectify the output signal to satisfy the voltage and frequency standards before connecting the system to the grid [35].





## Control Strategies for Wave Energy Converters: *A state-of-the-Art* review

” *The world is full of obvious things which nobody by any chance ever observes.*

– Sherlock Holmes –

3.1	Primary Controllers: Function . . . . .	33
3.2	Optimal unconstrained control law: Impedance-matching principle. . .	33
3.3	Classical control strategy . . . . .	36
3.3.1	Passive Loading Control . . . . .	37
3.3.2	Reactive Control . . . . .	38
3.3.3	Latching Control . . . . .	38
3.3.4	Declutching Control . . . . .	38
3.4	Modern control strategies . . . . .	39
3.4.1	Hydrodynamic model . . . . .	42
3.4.2	Cost function . . . . .	44
3.4.3	PTO system efficiency. . . . .	45
3.4.4	Real-time capabilities . . . . .	47
3.5	Summary . . . . .	48

Wave energy systems typically require two controllers: a primary controller for the power take-off (PTO) system, that maximise energy harvesting and determines the optimal set points for device velocity or PTO force, and the secondary controller for the grid power converters connected to the electric generator, that regulates the voltage, current, and frequency to ensure grid integration. A schematic representation of these two controllers is depicted in Figure 3.1. The former, namely research on optimal controllers for the primary stage of energy conversion in WECs, is what this dissertation aims to contribute. Therefore the literature review studied and presented in this chapter focus on control strategies for the primary conversion of WECs. The reasons behind this are twofold: first, the ocean wave energy community is aware [61–64] that optimal controllers can lower the levelised cost of energy (LCOE), thereby making ocean wave energy more attractive to investors and more price-competitive relative to other forms of renewable energy, and second, the design of an energy-maximising controller for WECs does not fit the ‘traditional’ control problem, i.e., tracking/regulating. As a result, off-the-shelf control strategies cannot be directly implemented as controllers for WECs.

**Levelised cost of energy (LCOE):** (dollars per unit energy; here, \$/kWh) may be defined as the quotient of total capital and operational expenditures of wave energy generation to the amount of energy generated over the system’s lifetime [62]

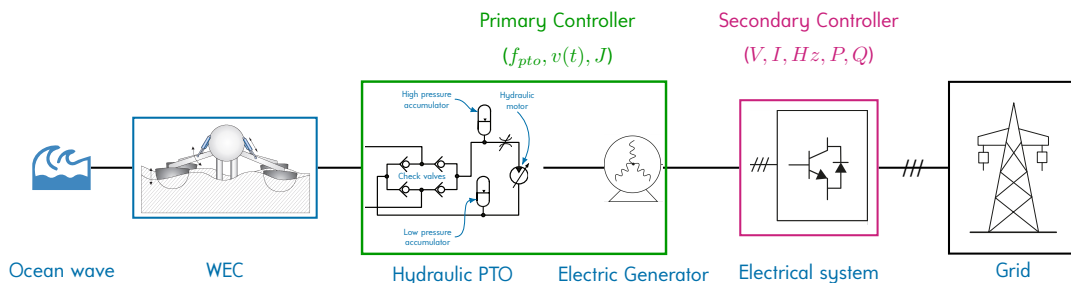


**Figure 3.1.:** Schematic representation of controllers for OWE converters.

Depending on the nature of the primary controllers, these can be considered passive or active controllers. A passive controller infers a purely resistive control strategy characterised by a unidirectional energy flow. On the other side, using a bidirectional energy flow, active controllers feed back energy into the PTO for an (ideally) small fraction of the wave cycle to increase the absorbed energy from the ocean waves. The following sections will give examples for both types, passive and active controllers.

---

## 3.1. Primary Controllers: Function

Recall from Section 2.3.3 that the dynamics of a WEC, under potential flow theory, can be modelled by the well-known Cummins' equation, Eq. (2.15), shown below for convenience:

$$(M + \mu_\infty) \ddot{\zeta}(t) = -K_h \zeta(t) - K_{rad}(t) * \dot{\zeta}(t) + K_{exc}(t) * \eta(t) - F_{pto}(t) + F_{ext}(t).$$

As discussed in Section 2.3.3, the excitation force  $F_{exc}$  in the above equation is independent of the internal variables that describe the system's evolution (displacement, velocity or acceleration). Therefore, from a system dynamics perspective, the excitation force can be considered an external input to the system (over which the primary controller has no influence), and its dependency is restricted to the free surface elevation  $\eta(t)$ . The two other terms to study from Cummins' equation are the external forces  $F_{ext}$  and the PTO force  $F_{pto}$ , which will be covered in the following paragraphs.

External forces, often combined under the term  $F_{ext}$  and may include mooring forces, non-linear forces as extensions to Cummins' equations such as viscous forces or restoring forces, are almost always expressed as functions of the state vector of the system (displacement, velocity, See Section 2.3.4). Again, the primary controller does not directly determine these external forces' magnitude.

According to the above analysis, the *only* independent force over which the primary controller has a direct influence is the PTO force. Therefore, we are able now to state the function of the primary controller: *Determine the optimal behaviour for the PTO force to optimise the operation of the ocean wave energy (OWE) device, which includes maximising the absorbed energy while converting it as efficiently as possible to minimise the cost of the delivered energy, preserving the structural integrity of the device, reducing wear on the device components and operating in a broad range of sea states.*

Having defined the main function of a WEC's primary controller, the following sections examine control strategies that strive to achieve the aforementioned primary controller's function.

---

## 3.2. Optimal unconstrained control law:

### Impedance-matching principle

To date, a wide range of control strategies for OWE converters is available in the literature. The first ideas for maximising the amount of absorbed energy date back to the 1970's, when

Kjell Budal and Johannes Falnes [65–67], and David Evans [68] presented their control laws in separate publications on the analysis of the system dynamics in the frequency domain.

For simplicity of presentation, a WEC oscillating in only one mode, for instance, heave or pitch (Recalled modes of oscillation from Figure 2.10), is considered for the remainder of the dissertation. Also, this analysis does not consider external forces such as mooring or end-stop forces. In the following paragraphs, a brief derivation of the impedance matching principle for OWE converters is provided; interested readers can find the full development of this principle in [37, 42, 55].

Now, consider Cummins' equation, Eq. (2.15), applying the *Fourier transform* and rewriting it as a force-to-velocity model; Cummins' equation in the frequency domain is given by:

$$V(\omega) = \frac{1}{Z_{int}(\omega)} [F_{exc}(\omega) - F_{pto}(\omega)], \quad (3.1)$$

where  $V(\omega)$  is the Fourier transform of the device velocity,  $v(t) = \dot{\zeta}(t)$ ;  $F_{exc}(\omega)$  and  $F_{pto}(\omega)$  are the Fourier transforms of the excitation force  $F_{exc}(t)$  and PTO force  $F_{pto}(t)$ , respectively.  $Z_{int}(\omega)$  is termed the intrinsic mechanical impedance of the OWE converter, defined as:

$$Z_{int}(\omega) = B_{rad}(\omega) + j\omega \left[ M + A_{rad}(\omega) - \frac{K_h}{\omega^2} \right], \quad (3.2)$$

where  $B_{rad}(\omega)$  is the radiation resistance,  $A_{rad}(\omega)$  is the frequency-dependent added mass, often replaced by its high-frequency asymptote  $\mu_\infty$  [55].

Regarding the PTO force, it is commonly modelled as the combination of linear terms opposing the motion of the WEC [35], where the force comprises a term proportional to the WEC velocity and another term proportional to the WEC displacement. The mathematical expression is as follows:

$$F_{pto}(t) = D_{pto} \dot{\zeta}(t) + k_{pto} \zeta(t), \quad (3.3)$$

where  $D_{pto}$  and  $k_{pto}$  are the so-called damping coefficient and spring coefficient of the PTO system, the first term on the right-hand-side of Eq. (3.3) refers to a resistive or dissipative effect. It is directly linked with the capacity of the WEC to harvest OWE [35]. The second term refers to a reactive force proportional to displacement, which models the reactive effect associated with the energy transfer between the PTO system and the moving element of the WEC. The reactive power is proportional to the difference between the maximum value of kinetic and potential energy. Ultimately, because the time-averaged reactive power is zero, the reactive-force term does not affect the absorbed power [35].



Equations (2.15) and (3.1) can be represented as a simple mechanical oscillator in the form of a mass–spring–damper system or its analogue in the electrical domain, as shown in Figure 3.2. This equivalent representation allows the derivation of conditions for *unconstrained* optimal energy absorption if system constraints are ignored for the time being.

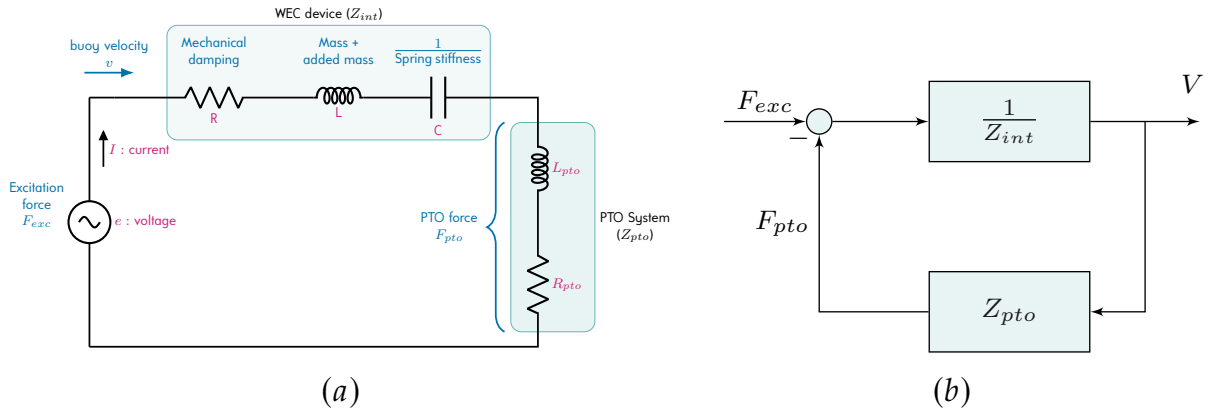


**Figure 3.2.:** Equivalent representation of an OWE converter dynamics by (a) electrical circuit (redrawn from [21]). (b) Closed loop for the complex-conjugate control

From the electrical equivalent representation depicted in Figure 3.2(a), the PTO force can be regarded as the external load to the circuit, which has to be designed to ensure maximum power transfer from the source, i.e., excitation force  $F_{exc}$ . By the so-called impedance-matching (or maximum power transfer) theorem [69], the optimal PTO system impedance should satisfy the following condition:

$$Z_{pto}(\omega) = Z_{int}^*(\omega), \quad (3.4)$$

where  $Z_{int}^*$  denotes the complex conjugate of  $Z_{int}$  to maximise the energy absorbed from the ocean waves.

Equation (3.4) indicates that the power absorbed by the WEC from the ocean waves is maximised when the PTO system impedance is the complex conjugate of the system's intrinsic mechanical impedance [42]. Given this result, the PTO force should be set as (see Figure 3.2 for a closed-loop representation):

$$F_{pto}(\omega) = Z_{pto}(\omega) V(\omega) = Z_{int}^*(\omega) V(\omega). \quad (3.5)$$

This control policy is called complex-conjugate or reactive control (RC).

From the result in Eq. (3.4), we can make the following remarks:

- 1) The proposed optimal solution in Eq. (3.4) for the tuning of the PTO force,  $F_{pto}$ , is frequency dependent, which implies that there is an optimum value for each wave frequency. Additionally, it poses a challenge to tuning the PTO force with the parameterisation presented in Eq. (3.3) for irregular seas consisting of various frequencies [55].
- 2) To maximise the total energy extraction (rather than the instantaneous power), it is essential to continuously tune the control parameters ( $D_{pto}$  and  $k_{pto}$ ) of the PTO system for each sea state to maintain the WEC operating at its optimal efficiency [35].
- 3) The inclusion of both terms,  $D_{pto}$  and  $k_{pto}$ , implies bidirectional reactive power flowing between the PTO system and the absorber [35]. One of the main limitations of this control strategy is that it creates a particular requirement on PTO systems to allow for bidirectional power flow. Still, it can yield energy losses if not tuned correctly [55, 70, 71].
- 4) In addition to the strong assumptions on regular waves, linear hydrodynamics, and ideal PTO, the proposed optimal solution does not account for physical constraints, such as WEC displacement, velocity, or PTO force maximum value, to mention a few. This is paradoxical given that this control law maximises device displacement [55].

Despite its shortcomings, the impedance-matching theorem-based control policy presented above is a crucial foundation for other control strategies described in the literature. In the following section, we will describe some control schemes based on the impedance-matching principle.

---

### 3.3. Classical control strategy

The result obtained from Section 3.2 for unconstrained optimum energy absorption can alternatively be expressed in terms of an optimum velocity profile as:

$$V^{opt}(\omega) = \frac{F_{exc}(\omega)}{2R_{int}(\omega)}, \quad (3.6)$$

where  $V^{opt}(\omega)$  is the optimum trajectory for the floater velocity and  $R_{int}(\omega)$  is intrinsic mechanical resistance (i.e., the real part of the OWE converter intrinsic mechanical



impedance:  $\Rightarrow R_{int}(\omega) = B_{rad}(\omega)$ ). Eq.(3.6) implies that the absorbed power is maximised when both the amplitude and phase conditions are satisfied at the same time:

$$|V^{opt}(\omega)| = \frac{|F_{exc}(\omega)|}{|2R_{int}(\omega)|}, \quad \angle V^{opt}(\omega) = \angle F_{exc}(\omega), \quad (3.7)$$

wherein  $\angle$  stands for the phase of the complex variable.

In summary, the optimal velocity trajectory of the device should be *proportional* to the excitation force  $F_{exc}$ , with the constant of proportionality as  $\frac{1}{2R_{int}(\omega)}$ . But also should be *in-phase* with excitation force  $F_{exc}$ .

Although the control policy derived from the conditions of Equations (3.6) and (3.7) is not applicable in a generic sense, i.e.,  $\forall \omega \in \mathbb{R}$ , it intuitively captures the underlying dynamics behind maximum energy absorption. It gives rise to various impedance-matching-based control strategies, including Latching or Declutching, among others.

Passive Loading, Latching and Declutching control strategies will be briefly described without going into great depth, as it has been demonstrated in several earlier studies that these strategies are inherently suboptimal. Interested readers can find additional information in [30, 55, 72–74]. Also, a comparison of control strategies for wave energy converters can be found in [75–79]

### 3.3.1 Passive Loading Control

Passive control, also known as Resistive control, is perhaps the simplest control strategy in OWE literature. This control approach consists in setting the PTO force by using only the real part of  $Z_{pto}$ , i.e., The PTO force is set proportional to the device velocity, with the damping coefficient  $R_{pto}$  as the constant of proportionality. Using a passive controller offers the advantage of requiring a less complex PTO system, which avoids the need for the PTO to supply power back to the WEC (avoiding reactive power) [55]. The damping coefficient is frequency-dependent and can be determined numerically or from experimental tank testing [35]. The damping coefficient is set to  $R_{pto}(\omega) = B_{rad}(\omega)$  when optimal control is being used.

### 3.3.2 Reactive Control

Contrary to resistive control, the PTO impedance  $Z_{pto}$  is allowed to be complex in reactive control. For the case of optimum reactive control,  $Z_{pto}$  is set equal to  $Z_{int}^*$ , as presented in Eq. (3.5). If reactive control is employed to control a WEC, the PTO system must be able to manage reactive power flow [80]. This indicates that the instantaneous power conversion through the PTO device may need to be reversed for brief periods of the wave cycle [35]. With reactive loading control, the OWE converter's frequency band can be broadened on either side of its resonant frequency [30, 81]. Finally, it has been shown that this control strategy can enhance OWE absorption [82, 83], but at the expense of a reversible and more complex PTO system.

### 3.3.3 Latching Control

Latching control, initially proposed in [65], is one of the most common control strategies found in OWE literature, and one of the reasons is its simplicity of implementation [37]. It is a non-linear control technique that works by stalling the WEC floater at its extremes (i.e., when its velocity is zero) and releasing it when the wave force is back in phase with the device to maximise energy absorption [21, 55]. Therefore some authors categorised it as *phase control* technique [35, 42]. The time the device must be latched is the control variable within this control strategy [30].

Latching controllers requires a PTO system able to react quickly to a given control set value [29], and it has been shown it considerably increases the absorbed energy for a range of different devices operating in irregular wave conditions [72, 73, 80]. The latching of the buoy is done when the velocity is equal to zero, however, complex algorithms are required to determine the precise moment to release it. Additionally, latching can result in extremely large structural forces [35].

### 3.3.4 Declutching Control

Like the latching strategy, declutching belongs to the class of discrete control algorithms. This approach involves unloading the device at specific moments during the cycle to allow the device to "catch up" with the excitation force, bringing the device's velocity into phase with the excitation force. In hydraulic PTO systems, declutching is accomplished by switching a by-pass valve on and off, whereas in electromechanical PTO systems, declutching is





accomplished via a clutch mechanism [84]. According to [35], it is believed that declutching was first presented by [81] and [74] later investigated in depth.

Declutching, also known as *freewheeling* or *unlatching*, has been studied in [85] for the specific device SEAREV, where it was reported that the declutching strategy increases WEC's efficiency up to a factor of two under certain wave conditions, even when compared to the case where a passive loading control strategy controls the PTO. According to [86], declutching is an optimal non-linear damping strategy when the device's resonant period is longer than the wave period. Active bipolar damping control, a combination of latching and declutching approach, has been simulated and implemented in [87], demonstrating that the power capture may significantly increase relative to optimal linear damping. Several studies, including [74, 88], have shown a significant increase in energy absorption compared to latching or declutching implemented individually.

---

### 3.4. Modern control strategies

Modern control strategies are defined in this dissertation as those control strategies whose control variable is chosen based on the solution of an optimal control problem (OCP). In Section 3.1, the main function of the WEC's primary controller was verbally defined. In this section, we attempt to mathematically represent the WEC's primary controller function.

The WEC control problem may generally be formulated as an optimal control problem as follows:

$$F_{pto}^{opt} = \arg \max J(F_{pto}) \quad (3.8a)$$

subject to:

$$\left. \begin{aligned} \dot{\underline{x}}(t) &= f(\underline{x}, F_{pto}, F_{exc}, t) \\ |\zeta(t)| &\leq \zeta_{max} \\ |\dot{\zeta}(t)| &\leq \dot{\zeta}_{max} \\ |F_{pto}(t)| &\leq F_{pto,max} \end{aligned} \right\} \begin{array}{l} \text{WEC dynamics} \\ \text{State and input constraints} \end{array} \quad (3.8b)$$

where  $J(F_{pto})$  is the cost function of the OCP, and its definition has been left open for reasons that will become apparent in the coming paragraphs.

In general, the OCP denoted in Eq. (3.8) cannot be solved analytically, and its solution must be approximated using numerical methods, such as direct or indirect methods, among others [89, 90].

Indirect methods, which "*first optimise and then discretise*", provide a more accurate solution compared with direct methods. However, the need for previous knowledge of the solution's structure, which requires an extensive understanding of optimum control, limits indirect methods for use in practical applications. Such information is difficult to get in many circumstances, even for experts in optimum control [91].

Numerical solutions based on direct methods, on the other hand, "*first discretise and then optimise*", as the OCP is transcribed into a Non-linear Programming Problem (NLP) by discretising the continuous-time system model and cost function [91]. The NLP that results from the discretisation may be considered an OCP for a discrete-time system that arises from discretising the original system on the specified sampling time [91].

Most energy-maximising control strategies reported in the WEC control literature are based on direct methods for solving the OCP [37]. *Model Predictive Control* and *Spectral/Pseudo-spectral control* are two most often encountered control strategies in the OWE area [37, 92]. In the following paragraphs, the principle of each of these control strategies is briefly presented.

MPC is an advanced control strategy for linear and non-linear constrained systems based on optimal control [91]. As its name suggests, it employs a mathematical *model* of the system's dynamics, typically in the form of state space models, to *predict* its future evolution. Based on the system's evolution prediction, the controller tries to minimise a given cost function over a predetermined prediction horizon [91]. From this solution, only the first set of decision variables are implemented, and, at the following sampling interval, a new control policy is calculated based on the most recent information on the system evolution.

Due to its digital nature, MPC is often evaluated in a discrete-time framework, despite its frequent application to continuous-time systems. A continuous-time system may be discretised to provide a discrete-time equivalent. The relationship to direct optimum control becomes apparent in this setting, even though other approaches may also be employed to solve the MPC OCP [91].

On the other hand, Spectral (SPM) and pseudo-spectral methods (PSM) provide a compelling alternative to MPC for solving the OCP under constraints using a specific parameterisation of the solution [93]. The idea behind spectral and pseudo-spectral methods is to approximate the states and control variables by a linear combination of an  $n$ -dimensional vector space spanned by an orthogonal basis of real functions  $\Phi(t) = \{\phi_i(t)\}_{i=1}^N$  [94], commonly defined in terms of the standard inner product in  $L^2$ -spaces. Typically, the



system's states and control are approximated as follows:

$$x_i(t) \approx x_i^N(t) = \sum_{j=1}^N c_{ij}^x \phi_j(t) = \hat{C}_i^x \Phi(t) \quad (3.9a)$$

$$u_i(t) \approx u_i^N(t) = \sum_{j=1}^N c_{ij}^u \phi_j(t) = \hat{C}_i^u \Phi(t) \quad (3.9b)$$

where  $x_i$ ,  $x_i^N$ ,  $u_i$ ,  $u_i^N$ , are the  $i$ -th components of the system's state space vector  $\underline{x}$ , approximated system's state space vector  $\underline{x}^N$ , control input vector  $\underline{u}$ , and approximated system's state space vector  $\underline{u}^N$ , respectively.  $\hat{C}_i^x = [c_{i1}^x, \dots, c_{iN}^x]^T \in \mathbb{R}^N$  and  $\hat{C}_i^u = [c_{i1}^u, \dots, c_{iN}^u]^T \in \mathbb{R}^N$  denote the set of expansion coefficients employed to approximate the system's state and control input vectors, respectively, and  $\Phi(t) = [\phi_1(t), \dots, \phi_N(t)]$  represents the set of orthogonal basis functions.

**A brief history of MPC:** Model predictive control strategy was first introduced in the 1970s and 1980s to address the particular control demands of power plants and petroleum refineries [95]. Its acceptance in industry as in the academic literature is mainly due to its conceptual simplicity and ability to handle complex systems with hard control constraints and multiple inputs and outputs [96]. To date, the range of applications in engineering is immense, from food processing, automotive, aerospace, power electronics, manufacturing and building climate and energy [95, 97]. One of the earliest forms, Model Predictive Heuristic Control (MPHC), published in [98], employs impulse response models to predict the system dynamics. In contrast, the variant published in [99], termed Dynamic Matrix Control (DMC), employs step response models to predict the system behaviour. Later in the 1980s, Clarke et al. published the Generalised Predictive Control (GPC) based on the controlled auto-regressive moving average (CARIMA) input-output model [100], while [101] introduced the state space formulation for model predictive control. The reader is referred to [96, 97, 102, 103] for further information (as a starting point) on state-of-the-art advances in MPC.

The set of expansion coefficients are determined by forcing the projection of the residual function,  $R$  (defined in equation (3.10)), over the set of test functions  $\Sigma(t) = \{\sigma_j(t)\}_{j=1}^N$  to be zero [92]. Assuming that the system's dynamics can be modelled as  $\dot{\underline{x}}(t) = f(\underline{x}, \underline{u}, F_{exc}, t)$  (note that the PTO force  $F_{pto}$  has been replaced by the standard control input nomenclature:  $u$ ), the residual function is defined as:

$$R_i(\hat{C}_i^x, \hat{C}_i^u, t) = x_i^N(t) - f(\hat{C}_i^x, \hat{C}_i^u, F_{exc}, t) \quad (3.10)$$

For a given value of  $\hat{C}_i^u$ , the corresponding vector  $\hat{C}_i^x$  is obtained by solving the following system of equations:

$$\langle R_i(t), \sigma_i(t) \rangle = 0 \quad \text{for } i, j = 1, \dots, N \quad (3.11)$$

where  $\langle \cdot, \cdot \rangle$  represents the inner product operator defined as:

$$\langle f(t), g(t) \rangle = \int_0^T f(t) g(t) dt \quad (3.12)$$

It has been shown that spectral and pseudo-spectral methods may scale in complexity and performance by varying the number of approximating basis functions [92]. In contrast to MPC, which relies primarily on local zero-order holder (ZOH) functions to approximate the optimum solution, spectral methods are generally based on global functions specified throughout the control horizon [104].

**Fundamental difference between Spectral and Pseudo-spectral methods:** The distinction between spectral and pseudo-spectral methods is made by the specification of the finite-dimensional orthogonal set of test functions  $\gamma_i$  that is used to solve for the annulment of the so-called residual function [94]. If the set of test functions  $\gamma_i$  is a subset of the basis functions  $\phi_i$  used to approximate the system's state vector, then the method is known as a *spectral or Galerkin* method. Alternatively, if the test functions set is composed of translated Dirac-Delta  $\delta(t - t_i)$ , the method is referred to as pseudo-spectral, collocation, or interpolation method [94].

After outlining the essential ideas behind MPC and SPM/PSM, the discussion of these two control techniques will go on to the hydrodynamic model for the device-ocean wave-interaction that was utilised (linear or non-linear), the cost function  $J(\underline{u}(t))$ , the PTO system's efficiency, and their real-time capabilities.

### 3.4.1 Hydrodynamic model

In the OWE sector, a great portion of the research proposing MPC or spectral methods (SPM or PSM) to control the PTO system relies on linear models based on Cummins' equation (2.15) [37]. MPC was first proposed to be used in the OWE field by Paul Gieske in [39] to control the Archimedes Wave Swing. The mathematical model used in [39] is based on Cummins' equation with the inclusion of some non-linear forces (but later linearised), e.g., friction forces in the bearings and drag forces. Other studies that rely on linear models include [70, 105–113], to name a just a few examples.



In the case of spectral methods, it was first brought to the ocean wave field by Bacelli et al. in [114, 115] using a truncated Fourier series to approximate the control and state variables. Cummins' equation is supplemented with a linear model for viscous force in [114, 115]. Herber and Allison in [40] suggested pseudo-spectral methods for solving the OCP in OWE sector using the General Pseudo-spectral Optimisation Software (GPOPS), which utilises the Radau Pseudo-spectral Method (RPM) with Legendre-Gauss-Radau (LGR) collocation points and a *hp*-adaptive mesh refinement algorithm [40, 116]. Similarly, [40] uses a linearised drag force model for approximating the viscous force.

Later on, [117] presents a general mathematical framework for the solution of the WEC OCP, employing both spectral and pseudo-spectral methods, where the Galerkin method is extensively discussed when applied to a heaving point absorber.

There are advantages and disadvantages to using linear models to represent the system dynamics of the WEC under study. On the one hand, linear models have been used because of their simplicity and computing efficiency. However, part of the underlying assumptions followed in the derivation of Cummins' equation has recently been called into question [118, 119]. This is because the controller aims to maximise the motion amplitude to maximise the absorbed energy, whereas Cummins' equation relies on small displacements around the equilibrium position of the floater.

To enhance the linear model from Cummins' equation, numerous studies have added more elements to Cummins' equation. For instance, the models employed in [120–123] incorporate non-linear restoring forces, while the models presented in [121–126] include non-linear viscous forces.

Apart from the extensions to Cummins' equation discussed above, very few studies have considered the non-linear contribution of the static and dynamic Froude–Krylov (FK) force [127], which directly arises as the integration of the incident pressure field over the wetted surface of the device [128]. Demonte Gonzalez et al. in [129] and Malekar in [130] considered non-linear FK forces. However, these studies rely on a regular wave, which is a strong and unrealistic assumption if a practical implementation is desired.

In a recent study published by Faedo et al. [127] an integrated framework to include the non-linear FK forces is proposed. Faedo et al. claim that **a)** *the proposed algorithm for non-linear FK forces is capable of recovering the exact analytical solution based solely on data* [127], and that **b)** *the proposed controller outperforms a benchmark control strategy in OWE literature, reactive control in this case, in terms of energy absorption (with an increase of up to 3 times in performance), while effectively incorporating state and input constraints,*

and more conservative requirements in terms of operational space (i.e., motion range), while requiring less reactive (bidirectional) power flow to achieve optimality [127].

Another non-linear term typically added to Cummins' equation is mooring forces [131, 132]. Not related to hydrodynamics specifically, but the addition of the PTO system's efficiency (discussed in Section 3.4.3) causes non-linearities in the OCP.

### 3.4.2 Cost function

As its name suggests, a proper energy-maximising WEC controller should aim to maximise the amount of energy transferred from the ocean waves to the grid for a broad range of sea states over a specific time period  $T$ . For instance, for one degree of freedom (1-DoF) WEC oscillating in heave, the cost function  $J$  to be used in Eq. (3.8) may be mathematically formulated as:

$$J(\underline{u}) = E_{abs} = - \int_t^{t+T} P_e(\tau) d\tau = - \int_t^{t+T} \Gamma(\tau) P_m(\tau) d\tau \quad (3.13)$$

where  $E_{abs}$  denotes the absorbed energy from the ocean waves,  $P_e$  denotes the electrical power delivered to the grid,  $P_m$  represents the instantaneous hydro-mechanical power absorbed by the PTO system,  $\Gamma(t)$  models the overall efficiency of the PTO system, and  $\tau$  is the variable of integration. With the instantaneous hydro-mechanical absorbed power given by:

$$\begin{aligned} P_m(t) &= F_{pto}(t) \dot{\zeta}(t) \\ &= u(t) v(t) \end{aligned} \quad (3.14)$$

where  $F_{pto}(t) = u(t)$  represents the PTO force (control input).

The cost function  $J(\underline{u})$  given in Eq. (3.13), even when departing from the traditional regulation or tracking control objectives encountered in standard optimal control strategies, may be recast as a standard quadratic problem (QP); see for example [133]. It has been reported, however, that the convexity of such a cost function (seeking to maximise the amount of absorbed energy) is not generally guaranteed [22, 70]. Therefore, as discussed in [70] the inclusion of additional terms to the cost function, which are essentially regularisation terms to assure convexity, is advocated.



Such regularisation terms can be found in most of the MPC studies reviewed to guarantee a convex OCP at each sampling period. Studies considering a term proportional to the squared of the control input  $\underline{u}^2$  include: [109, 132, 134–141]. Other studies additionally include a term proportional to the squared device displacement  $\zeta(t)^2$  [70, 140, 142, 143], whilst [107] and [133] add a term proportional to the control slew rate.

Finally, even with the inclusion of the above-discussed regulating terms into the cost function  $J(\underline{u})$ , the consideration of physical constraints in WEC displacement and PTO force may not guarantee the existence of optimal control solutions [22].

### 3.4.3 PTO system efficiency

The inclusion of the PTO system efficiency is crucial in optimising the energy absorbed from ocean waves [35, 55]. Nonetheless, until recent years, the great bulk of effort on WEC control design was devoted to maximising mechanical power rather than electrical power delivered to the grid [144]. In this manner, the hydrodynamic performance of the device is prioritised, frequently neglecting the dynamics and losses in the electromechanical conversion chain. In addition, active controllers entail a two-way energy flow from the ocean to the grid and vice versa. This bidirectional energy flow may result in energy loss owing to the dissipative processes intrinsic to energy exchange between the PTO system and the floater of the WEC [145].

Of the studies that incorporate the efficiency of the PTO system in the energy-maximising control strategy, virtually all of them (with few exceptions, see for instance [124, 144, 146]), modelled the efficiency of the whole PTO system using a single value (actually two, one value when the energy is flowing from the ocean waves to the grid, and another value in the other direction). So that the instantaneous electric power is expressed as follows:

$$P_e(t) = \Gamma(t) P_m(t), \quad \text{with} \quad \Gamma(t) = \begin{cases} \mu_{gen} & \text{if } P_m(t) \geq 0 \\ \mu_{mot} & \text{if } P_m(t) < 0 \end{cases} \quad (3.15)$$

where  $\mu_{gen}$  is the global efficiency of the PTO system when it delivers energy to the grid and  $\mu_{mot}$  is the global efficiency when the PTO system consumes power from the grid.

The model proposed in Eq. (3.15) brings another layer of difficulty to the energy-maximising controllers due to its discontinuity, i.e., non-differentiability between the two cases:  $P_m(t) \geq 0$  and  $P_m(t) < 0$ . Such a discontinuous function is undesirable in gradient-based optimisation approaches.

In the following paragraphs, studies incorporating the PTO system efficiency in the form of Eq. (3.15) (unless otherwise stated) in their energy-maximising control proposals are discussed.

Strager et al. in [147], one of the earliest documented studies, discusses the performance of a reactive controller for a single point absorber of a Wavestar WEC with a non-ideal efficiency for the PTO system under regular waves, and the performance of regular and irregular waves was studied in [148, 149]. For regular and irregular waves, partial reactive control was suggested in [150] as a causal suboptimal control approach for a heaving single-body wave energy converter, along with studies of the impact of the actuators' efficiency on the annual mean absorbed power.

In [151], similar to [110, 112], an MPC approach to maximise the energy extracted explicitly considers the PTO system's efficiency. Nguyen et al. in [113] experimentally evaluate a non-linear MPC strategy capable of taking into account PTO system efficiency for a scaled-down version of the well-known Wavestar device.

An interesting study presented by Sergiienko et al. in [144] compares four variations of efficiency-aware model-predictive controllers applied to a floating spherical WEC connected to a rotary generator. The control strategies studied in [144] are: **a)** pure maximisation of mechanical power, **b)** maximisation of mechanical power with a control penalty factor, **c)** maximisation of electrical power using a single value for the overall efficiency of the PTO system (as in Eq. (3.15)), and **d)** maximisation of electrical power using wave-to-wire model (i.e., full electromechanical system model).

Findings presented in [144] show that a controller whose cost function is based on mechanical power is not suitable for practical applications as it can yield negative average generated power. Similar results have been documented in [55, 70, 71, 124, 152]. In addition, [144] concludes that replacing the power take-off dynamics with a single efficiency coefficient for the whole energy conversion chain does not guarantee maximum electrical power generation.

Based on spectral methods, Mérigaud and Tona in [71] incorporate the non-ideal PTO system and use a modified hyperbolic tangent function to smooth the discontinuity present in Eq. (3.15). Bacelli et al. in [124], also working with spectral methods, modelled the energy delivered to the grid as the mechanical power *minus* the inherent losses of the PTO systems using efficiency curves. Efficiency curves can be a function of various parameters such as load factor, duration and frequency of use, or temperature [124]. A similar approach is taken in [153].





Finally, using another mathematical tool, rather than MPC and SPM/PSM, Faedo et al. present in [127] an energy-maximising controller, built upon so-called *moment-based theory*, which incorporates the non-ideal efficiency of the PTO system. [127] employs a discontinuous efficiency map for approximating the overall energy conversion chain in the PTO system, similar to Eq. (3.15). A *sigmoid* function is used to smooth the transition from one case  $P_m(t) \geq 0$  to the other  $P_m(t) < 0$ .

#### 3.4.4 Real-time capabilities

Though several energy-maximising control strategies for wave energy converters are described in the field literature, e.g., see the review papers [55, 92, 144], and some of them have been experimentally tested, e.g., [112, 113, 154], few of the proposed energy-maximising controllers can solve in real time the OCP that arises at each sampling time (or at least offer information about the time required to solve the OCP).

Consider, for instance, the solution presented by Tona et al. to the Wave Control Competition [155], assessed in simulation [110] and experimentally [112]. One of its key features is the inclusion of an equivalent discrete objective function in which the instantaneous mechanical power values are weighted across the prediction horizon, with the prime constraint that the optimal weightings are usually pre-calculated using an optimisation algorithm, such as the Nelder-Mead simplex algorithm based on repeated simulations of the nominal model utilised for the design over a range of sea states [112]. A similar approach is taken in [149].

Along the same line, the non-linear model predictive controller proposed in [131] does not focus on real-time applicability. Mériçaud and Tona published in [71] a power-maximising control strategy with the inclusion of an overall value for the efficiency of the PTO, where the proposed strategy "is concerned with the calculation of optimal control solutions in an 'off-line' fashion", as stated by the authors.

These proposed control strategies are susceptible to modelling errors and can not account for changes in the device response over time, rendering them "less robust".

Haider et al. in [156] described the implementation of a non-linear model predictive controller with a non-quadratic piece-wise discontinuous cost function, which is one of the few research addressing execution time and deployment of the control algorithm in real-time target machines [156, 157]. The proposed controller is deployed on Speedgoat Performance real-time target machine based on the non-linear optimisation solver ACADO toolkit for MATLAB/Simulink [158].

In a recent publication, Faedo et al. presented a non-linear moment-based optimal controller for wave energy converters that considers the PTO system's efficiency [159], demonstrating that the computational time required to solve the OCP at each sampling time is significantly lower than the limit time specified in the controller design (sampling time of 0.1 s).

---

## 3.5. Summary

This chapter reviews the most prominent studies in the ocean wave energy literature for control strategies for point absorbers WECs. We defined the main function of the primary controller, which is to determine the optimal behaviour for the PTO force to optimise the operation of the WEC for a wide range of sea states, maximising the absorbed energy while respecting the system constraints.

The conditions for an optimal unconstrained control law have been presented based on the frequency-domain version of Cummins' equation. These conditions are known as the *impedance-matching principle*. We discussed how, despite its simplicity, this finding provides a great understanding of the necessary conditions to maximise the amount of energy extracted from ocean waves, given a set of specified assumptions. It serves as the basis for several control strategies discussed in the literature.

By design, control techniques based on the impedance-matching principle are suboptimal. Their main advantage relies on their simplicity of low computational requirements, which makes this family of strategies desirable for practical application. However, the improper handling of system constraints has a negative impact on their performance.

Moving to more recent researches, we examined how the nature of the energy-maximising control problem lends itself to optimal control theory, where the control objective is, in essence, to maximise the absorbed energy from incoming ocean waves, subject to a set of physical constraints. We summarised the key concepts of the two most promising control strategies found in the ocean wave energy field within this category, namely *Model Predictive Control* and *Spectral/Pseudo-spectral control*.

Then, the discussion on MPC and SPM/PSM shifted to their shared core components, notably the hydrodynamic model for the device-ocean wave interaction, the cost function, the PTO system's efficiency, and their real-time capabilities.



We found that most of the research relies on a linear hydrodynamic formulation based on Cummins' equation to describe the motion of the WEC. As expansions to Cummins' equation, only a small number of studies include non-linear terms, mostly for restoring and viscous forces. And only a small number of studies have explored the non-linear contribution of the static and dynamic Froude–Krylov (FK) force.

Regarding the cost function, we found that most studies include additional terms into the cost function  $J(\underline{u})$  to guarantee its convexity. And as for the inclusion of the PTO system efficiency, we found that even though more studies are now including it within their control strategies, this specific issue is still an active research topic.

The last component we discussed is the real-time implementation capabilities. For this issue, we found that even though some of the proposed control strategies can effectively achieve real-time implementation, only preliminary (i.e., simulation-based) results are generally presented, and the issue of real-time control of converted energy in WEC systems is still an active topic of research.

Motivated by the discussion provided in this chapter and the specific issues found in the state-of-the-art WEC control, this research project has focused on the study of control strategies able to offer real-time implementation of energy-maximising non-linear control strategies for WECs, with a particular emphasis on point absorbers.



---

# Optimal Control for Wave Energy Converters: Contributions

” *The journey of a thousand miles begins  
with one step.*

- Lao Tzu -

4.1	Contributions overview. . . . .	52
-----	---------------------------------	----

---

## 4.1. Contributions overview

In this section, we have summarised the major contributions made by this research project, and in the following sections, we have included the Version of Record for each manuscript.

Based on the literature review discussed in the preceding chapter, one of the limitations of implementing Model Predictive Control in real-time is the computational cost of this control strategy due to the complexity of the optimal control problem. To offer an alternative approach to reduce the optimal control problem (OCP) size, we have proposed a Moving Window Blocking (MWB) technique to reduce the number of degrees of freedom, e.g., decision variables, using input parameterised solutions. This will reduce the time required for solving the OCP arising at each time step.

To evaluate the advantages of the moving window blocking approach, a Matlab simulation is conducted and compared with two other different control strategies: "standard" MPC, here referred to as Full-Degree of Freedom (F-DoF) MPC, and the Generalised Predictive Control (GPC) strategy.

In this study, we used a blocking approach where the control input is parameterised in blocks of size  $N_b$  having same value, e.g.  $u_k = u_{k+1} = \dots = u_{k+N_b-1}$  for the first block,  $u_{k+N_b} = u_{k+N_b+1} = \dots = u_{k+2N_b-1}$  for the second block, etc. In contrast to the usual Generalised Predictive Control (GPC) technique, in which the values for decision variables are "congested" at the beginning and held constant after a "control horizon", the MWB parameterisation allows the decision variables to be distributed throughout the prediction horizon. Figure 4.1 illustrates such a parameterisation.

Figure 4.1 shows the prediction of the control input, e.g., PTO force, for 10 s ahead with a sampling time of 100 ms. For this example, the number of decision variables for Full-Degrees of Freedom MPC is 100, and block size  $N_b = 5$ , resulting in a reduced number of 20 decision variables.

This distinctive feature, i.e., having decisions available distributed throughout the prediction horizon, makes the blocking approach appropriate for wave energy applications for the following reasons: first, the solution obtained from the original problem using full degrees of freedom, when constraints are taken into account, applied to the WEC system is constantly saturated due to the physical limitation of the actuator, as shown in Figure 4.1, and can therefore be accurately represented by blocks; and second, depending on the wave future values, it may be more important to have decisions available distributed throughout the prediction horizon and not just at the beginning of it, for instance when the wave reaches its



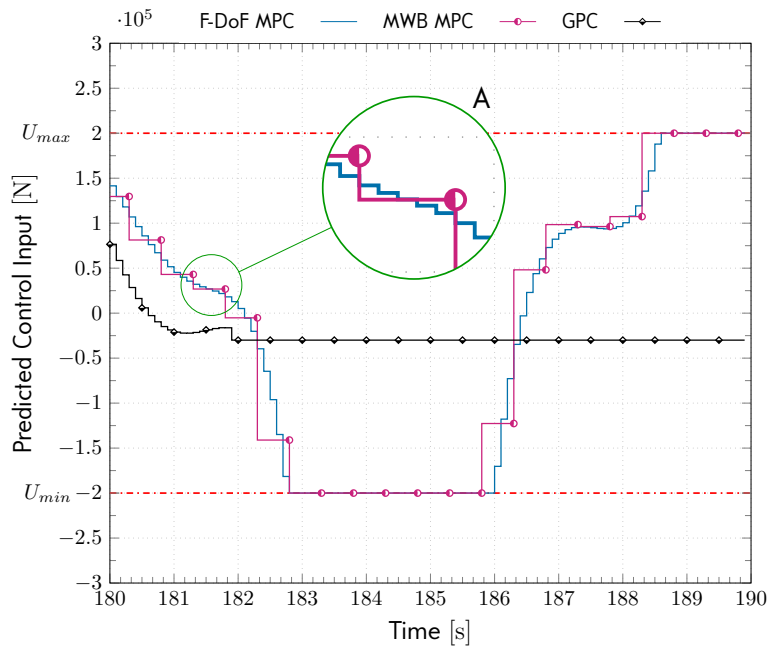


**Figure 4.1.:** Prediction of the control input, e.g., PTO force, for 10 s ahead with a sampling time of 100 ms. The total number of decision variables for Full-Degrees of Freedom MPC is 100, and block size  $N_b = 5$ , resulting in a reduced number of 20 decision variables.

crest and trough (maximum/minimum values).

A numerical simulation of a generic single device point absorber wave energy converter controlled by this approach demonstrates the advantages of this strategy. In comparison to the optimal solution provided by Full Degrees of Freedom MPC, MWB-MPC enables solutions that are up to 12.5 times faster and could absorb as much as 98.8 % of the energy provided by F-DoF MPC.

Lastly, it should be noted that the main contribution of the MWB approach is not just the reduction in computation time required to solve the OCP at each sampling time but also the ability to maintain nearly the same performance as F-DoF MPC via shifting input parameterisation, a feature that GPC does not provide.

The control strategy discussed in *Manuscript 1* is based on the maximisation of mechanical power rather than the electrical power delivered to the grid. However, as we have learnt from the literature review, optimal controllers based exclusively on the maximisation of mechanical energy are deceptive because they do not take into account the efficiency of the PTO system, a crucial factor to consider in active controllers owing to two-way energy flow from the ocean to the grid and vice versa. Recognising this limitation, in *Manuscript 2*, we present a controller capable of incorporating the PTO system's efficiency as a single number for the whole system.

Incorporating the PTO system's efficiency results in a non-linear and non-convex optimum control problem, even though the hydrodynamic model employed to describe fluid-structure

interaction is linear. To the best of our knowledge, none of the published solutions can solve the entire optimal control problem in real-time. To fill this need, *Manuscript 2* presents a non-linear model predictive control (NMPC) approach based on the real-time iteration (RTI) scheme. The proposed controller incorporates the PTO system's efficiency when solving the optimal control problem at each time step, in a control law that maximises the energy recovered from the ocean waves.

The controller proposed in *Manuscript 2* differentiates from others in that it does not require offline computations to solve the non-linear programming problem that arises from incorporating the PTO's efficiency into the optimal control problem. In addition, this controller technique can adjust to changing sea conditions to provide the best possible solution.

Numerical simulations of the proposed RTI-NMPC controller for a single point absorber of a Wavestar-scale model wave energy converter with a non-ideal PTO system efficiency indicate that the RTI-NMPC approach can significantly improve wave energy converter performance. Figure 4.2 shows the energy absorbed by the WEC when controlled by a resistive controller, linear MPC without the PTO efficiency and the proposed RTI-NMPC after a simulation time of around one hundred times the peak period, i.e.,  $100 \times T_p$ . The proposed controller harvests roughly two and a half times the amount of energy extracted by a resistive controller and nearly three times that of linear MPC while keeping the amount of power "borrowed" from the grid to a bare minimum.

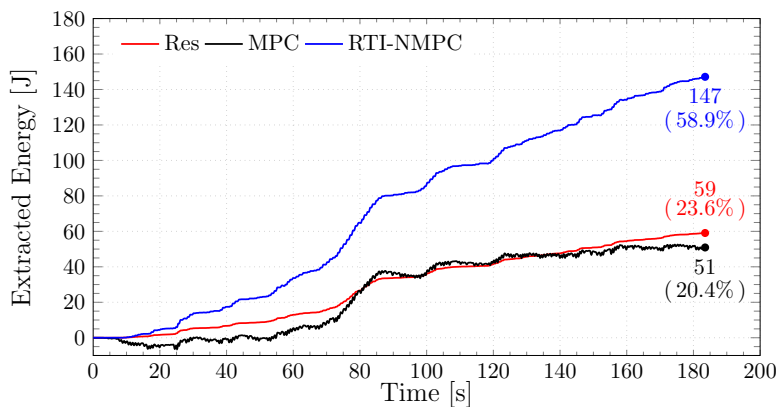


**Figure 4.2.:** Energy absorbed by the Wavestar model for sea state SS6 with different control strategies. In blue RTI-NMPC, in black linear MPC without the PTO efficiency, and in red resistive control. The value in parenthesis represents the percentage of energy absorbed concerning the maximum theoretical amount, 249.5 J

An interesting observation we can make based on the results discussed in *Manuscript 2* is that the standard MPC, despite attempting to provide an optimal solution at each sample time, the overall optimisation procedure becomes meaningless at the current time step due to the absence of the PTO system's efficiency in the OCP, which results in significant differences in the predictions of the generated energy and thus an ill-posed optimisation. This ultimately





leads to suboptimal control law, or even a net negative absorbed energy depending on the sea state and tuning parameters employed in the simulation (see Table 6: Energy absorbed and mean power for resistive control, MPC, and RTI-NMPC for each sea state from *Manuscript 2*).

Related to the preceding point, another interesting finding of this work is that standard MPC cannot harvest more energy than a simple resistive controller in certain instances, which makes it a very interesting feat that, apparently, many previous studies have otherwise ignored. This is also reflected in the reactive power that MPC "consumes" at specific points during the simulation, as opposed to the resistive controller, which draws no power from the grid. Therefore, we conclude that standard MPC is not worth the effort for this particular application, especially considering the extra costs when designing/buying a PTO system that can offer a bidirectional energy flow.

A second contribution delivered in *Manuscript 2* is the derivation of a computationally efficient algorithm  $O(N^2)$  for "only-output" cost functions, which offers significant time savings for computing the Hessian for large prediction horizons. Table 4.1 (Table 7 in *Manuscript 2*) shows how the time saved from computing the Hessian using the algorithm  $O(N^2)$  increases as the number of steps ahead in the prediction horizon increases. Even while we recognise that the time required to calculate the Hessian is not the only factor to consider when attempting to solve an OCP, it is, without question, the most crucial.

**Table 4.1.:** Average time for computing the Hessian  $E$  using algorithm  $O(N^2)$  and standard matrix-vector operations.

Prediction horizon $N_p$ [Steps ahead]	Algorithm $O(N^2)$ Avg. Time [ms]	Std matrix-vector operations Avg. Time [ms]	Gain [-]
100	$0.318 \pm 0.039$	$0.547 \pm 0.141$	1.720
200	$1.236 \pm 0.126$	$3.766 \pm 0.245$	3.047
300	$2.848 \pm 0.212$	$10.179 \pm 0.583$	3.574
365	$4.500 \pm 0.441$	$17.892 \pm 1.040$	3.976
400	$5.426 \pm 0.274$	$22.795 \pm 0.497$	4.201
500	$8.803 \pm 0.331$	$42.671 \pm 0.789$	4.847

The computational time savings achieved by implementing the  $O(N^2)$  condensing algorithm could allow for the use of larger prediction horizons and/or faster sample rates, as long as more precise prediction algorithms are available.

To examine the real-time capabilities of the proposed controller, we used two prediction horizons for each sea state, corresponding to one peak period ( $1 \times T_p$ ) and two peak periods ( $2 \times T_p$ ) of the dominant wave. For instance, that would be 185 and 365 steps ahead for sea state SS6 with a  $T_p = 1.836$  s using a sampling time of 10 ms. And we found that except for the case of a prediction horizon of 365 steps ahead, all other case studies could be implemented in real-time, i.e., the overall time required to solve the OCP at each time step is less than the 10 ms used as sampling time. For the case of 365 steps ahead, the implementation would take around 11.840 ms in the worst-case scenario. In *Manuscript 2*, we also considered potential solutions if such a large prediction horizon were necessary. In summary, numerical simulations suggest that the proposed algorithm would allow faster computations required to achieve real-time performance.

The work presented in *Manuscript 3* builds on the proposed RTI-NMPC strategy with a couple of additional feats. A key extension is that the assumptions about the incident wave moment at the current time step and for the prediction horizon window are removed.

By removing the assumption of having the exact value for the excitation force (or moment), this value has to be estimated. To that end, wave excitation force (or moment) is usually estimated via measuring other quantities, such as the position or velocity of the float.

The approach followed in *Manuscript 3* is based on a Kalman filter coupled with a random-walk model for the wave excitation moment. The main features of this solution are (1) only standard WEC measurements (position, velocity), (2) there is no significant lag compared to "true" values, and (3) no (implicit) unrealistic assumption about the time-invariant nature of the sea state is made; therefore it can be implemented in any sea state.

In regards to the prediction of the wave excitation force, and based on the literature review, the work presented in *Manuscript 3* used a linear autoregressive (AR) model. The AR model implies that the wave excitation force at any given time  $t_k$  is linearly dependent on its past values via a set of coefficients.

In our study of AR models, we found widely disparate claims of the model order necessary for wave excitation force prediction, ranging from 10 to 200 lag terms.

Therefore, we used the following procedure to determine the appropriate order of fit for the AR model. First, the WEC system was simulated without using a control law (simulation was performed in WEC-Sim code) to extract the wave excitation force from the simulation. We then used this information to conduct a partial autocorrelation analysis of the wave excitation



force signal. We found that a 18-lag model was sufficient to predict the wave excitation force. In addition, to maintain the accuracy of the AR model, it is updated every second during the simulation, regardless of the selected sea state.

A further important novelty is that the simulations are performed using a time-domain hydrodynamics model (WEC-Sim). WEC-Sim is a time-domain open-source code that solves the system dynamics of WECs consisting of rigid bodies, PTO systems, mooring systems, and control systems. WEC-Sim calculates the dynamic response of the WEC device by solving the WEC's equation of motion for each rigid body about its centre of gravity  $C_g$  in the 6 degrees of freedom based on Cummins' equation.

Regarding the overall performance of the proposed controller, once again, the simulation results presented in *Manuscript 3* show that RTI-NMPC outperforms a resistive controller, harvesting roughly 1.75 times the amount of energy extracted by a resistive controller while keeping the amount of power "borrowed" from the grid to a bare minimum.

To summarise, numerical simulations in *Manuscript 2* and *Manuscript 3* suggest that the proposed control strategy, i.e., non-linear model predictive control based on the real-time iteration approach, could be employed to significantly increase the absorbed energy from ocean waves, thereby lowering the levelised cost of electricity.

Finally, the code utilised in the simulations across the three publications is freely accessible via a Code Ocean capsule or GitHub repository to encourage peer collaboration and openness.



---

## Summary of Findings and future work

” *Anyone who stops learning is old, whether at twenty or eighty. Anyone who keeps learning stays young. The greatest thing in life is to keep your mind young.*

– Henry Ford –

5.1	Summary of Findings . . . . .	60
5.2	Future work . . . . .	63

---

## 5.1. Summary of Findings

The idea of extracting energy from ocean waves and turning it into electricity, even when this is appealing, is not novel. In 1974, Professor Stephen Salter of the University of Edinburgh conceived the concept of "ducks": house-sized buoys moored to the sea floor that would convert the swell into rotational motion to drive generators.

Five decades have passed since this milestone in the ocean wave energy area. Yet, we still do not have a commercial-scale wave energy converter regularly delivering power to the grid. It is no doubt that wave energy converters are still in the early stages of technological development compared to other renewable energy alternatives that are more mature, such as wind or solar energy.

Obtaining cost competitiveness is the major challenge facing ocean wave energy technology. Because they must be engineered to endure large wave loads and severe sea states while still extracting energy at a reasonable price. Reducing the structural cost of WECs and improving energy capture are two paths to reduce wave energy's levelised cost of energy (LCOE), hence enhancing its attractiveness as a major renewable energy source. This dissertation aims to contribute to the second path, i.e., to improve energy capture using an advanced control strategy tailored for WEC applications to optimise their power performance.

Before implementing an advanced control strategy able to operate in real-time, the first contribution of this dissertation, presented in *Manuscript 1*, provides an alternative approach for reducing the size of the optimal control problem. Using a Moving Window Blocking (MWB) technique, we can reduce the number of decision variables, thereby reducing the time required to solve the OCP arising at each time step. Numerical simulations of a generic wave energy converter controlled by a linear model predictive control coupled with the MWB technique demonstrate the advantages of this approach. Compared to the optimal solution provided by Full Degrees of Freedom MPC, MWB-MPC enables solutions that are up to 12.5 times faster and could absorb as much as 98.8% of the energy provided by F-DoF MPC.

Moving to advanced energy-maximising control strategies, we learnt from the literature review that optimal controllers based exclusively on the maximisation of mechanical energy are misleading because they do not take into account the efficiency of the PTO system, a crucial factor to consider in active controllers owing to two-way energy flow from the ocean to the grid and vice versa. As a contribution to this gap, we present in *Manuscript 2* a controller capable of incorporating the PTO system's efficiency into the OCP.



*Manuscript 2* introduces a non-linear model predictive control (NMPC) approach based on the real-time iteration (RTI) scheme to maximise the energy recovered from the ocean waves. The proposed controller incorporates the PTO system's efficiency when solving the optimal control problem at each time step. This controller differentiates from others in that it does not require offline computations to solve the non-linear programming problem that arises from incorporating the PTO's efficiency into the optimal control problem. In addition, this controller technique can adjust to changing sea conditions to provide the best possible solution.

Numerical simulations of the proposed RTI-NMPC controller indicate that the RTI-NMPC approach can significantly improve wave energy converter performance. The proposed controller outperformed the other two controllers used for comparison, i.e., a resistive controller and linear MPC while keeping the amount of power "borrowed" from the grid to a bare minimum.

Based on the results discussed in *Manuscript 2*, we can make an interesting observation: even though the standard MPC tries to provide an optimal solution at each sample time, the overall optimisation problem becomes meaningless at the current time step because the efficiency of the PTO system is not included in the OCP. Consequently, the predictions of the extracted energy vary significantly from one time step to the next, resulting in an ill-posed optimisation problem. This ultimately leads to suboptimal control law, or even a net negative absorbed energy depending on the sea state and tuning parameters employed in the simulation.

Another interesting finding of this work is that standard MPC cannot harvest more energy than a simple resistive controller in certain instances, making it a very interesting feat that apparently many previous studies have overlooked. This is also reflected in the reactive power that MPC "consumes" at specific points during the simulation, as opposed to the resistive controller, which draws no power from the grid. Therefore, we conclude that standard MPC is not worth the effort for this particular application, especially considering the extra costs when designing/buying a PTO system that can offer a bidirectional energy flow.

A second contribution delivered in *Manuscript 2* is the derivation of a computationally efficient algorithm  $O(N^2)$  for "only-output" cost functions, which offers significant time savings for computing the hessian for large prediction horizons. The computational time savings achieved by implementing the  $O(N^2)$  condensing algorithm could allow for the use of larger prediction horizons and/or faster sample rates, as long as more precise prediction algorithms are available.

The work presented in *Manuscript 3* builds on the proposed RTI-NMPC strategy with several other feats. An important extension is the elimination of assumptions about the knowledge of the wave excitation force at the current time step and for the prediction horizon window. Using a Kalman filter paired with a random-walk model, we are able to estimate the wave excitation force. A linear autoregressive (AR) model is employed to forecast the wave excitation force based on the literature review.

One of the most noteworthy findings from our study of AR models in wave energy literature is the widely disparate claims of the model order required for wave excitation force prediction, which ranges from 10 to 200 lag terms. Therefore, we provide a procedure based on partial auto-correlation analysis to determine the AR model's minimum order to forecast the wave excitation force.

In conclusion, numerical simulations in *Manuscript 2* and *Manuscript 3* suggest that the proposed control strategy, i.e., non-linear model predictive control based on the real-time iteration approach, could be employed to increase the absorbed energy from ocean waves significantly, thereby decreasing the levelised cost of electricity.





---

## 5.2. Future work

Throughout this project, we have learnt that improving the energy capture of wave energy converters is a very complex, non-traditional and multifaceted problem. It depends not just on the control strategy deployed but also on factors such as the physical design of the WEC and ocean conditions. We also acknowledge that this study is in no way conclusive, hence in the following paragraphs, we outline a few potential future research paths that we believe are worth exploring:

- a) Although the theoretical background of the proposed control strategy, i.e., Non-linear model predictive control based on real-time iteration, supports the implementation of this strategy for non-linear models, in this work, the non-linearity is derived from the incorporation of the PTO system's efficiency. In contrast, the hydrodynamic model used to describe fluid-structure interaction is based on linear wave theory. Hence, it would be interesting to evaluate the controller's performance using non-linear models.
- b) Due to the lack of experimental resources for this study, the optimum controller proposed in *Manuscripts 2* and *3* has only been evaluated using Matlab and wecSim-based numerical simulations. It would be fascinating to examine the performance of a scaled-down physical model in a wave tank.
- c) In this work, the robustness of the proposed controller was not investigated, and the performance depends on the accuracy of the model used for the predictions. In addition, the combination of learning methods with Model Predictive Control (MPC) has recently received considerable attention in the scientific literature. Therefore, it would be interesting to include learning techniques in the loop so that the model may be continuously updated, reducing MPC schemes' dependency on accurate models. A good starting point is the paper recently published by Gros and Zanon [160].
- d) There is no theoretical guarantee that a global solution will be found at each sampling period, which is one of the limitations of the work reported in this dissertation. Attempting to specify the requirements for the global optimum is thus a viable path for future research.
- e) Finally, the work described in this dissertation focuses on single point-absorbers wave energy converters. However, according to the wave energy literature, to further reduce the levelised cost of energy, it is necessary to extend the design of

wave energy converters to arrays of devices, also known as WEC farms. One of the challenges associated with WEC farms is that the devices comprising the WEC array are often deployed nearby, mostly due to practical reasons [161]. However, this design has several disadvantages. The interaction between the devices is very complex since a wave energy converter is at the same time a wave generator as it heaves up and down; hence the wave generated by one buoy will affect the capture efficiency of the follow-up buoys. The interaction between the buoys demands an accurate and control-oriented dynamic model. Therefore, based on the drawn conclusions and identified limitations of the proposed methods, a potential research direction is designing a distributed control system for multiple devices considering the hydrodynamic interaction between the devices.



## References

- [1] IEA (International Energy Agency). *Net Zero by 2050: A roadmap for the global energy system*. Special Report. 4<sup>th</sup> revision. France: International Energy Agency, Oct. 2021, pp. 1–224 (cit. on p. 2).
- [2] IEA (International Energy Agency). *World Energy Outlook 2021*. Technical Report. France: International Energy Agency, Dec. 2021, pp. 1–386 (cit. on p. 2).
- [3] IRENA (International Renewable Energy Agency). *Global Renewables Outlook: Energy transformation 2050*. Technical Report. Abu Dhabi: International Renewable Energy Agency, Apr. 2020, pp. 1–291 (cit. on p. 2).
- [4] B. G. Reguero, I. J. Losada and F. J. Méndez. ‘A global wave power resource and its seasonal, interannual and long-term variability’. In: *Applied Energy* 148 (June 2015), pp. 366–380 (cit. on p. 2).
- [5] Gunnar Mørk, Stephen Barstow, Alina Kabuth and M. Teresa Pontes. ‘Assessing the global wave energy potential’. In: *Proceedings of the International Conference on Offshore Mechanics and Arctic Engineering - OMAE*. Vol. 3. ASME, Dec. 2010, pp. 447–454 (cit. on p. 2).
- [6] Kester Gunn and Clym Stock-Williams. ‘Quantifying the global wave power resource’. In: *Renewable Energy* 44 (Aug. 2012), pp. 296–304 (cit. on p. 2).
- [7] V. Sanil Kumar, K. K. Dubhashi, T. M. Balakrishnan Nair and Jai Singh. ‘Wave power potential at a few shallow-water locations around Indian coast’. In: *Current Science* 104.9 (2013), pp. 1219–1223 (cit. on p. 2).

- [8] Iraide López, Jon Andreu, Salvador Ceballos, Iñigo Martínez De Alegría and Iñigo Kortabarria. 'Review of wave energy technologies and the necessary power-equipment'. In: *Renewable and Sustainable Energy Reviews* 27 (Nov. 2013), pp. 413–434 (cit. on pp. 2, 8, 9, 27).
- [9] Olivia Langhamer, Kalle Haikonen and Jan Sundberg. 'Wave power—Sustainable energy or environmentally costly? A review with special emphasis on linear wave energy converters'. In: *Renewable and Sustainable Energy Reviews* 14 (4 May 2010), pp. 1329–1335 (cit. on p. 2).
- [10] Andrea E. Copping, Lenaïg G. Hemery, Dorian M. Overhus et al. 'Potential Environmental Effects of Marine Renewable Energy Development—The State of the Science'. In: *Journal of Marine Science and Engineering* 2020, Vol. 8, Page 879 8 (11 Nov. 2020), p. 879 (cit. on p. 2).
- [11] Francesco Fusco, Gary Nolan and John V. Ringwood. 'Variability reduction through optimal combination of wind/wave resources – An Irish case study'. In: *Energy* 35 (1 Jan. 2010), pp. 314–325 (cit. on p. 2).
- [12] Christina Kalogeri, George Galanis, Christos Spyrou et al. 'Assessing the European offshore wind and wave energy resource for combined exploitation'. In: *Renewable Energy* 101 (Feb. 2017), pp. 244–264 (cit. on p. 2).
- [13] Carlos V.C. Weiss, Raúl Guanche, Bárbara Ondiviela, Omar F. Castellanos and José Juanes. 'Marine renewable energy potential: A global perspective for offshore wind and wave exploitation'. In: *Energy Conversion and Management* 177 (Dec. 2018), pp. 43–54 (cit. on p. 2).
- [14] Sarah Gallagher, Roxana Tiron, Eoin Whelan et al. 'The nearshore wind and wave energy potential of Ireland: A high resolution assessment of availability and accessibility'. In: *Renewable Energy* 88 (Apr. 2016), pp. 494–516 (cit. on p. 2).
- [15] Joakim Widén, Nicole Carpman, Valeria Castellucci et al. 'Variability assessment and forecasting of renewables: A review for solar, wind, wave and tidal resources'. In: *Renewable and Sustainable Energy Reviews* 44 (Apr. 2015), pp. 356–375 (cit. on p. 2).
- [16] C. Pérez-Collazo, D. Greaves and G. Iglesias. 'A review of combined wave and offshore wind energy'. In: *Renewable and Sustainable Energy Reviews* 42 (Feb. 2015), pp. 141–153 (cit. on p. 2).
- [17] Wataru Sasaki. 'Predictability of global offshore wind and wave power'. In: *International Journal of Marine Energy* 17 (Apr. 2017), pp. 98–109 (cit. on p. 2).



- [18] Julia Fernandez, Jens Peter and Hans Christian. *Predictability and Variability of Wave and Wind wave and wind forecasting and diversified energy systems in the Danish North Sea*. DCE Technical reports 156. Aalborg Universitet, 2013, pp. 1–197 (cit. on p. 2).
- [19] IRENA (International Renewable Energy Agency). *Innovation Outlook: Ocean Energy Technologies*. 2020, pp. 1–112 (cit. on pp. 2, 8, 16).
- [20] Kaan Koca, Andreas Kortenhuis, Hocine Oumeraci, Barbara Zanuttigh and Elisa Angelelli. 'Recent Advances in the Development of Wave Energy Converters'. In: *The 10th European Wave and Tidal Energy Conference, Aalborg, Denmark September (2013)*, p. 7 (cit. on pp. 3, 9, 12).
- [21] Daniel Gallutia, Majid Tahmasbi Fard, Mariantonieta Gutierrez Soto and JiangBiao He. 'Recent advances in wave energy conversion systems: From wave theory to devices and control strategies'. In: *Ocean Engineering* 252 (May 2022), p. 111105 (cit. on pp. 3, 35, 38).
- [22] Bingyong Guo and John V. Ringwood. 'A review of wave energy technology from a research and commercial perspective'. In: *IET Renewable Power Generation* (Oct. 2021) (cit. on pp. 3, 18–20, 44, 45).
- [23] Tunde Aderinto and Hua Li. 'Ocean Wave energy converters: Status and challenges'. In: *Energies* 11 (2018) (cit. on pp. 3, 8, 11).
- [24] Arqam Ilyas, Syed A.R. Kashif, Muhammad A. Saqib and Muhammad M. Asad. 'Wave electrical energy systems: Implementation, challenges and environmental issues'. In: *Renewable and Sustainable Energy Reviews* 40 (Dec. 2014), pp. 260–268 (cit. on pp. 3, 10).
- [25] Wanan Sheng. 'Wave energy conversion and hydrodynamics modelling technologies: A review'. In: *Renewable and Sustainable Energy Reviews* (2019), pp. 482–498 (cit. on pp. 4, 8).
- [26] Alain Clément, Pat McCullen, António Falcão et al. *Wave energy in Europe: Current status and perspectives*. Oct. 2002 (cit. on p. 8).
- [27] Bingyong Guo, Ron J. Patton, Siya Jin and Jianglin Lan. 'Numerical and experimental studies of excitation force approximation for wave energy conversion'. In: *Renewable Energy* 125 (Sept. 2018), pp. 877–889 (cit. on p. 8).
- [28] Ligu Wang, Jan Isberg and Elisabetta Tedeschi. 'Review of control strategies for wave energy conversion systems and their validation: the wave-to-wire approach'. In: *Renewable and Sustainable Energy Reviews* 81. June 2017 (2018), pp. 366–379 (cit. on pp. 8, 14).

- [29] António F.de O. Falcão. 'Wave energy utilization: A review of the technologies'. In: *Renewable and Sustainable Energy Reviews* 14.3 (2010), pp. 899–918 (cit. on pp. 8, 10, 11, 25, 26, 38).
- [30] B. Drew, A. R. Plummer and M. N. Sahinkaya. 'A review of wave energy converter technology'. In: *Proceedings of the Institution of Mechanical Engineers, Part A: Journal of Power and Energy* 223.8 (2009), pp. 887–902 (cit. on pp. 8–10, 26, 27, 29, 37, 38).
- [31] Balazs Czech and Pavol Bauer. 'Wave energy converter concepts : Design challenges and classification'. In: *IEEE Industrial Electronics Magazine* 6 (2 2012), pp. 4–16 (cit. on pp. 8, 10).
- [32] Rico Hjern Hansen. 'Design and Control of the PowerTake-Off System for a Wave Energy Converter with Multiple Absorbers'. PhD thesis. Aalborg University, 2013 (cit. on pp. 9, 11, 14).
- [33] Omar Farrok, Koushik Ahmed, Abdirazak Dahir Tahlil et al. 'Electrical power generation from the oceanic wave for sustainable advancement in renewable energy technologies'. In: *Sustainability (Switzerland)* 12 (6 Mar. 2020) (cit. on p. 10).
- [34] Rico H. Hansen, Morten M. Kramer and Enrique Vidal. 'Discrete displacement hydraulic power take-off system for the wavestar wave energy converter'. In: *Energies* 6.8 (Aug. 2013), pp. 4001–4044 (cit. on p. 12).
- [35] Arthur Pecher and Jens Peter Kofoed. *Handbook of Ocean Wave Energy*. 2017 (cit. on pp. 12, 24–29, 34, 36–39, 45).
- [36] Tom S Garrison. *Oceanography: an invitation to marine science*. Cengage Learning, 2012 (cit. on p. 12).
- [37] Nicolás Faedo. 'Optimal control and model reduction for wave energy systems: A moment-based approach'. 2020, p. 328 (cit. on pp. 13, 24, 34, 38, 40, 42).
- [38] Rico H. Hansen and Morten M. Kramer. 'Modelling and control of the wavestar prototype'. In: *9th European Wave and Tidal Energy Conference (EWTEC)*. Southampton, UK, 2011, pp. 1–10 (cit. on p. 14).
- [39] Paul Gieske. 'Model Predictive Control of a Wave Energy Converter: Archimedes Wave Swing'. PhD thesis. Delft University of Technology, 2007, p. 101 (cit. on pp. 14, 15, 42).
- [40] Daniel R Herber and James T Allison. 'Wave energy extraction maximization in irregular ocean waves using pseudospectral methods'. In: *Proceedings of the ASME Design Engineering Technical Conference*. Vol. 3 A. Portland, Oregon, USA, 2013 (cit. on pp. 15, 43).



- [41] Klaus Hasselmann, T. Barnett, E. Bouws et al. *Measurements of wind-wave growth and swell decay during the Joint North Sea Wave Project (JONSWAP) Wind Work and Radiative Internal Wave Flux in a Hybrid Slab Model View project Ocean Dynamics book View project*. Deutsches Hydrographisches Institut, 1973 (cit. on p. 15).
- [42] Johannes Falnes. *Ocean Waves and Oscillating Systems: Linear Interactions Including Wave-Energy Extraction*. Cambridge University Press, 2002, pp. 1–287 (cit. on pp. 15, 19, 22, 34, 35, 38).
- [43] Giuseppe Giorgi, Markel Penalba and John V Ringwood. ‘Nonlinear Hydrodynamic Models for Heaving Buoy Wave Energy Converters’. In: *Proceedings of the 3rd Asian Wave and Tidal Energy Conference*. 2016, pp. 144–153 (cit. on pp. 18, 20, 23, 24).
- [44] Giuseppe Giorgi and John V. Ringwood. ‘Nonlinear Froude-Krylov and viscous drag representations for wave energy converters in the computation/fidelity continuum’. In: *Ocean Engineering* 141 (Sept. 2017), pp. 164–175 (cit. on p. 18).
- [45] Christian Windt, Josh Davidson and John V Ringwood. ‘High-fidelity numerical modelling of ocean wave energy systems: A review of computational fluid dynamics-based numerical wave tanks’. In: *Renewable and Sustainable Energy Reviews* 93 (2018), pp. 610–630 (cit. on p. 19).
- [46] M Folley. *Numerical Modelling of Wave Energy Converters: State-of-the-Art Techniques for Single Devices and Arrays*. Ed. by Matt Folley. Elsevier Science, 2016 (cit. on p. 19).
- [47] Inc. WAMIT. *Wamit, Inc.* (Cit. on p. 19).
- [48] Markel Penalba, José-Antonio Cortajarena and John Ringwood. ‘Validating a Wave-to-Wire Model for a Wave Energy Converter—Part II: The Electrical System’. In: *Energies* 10.7 (2017), p. 1002 (cit. on p. 19).
- [49] ANSYS Aqwa. *ANSYS Aqwa* (cit. on p. 19).
- [50] Markel Penalba, Nathan P Sell, Andy J Hillis and John V Ringwood. ‘Validating a wave-to-wire model for a wave energy converter-part I: The hydraulic transmission system’. In: *Energies* 10.7 (2017) (cit. on p. 19).
- [51] Alexis Merigaud, Jean-Christophe Gilloteaux and John V Ringwood. ‘A Nonlinear Extension for Linear Boundary Element Methods in Wave Energy Device Modelling’. In: *Proceedings of the ASME 2012 31st International Conference on Ocean, Offshore and Arctic Engineering*. 2013 (cit. on p. 20).
- [52] Danial Golbaz, Rojin Asadi, Erfan Amini et al. ‘Ocean Wave Energy Converters Optimization: A Comprehensive Review on Research Directions’. In: (May 2021) (cit. on p. 21).

- [53] W.E. Cummins. *The impulse response fitting and ship motions*. Tech. rep. Hamburg: Institut fuer Schiffbau der Universitaet, Hamburg, 1962, p. 20 (cit. on p. 22).
- [54] Markel Peñalba Retes, Giuseppe Giorgi and John V Ringwood. 'A Review of Non-Linear Approaches for Wave Energy Converter Modelling'. In: *The 11th European Wave and Tidal Energy Conference*. 2015, pp. 1–10 (cit. on p. 22).
- [55] John V. Ringwood, Giorgio Bacelli and Francesco Fusco. 'Energy-maximizing control of wave-energy converters: The development of control system technology to optimize their operation'. In: *IEEE Control Systems* 34.5 (2014), pp. 30–55 (cit. on pp. 22, 34, 36–38, 45–47).
- [56] Z Yu and J Falnes. 'State-space modelling of a vertical cylinder in heave'. In: *Applied Ocean Research* 17.5 (1995), pp. 265–275 (cit. on p. 22).
- [57] David I.M. Forehand, Aristides E. Kiprakis, Anup J. Nambiar and A. Robin Wallace. 'A fully coupled wave-to-wire model of an array of wave energy converters'. In: *IEEE Transactions on Sustainable Energy* 7.1 (Jan. 2016), pp. 118–128 (cit. on p. 23).
- [58] Giuseppe Giorgi. 'Nonlinear hydrodynamic modelling of wave energy converters under controlled conditions'. PhD thesis. Maynooth University, 2018 (cit. on p. 24).
- [59] Dezhi Ning and Boyin Ding. *Modelling and Optimization of Wave Energy Converters*. CRC Press, 2022 (cit. on p. 25).
- [60] S. Raghunathan. 'The wells air turbine for wave energy conversion'. In: *Progress in Aerospace Sciences* 31.4 (Jan. 1995), pp. 335–386 (cit. on p. 27).
- [61] Diana Bull, D. Scott Jenne, Christopher S. Smith, Andrea E. Copping and Guild Copeland. 'Levelized cost of energy for a Backward Bent Duct Buoy'. In: *International Journal of Marine Energy* 16 (Dec. 2016), pp. 220–234 (cit. on p. 32).
- [62] Grace Chang, Craig A. Jones, Jesse D. Roberts and Vincent S. Neary. 'A comprehensive evaluation of factors affecting the levelized cost of wave energy conversion projects'. In: *Renewable Energy* 127 (Nov. 2018), pp. 344–354 (cit. on p. 32).
- [63] Vincent S Neary, Michael Lawson, Mirko Previsic et al. 'Methodology for Design and Economic Analysis of Marine Energy Conversion (MEC) Technologies'. In: *Marine Energy Technology Symposium* (2014) (cit. on p. 32).
- [64] J. Cordonnier, F. Gorintin, A. De Cagny, A. H. Clément and A. Babarit. 'SEAREV: Case study of the development of a wave energy converter'. In: *Renewable Energy* 80 (2015), pp. 40–52 (cit. on p. 32).
- [65] K. BUDAR and J. FALNES. 'A resonant point absorber of ocean-wave power'. In: *Nature* 256.5517 (Aug. 1975), pp. 478–479 (cit. on pp. 34, 38).





- [66] K Budal and J Falnes. 'Optimum operation of improved wave-power converter'. In: *Mar. Sci. Commun.:(United States)* 3.2 (1977) (cit. on p. 34).
- [67] K Budal and J Falnes. 'Interacting point absorbers with controlled motion'. In: Academic Press, 1980, pp. 381–399 (cit. on p. 34).
- [68] D. V. Evans. 'A theory for wave power absorption by oscillating bodies'. In: *Journal of Fluid Mechanics* 77.1 (1976), pp. 1–25 (cit. on p. 34).
- [69] J. C. (Jan Corné) Olivier. *Electric circuits : a primer*. eng. Boston: Artech House, 2018 (cit. on p. 35).
- [70] Guang Li and Michael R. Belmont. 'Model predictive control of sea wave energy converters - Part I: A convex approach for the case of a single device'. In: *Renewable Energy* 69 (2014), pp. 453–463 (cit. on pp. 36, 42, 44–46).
- [71] Alexis Mérigaud and Paolino Tona. 'Spectral control of wave energy converters with non-ideal power take-off systems'. In: *Journal of Marine Science and Engineering* 8.11 (Oct. 2020), pp. 1–15 (cit. on pp. 36, 46, 47).
- [72] Aurélien. Babarit, Gaëlle Duclos and Alain H. Clement. 'Comparison of latching control strategies for a heaving wave energy device in random sea'. In: *Applied Ocean Research* 26.5 (July 2004), pp. 227–238 (cit. on pp. 37, 38).
- [73] Aurélien. Babarit and Alain H. Clement. 'Optimal latching control of a wave energy device in regular and irregular waves'. In: *Applied Ocean Research* 11.3 (2006), pp. 77–91 (cit. on pp. 37, 38).
- [74] Aurélien Babarit, Michel Guglielmi and Alain H. Clément. 'Declutching control of a wave energy converter'. In: *Ocean Engineering* 36.12-13 (Sept. 2009), pp. 1015–1024 (cit. on pp. 37, 39).
- [75] Ryan G. Coe, Giorgio Bacelli, David G. Wilson et al. 'A comparison of control strategies for wave energy converters'. In: *International Journal of Marine Energy* 20.August 2011 (2017), pp. 45–63 (cit. on p. 37).
- [76] Giorgio Bacelli, Ryan Geoffrey Coe, David G. Wilson et al. *A comparison of WEC control strategies*. Tech. rep. Albuquerque, NM, and Livermore, CA (United States): Sandia National Laboratories (SNL), Apr. 2016 (cit. on p. 37).
- [77] Apram Rahoo. 'Comparison of Control Strategies for Wave Energy Converters Masterprogram i förnybar elgenerering Master Programme in Renewable Electricity Production'. Master Thesis. Uppsala University, 2020 (cit. on p. 37).

- [78] Aleix Maria-Arenas, Aitor J. Garrido, Eugen Rusu and Izaskun Garrido. 'Control strategies applied to wave energy converters: State of the art'. In: *Energies* 12.16 (2019) (cit. on p. 37).
- [79] Giorgio Bacelli. 'Optimal Control of Wave Energy Converters'. PhD thesis. The National University of Ireland, 2014, p. 218 (cit. on p. 37).
- [80] Jorgen Hals, Torkel Bjarte-Larsson and Johannes Falnes. 'Optimum Reactive Control and Control by Latching of a Wave-Absorbing Semisubmerged Heaving Sphere'. In: *21st International Conference on Offshore Mechanics and Arctic Engineering, Volume 4*. ASME, Jan. 2002, pp. 415–423 (cit. on p. 38).
- [81] S H Salter, J R M Taylor and N J Caldwell. 'Power conversion mechanisms for wave energy'. In: July (2002), pp. 1–27 (cit. on pp. 38, 39).
- [82] U.A. Korde. 'Efficient primary energy conversion in irregular waves'. In: *Ocean Engineering* 26.7 (1999), pp. 625–651 (cit. on p. 38).
- [83] Duarte Valério, Pedro Beirão and José Sá da Costa. 'Optimisation of wave energy extraction with the Archimedes Wave Swing'. In: *Ocean Engineering* 34.17-18 (2007), pp. 2330–2344 (cit. on p. 38).
- [84] Enrico Anderlini. 'Control of wave energy converters using machine learning strategies'. PhD thesis. The University of Edinburgh, July 2017, p. 255 (cit. on p. 39).
- [85] Aurélien Babarit, Hakim Mouslim, Michel Guglielmi and Alain H Clément. 'Simulation of the SEAREV wave energy converter with a by-pass control of its hydraulic power take off'. In: *Proc. World Renewable Energy Congress, Glasgow, UK*. 2008, pp. 1004–1009 (cit. on p. 39).
- [86] B. Teillant, J. C. Gilloteaux and J. V. Ringwood. 'Optimal damping profile for a heaving buoy wave energy converter'. In: *IFAC Proceedings Volumes (IFAC-PapersOnline)*. 2010 (cit. on p. 39).
- [87] Matthew Folley and Trevor Whittaker. 'The control of wave energy converters using active bipolar damping'. In: *Proceedings of the Institution of Mechanical Engineers, Part M: Journal of Engineering for the Maritime Environment* 223.4 (2009), pp. 479–487 (cit. on p. 39).
- [88] A H Clément and A Babarit. 'Discrete control of resonant wave energy devices.' In: *Philosophical transactions. Series A, Mathematical, physical, and engineering sciences* 370.1959 (Jan. 2012), pp. 288–314 (cit. on p. 39).
- [89] John T. Betts. *Practical Methods for Optimal Control and Estimation Using Nonlinear Programming*. Society for Industrial and Applied Mathematics, 2010, p. 434 (cit. on p. 39).



- [90] D.E. Kirk. *Optimal Control Theory: An Introduction*. Dover Books on Electrical Engineering. Dover Publications, 2012 (cit. on p. 39).
- [91] Mario Zanon, Andrea Boccia, Vryan Gil S. Palma, Sonja Parenti and Ilaria Xausa. 'Direct optimal control and model predictive control'. In: *Optimal Control: Novel Directions and Applications*. Vol. 2180. Springer Verlag, 2017. Chap. 3, pp. 263–382 (cit. on p. 40).
- [92] Nicolás Faedo, Sébastien Olaya and John V. Ringwood. 'Optimal Control, MPC and MPC-Like Algorithms for Wave Energy Systems: An Overview'. In: *IFAC Journal of Systems and Control* (2017) (cit. on pp. 40–42, 47).
- [93] Divya Garg, William W. Hager and Anil V. Rao. 'Pseudospectral methods for solving infinite-horizon optimal control problems'. In: *Automatica* 47.4 (Apr. 2011), pp. 829–837 (cit. on p. 40).
- [94] Demián Garcia-Violini and John V. Ringwood. 'Energy maximising robust control for spectral and pseudospectral methods with application to wave energy systems'. In: *International Journal of Control* 94.4 (2021), pp. 1102–1113 (cit. on pp. 40, 42).
- [95] S. Joe Qin and Thomas A. Badgwell. 'A survey of industrial model predictive control technology'. In: *Control Engineering Practice* 11.7 (July 2003), pp. 733–764 (cit. on p. 41).
- [96] David Q. Mayne. 'Model predictive control: Recent developments and future promise'. In: *Automatica* 50.12 (Dec. 2014), pp. 2967–2986 (cit. on p. 41).
- [97] Max Schwenzer, Muzaffer Ay, Thomas Bergs and Dirk Abel. 'Review on model predictive control: an engineering perspective'. In: *International Journal of Advanced Manufacturing Technology* 117.5-6 (Aug. 2021), pp. 1327–1349 (cit. on p. 41).
- [98] J. Richalet, A. Rault, J. L. Testud and J. Papon. 'Model predictive heuristic control. Applications to industrial processes'. In: *Automatica* 14.5 (Sept. 1978), pp. 413–428 (cit. on p. 41).
- [99] Charles R Cutler and Brian L Ramaker. 'Dynamic matrix control: A computer control algorithm'. In: *Joint Automatic Control Conference*. 17. 1980, p. 72 (cit. on p. 41).
- [100] D. W. Clarke, C. Mohtadi and P. S. Tuffs. 'Generalized predictive control-Part I. The basic algorithm'. In: *Automatica* 23.2 (Mar. 1987), pp. 137–148 (cit. on p. 41).
- [101] Sifu Li, Kian Y. Lim and D. Grant Fisher. 'A state space formulation for model predictive control'. In: *AIChE Journal* 35.2 (Feb. 1989), pp. 241–249 (cit. on p. 41).
- [102] Liuping Wang. *Model Predictive Control System Design and Implementation Using MATLAB*. Springer, 2009 (cit. on p. 41).
- [103] John Anthony Rossiter. *A First Course in Predictive Control*. 2nd. CRC Press, 2018, p. 426 (cit. on p. 41).

- [104] Romain Genest and John V. Ringwood. 'Receding Horizon Pseudospectral Control for Energy Maximization With Application to Wave Energy Devices'. In: *IEEE Transactions on Control Systems Technology* 25.1 (Jan. 2017), pp. 29–38 (cit. on p. 42).
- [105] Ted K.A. Brekken. 'On model predictive control for a point absorber wave energy converter'. In: *2011 IEEE PES Trondheim PowerTech: The Power of Technology for a Sustainable Society, POWERTECH 2011*. IEEE, June 2011, pp. 1–8 (cit. on p. 42).
- [106] Jorgen Hals, Johannes Falnes and Torgeir Moan. 'Constrained Optimal Control of a Heaving Buoy Wave-Energy Converter'. In: *Journal of Offshore Mechanics and Arctic Engineering* 133.1 (2011), p. 011401 (cit. on p. 42).
- [107] J. Cretel, A. W. Lewis, G. Lightbody and G. P. Thomas. 'An application of Model Predictive Control to a wave energy point absorber'. In: *IFAC Proceedings Volumes (IFAC-PapersOnline)* 1.PART 1 (2010), pp. 267–272 (cit. on pp. 42, 45).
- [108] Markus Richter. 'Different Model Predictive Control Approaches for Controlling Point Absorber Wave Energy Converters'. PhD thesis. University Stuttgart, 2011, p. 86 (cit. on p. 42).
- [109] Dan El Montoya Andrade, Antonio De La Villa Jaén and Agustín García Santana. 'Considering linear generator copper losses on model predictive control for a point absorber wave energy converter'. In: *Energy Conversion and Management* 78 (2014), pp. 173–183 (cit. on pp. 42, 45).
- [110] Paolino Tona, Guillaume Sabiron and Hoai Nam Nguyen. 'An energy-maximising mpc solution to the wec control competition'. In: *Proceedings of the International Conference on Offshore Mechanics and Arctic Engineering - OMAE*. Vol. 10. Glasgow: American Society of Mechanical Engineers, June 2019 (cit. on pp. 42, 46, 47).
- [111] Paolino Tona. *Workshop: Control strategies applied to wave energy converters*. 2019 (cit. on p. 42).
- [112] Paolino Tona, Guillaume Sabiron, Hoai-Nam Nguyen, Alexis Merigaud and Caroline Ngo. 'Experimental Assessment of the Ifpen Solution To the Wec Control'. In: Figure 1. Glasgow, 2020, pp. 1–12 (cit. on pp. 42, 46, 47).
- [113] Hoai-Nam Nam Nguyen, Guillaume Sabiron, Paolino Tona, Morten Mejlhede Kramer and Enrique Vidal Sanchez. 'Experimental validation of a nonlinear mpc strategy for a wave energy converter prototype'. In: *Proceedings of the International Conference on Offshore Mechanics and Arctic Engineering - OMAE*. Vol. 6. South Korea: American Society of Mechanical Engineers (ASME), June 2016, pp. 1–10 (cit. on pp. 42, 46, 47).



- [114] Giorgio Bacelli, John V. Ringwood and Gilloteaux Jean-Christophe. 'A control system for a self-reacting point absorber wave energy converter subject to constraints'. In: *Proceedings of the 18th World Congress The International Federation of Automatic Control*. Vol. 18. PART 1. Milano, Italy: IFAC, 2011, pp. 11387–11392 (cit. on p. 43).
- [115] Giorgio Bacelli and John Ringwood. 'A Geometrical Interpretation of Force and Position Constraints in the Optimal Control of Wave Energy Devices'. In: (2011) (cit. on p. 43).
- [116] Anil V Rao, David A Benson, Christopher Darby et al. 'Algorithm 902: Gpops, a matlab software for solving multiple-phase optimal control problems using the gauss pseudospectral method'. In: *ACM Transactions on Mathematical Software (TOMS)* 37.2 (2010), pp. 1–39 (cit. on p. 43).
- [117] Giorgio Bacelli and John V. Ringwood. 'Numerical Optimal Control of Wave Energy Converters'. In: *IEEE Transactions on Sustainable Energy* 6.2 (Apr. 2015), pp. 294–302 (cit. on p. 43).
- [118] Christian Windt, Nicolás Faedo, Markel Penalba, Frederic Dias and John V. Ringwood. 'Reactive control of wave energy devices – the modelling paradox'. In: *Applied Ocean Research* 109 (Apr. 2021), p. 102574 (cit. on p. 43).
- [119] John V. Ringwood. 'Wave energy control: status and perspectives 2020'. In: *IFAC-PapersOnLine* 53 (2 Jan. 2020), pp. 12271–12282 (cit. on p. 43).
- [120] Guang Li. 'Nonlinear model predictive control of a wave energy converter based on differential flatness parameterisation'. In: *International Journal of Control* 90.1 (2017), pp. 68–77 (cit. on p. 43).
- [121] Alexis Mérigaud and John V. Ringwood. 'Towards realistic non-linear receding-horizon spectral control of wave energy converters'. In: *Control Engineering Practice* 81 (2018), pp. 145–161 (cit. on p. 43).
- [122] Clement Auger, Alexis Paul Louis Merigaud and John V. Ringwood. 'Receding-horizon pseudo-spectral control of wave energy converters using periodic basis functions'. In: *IEEE Transactions on Sustainable Energy* (2018), pp. 1–1 (cit. on p. 43).
- [123] Nicolas Faedo, Giordano Scarciotti, Alessandro Astolfi and John V. Ringwood. 'Nonlinear Energy-Maximizing Optimal Control of Wave Energy Systems: A Moment-Based Approach'. In: *IEEE Transactions on Control Systems Technology* (2021) (cit. on p. 43).
- [124] G. Bacelli, R. Genest and J. V. Ringwood. 'Nonlinear control of flap-type wave energy converter with a non-ideal power take-off system'. In: *Annual Reviews in Control* 40 (Jan. 2015), pp. 116–126 (cit. on pp. 43, 45, 46).

- [125] Adrian C.M. O'Sullivan and Gordon Lightbody. 'The Effect of Viscosity on the Maximisation of Electrical Power from a Wave Energy Converter under Predictive Control'. In: *IFAC-PapersOnLine* 50.1 (July 2017), pp. 14698–14704 (cit. on p. 43).
- [126] A. Karthikeyan, M. Previsic, J. Scruggs and A. Chertok. 'Non-linear Model Predictive Control of Wave Energy Converters with Realistic Power Take-off Configurations and Loss Model'. In: *CCTA 2019 - 3rd IEEE Conference on Control Technology and Applications*. Institute of Electrical and Electronics Engineers Inc., Aug. 2019, pp. 270–277 (cit. on p. 43).
- [127] N Faedo, G. Giorgi, J V Ringwood and G. Mattiazzo. 'Optimal control of wave energy systems considering nonlinear Froude–Krylov effects: control-oriented modelling and moment-based control'. In: *Nonlinear Dynamics* (May 2022), pp. 1–28 (cit. on pp. 43, 44, 47).
- [128] Giuseppe Giorgi and John V Ringwood. 'Analytical formulation of nonlinear froude-krylov forces for surging-heaving-pitching point absorbers'. In: *Proceedings of the International Conference on Offshore Mechanics and Arctic Engineering - OMAE*. Vol. 10. 2018 (cit. on p. 43).
- [129] Tania Demonte Gonzalez, Gordon G Parker, Enrico Anderlini and Wayne W. Weaver. 'Sliding mode control of a nonlinear wave energy converter model'. In: *Journal of Marine Science and Engineering* 9.9 (2021) (cit. on p. 43).
- [130] Isha Malekar. 'Nonlinear Model Predictive Control of Wave Energy Converter'. PhD thesis. Houghton, Michigan: Michigan Technological University, Jan. 2021 (cit. on p. 43).
- [131] Markus Richter, Mario E. Magana, Oliver Sawodny and Ted K. A. Brekken. 'Nonlinear Model Predictive Control of a Point Absorber Wave Energy Converter'. In: *Sustainable Energy, IEEE Transactions on* 4.1 (Jan. 2013), pp. 118–126 (cit. on pp. 44, 47).
- [132] Kai Uwe Amann, Mario Edgardo Magaña and Oliver Sawodny. 'Model Predictive Control of a Nonlinear 2-Body Point Absorber Wave Energy Converter With Estimated State Feedback'. In: *IEEE Transactions on Sustainable Energy* 6.2 (2015), pp. 336–345 (cit. on pp. 44, 45).
- [133] J. A.M. Cretel, G. Lightbody, G. P. Thomas and A. W. Lewis. 'Maximisation of energy capture by a wave-energy point absorber using model predictive control'. In: *Proceedings of the 18th World Congress The International Federation of Automatic Control*. Vol. 44. PART 1. Milano, Italy: IFAC, 2011, pp. 3714–3721 (cit. on pp. 44, 45).



- [134] Ted K.A. Brekken, Markus Richter, Oliver Sawodny and Mario E. Magaña. 'Power optimisation of a point absorber wave energy converter by means of linear model predictive control'. In: *IET Renewable Power Generation* 8.2 (2014), pp. 203–215 (cit. on p. 45).
- [135] Adrian Cornelius Michael O'Sullivan, Wanan Sheng and Gordon Lightbody. 'An Analysis of the Potential Benefits of Centralised Predictive Control for Optimal Electrical Power Generation From Wave Energy Arrays'. In: *IEEE Transactions on Sustainable Energy* 9.4 (Oct. 2018), pp. 1761–1771 (cit. on p. 45).
- [136] Daniela Oetinger, Mario E Magaña, Senior Member and Oliver Sawodny. 'Decentralized Model Predictive Control for Wave Energy Converter Arrays'. In: *Sustainable Energy, IEEE Transactions on* 5.4 (2014), pp. 1099–1107 (cit. on p. 45).
- [137] Adrian C.M. O'Sullivan and Gordon Lightbody. 'Co-design of a wave energy converter using constrained predictive control'. In: *Renewable Energy* 102 (2017), pp. 142–156 (cit. on p. 45).
- [138] Sebastien Olaya, Jean Matthieu Bourgeot and Mohamed Benbouzid. 'Optimal control for a self-reacting point absorber: A one-body equivalent model approach'. In: *Proceedings - 2014 International Power Electronics and Application Conference and Exposition, IEEE PEAC 2014*. IEEE, Nov. 2014, pp. 332–337 (cit. on p. 45).
- [139] Palle Andersen, Tom S. Pedersen, Kirsten M. Nielsen and Enrique Vidal. 'Model predictive control of a wave energy converter'. In: *2015 IEEE Conference on Control and Applications, CCA 2015 - Proceedings*. IEEE, Sept. 2015, pp. 1540–1545 (cit. on p. 45).
- [140] Siyuan Zhan, Bin Wang, Jing Na and Guang Li. 'Adaptive Optimal Control of Wave Energy Converters'. In: *IFAC-PapersOnLine* 51.29 (2018), pp. 38–43 (cit. on p. 45).
- [141] Alyssa Kody, Nathan Tom and Jeffrey Scruggs. 'Model predictive control of a wave energy converter using duality techniques'. In: *Proceedings of the American Control Conference 2019-July* (July 2019), pp. 5444–5451 (cit. on p. 45).
- [142] Guang Li and Mike R. Belmont. 'Model predictive control of sea wave energy converters - Part II: The case of an array of devices'. In: *Renewable Energy* 68.3 (2014), pp. 540–549 (cit. on p. 45).
- [143] G. Bracco, M. Canale and V. Cerone. 'Optimizing energy production of an Inertial Sea Wave Energy Converter via Model Predictive Control'. In: *Control Engineering Practice* 96 (Mar. 2020), p. 104299 (cit. on p. 45).



- [144] Nataliia Y Sergiienko, Giorgio Bacelli, Ryan G Coe and Benjamin S Cazzolato. 'A comparison of efficiency-aware model-predictive control approaches for wave energy devices'. In: *Journal of Ocean Engineering and Marine Energy* (2021) (cit. on pp. 45–47).
- [145] António F.O. Falcão and João C.C. Henriques. 'Effect of non-ideal power take-off efficiency on performance of single- and two-body reactively controlled wave energy converters'. In: *Journal of Ocean Engineering and Marine Energy* 1.3 (Aug. 2015), pp. 273–286 (cit. on p. 45).
- [146] Carolina Ericksson. 'Model Predictive Control of CorPower Ocean Wave Energy Converter'. KTH Royal Institute of Technology, June 2016, pp. 1–60 (cit. on p. 45).
- [147] T. Strager, A. Martin dit Neuville, P. Fernández López et al. 'Optimising Reactive Control in Non-Ideal Efficiency Wave Energy Converters'. In: *Volume 9A: Ocean Renewable Energy*. ASME, June 2014, V09AT09A002 (cit. on p. 46).
- [148] Enrique Vidal Sanchez, Rico Hjern Hansen and Morten Mejlhede Kramer. 'Control performance assessment and design of optimal control to harvest ocean energy'. In: *IEEE Journal of Oceanic Engineering* 40.1 (Jan. 2015), pp. 15–26 (cit. on p. 46).
- [149] Anup J. Nambiar, David I.M. Forehand, Morten M. Kramer, Rico H. Hansen and David M. Ingram. 'Effects of hydrodynamic interactions and control within a point absorber array on electrical output'. In: *International Journal of Marine Energy* 9 (Apr. 2015), pp. 20–40 (cit. on pp. 46, 47).
- [150] Romain Genest, Félicien Bonnefoy, Alain H. Clément and Aurélien Babarit. 'Effect of non-ideal power take-off on the energy absorption of a reactively controlled one degree of freedom wave energy converter'. In: *Applied Ocean Research* 48 (Oct. 2014), pp. 236–243 (cit. on p. 46).
- [151] Paolino Tona, Hoai-nam Nguyen, Guillaume Sabiron and Yann Creff. 'An Efficiency-Aware Model Predictive Control Strategy for a Heaving Buoy Wave Energy Converter'. In: *Ewtec*. 2015, pp. 1–10 (cit. on p. 46).
- [152] Giorgio Bacelli and Ryan G. Coe. 'Comments on Control of Wave Energy Converters'. In: *IEEE Transactions on Control Systems Technology* 29.1 (Jan. 2021), pp. 478–481 (cit. on p. 46).
- [153] Elisabetta Tedeschi, Matteo Carraro, Marta Molinas and Paolo Mattavelli. 'Effect of control strategies and power take-off efficiency on the power capture from sea waves'. In: *IEEE Transactions on Energy Conversion* 26.4 (Dec. 2011), pp. 1088–1098 (cit. on p. 46).





- [154] Bradley A. Ling, Bret Bosma and Ted K.A. Brekken. 'Experimental Validation of Model Predictive Control Applied to the Azura Wave Energy Converter'. In: *IEEE Transactions on Sustainable Energy* 11 (4 Oct. 2020), pp. 2284–2293 (cit. on p. 47).
- [155] John V Ringwood, Francesco Ferri, Kelley M Ruehl et al. 'A competition for WEC control systems'. In: *12th European Wave and Tidal Energy Conference*. Cork, Ireland, 2017, p. 9 (cit. on p. 47).
- [156] Ali S. Haider, Ted K.A. Brekken and Alan McCall. 'Application of real-time nonlinear model predictive control for wave energy conversion'. In: *IET Renewable Power Generation* 15 (14 Oct. 2021), pp. 3331–3340 (cit. on p. 47).
- [157] Ali Shahbaz Haider. 'Application of Nonlinear Model Predictive Controller for Ocean Wave Energy Conversion Systems.' PhD thesis. Oregon State University, 2021 (cit. on p. 47).
- [158] Boris Houska, Hans Joachim Ferreau and Moritz Diehl. 'ACADO toolkit—An open-source framework for automatic control and dynamic optimization'. In: *Optimal Control Applications and Methods* 32.3 (2011), pp. 298–312 (cit. on p. 47).
- [159] Nicolás Faedo, Giuseppe Giorgi, Guiliana Mattiazzo and John V Ringwood. 'Nonlinear Moment-Based Optimal Control of Wave Energy Converters With Non-Ideal Power Take-Off Systems'. In: *41st International Conference on Ocean, Offshore and Arctic Engineering, OMAE 2022*. Hamburg: ASME, 2022, p. 10 (cit. on p. 48).
- [160] Sebastien Gros and Mario Zanon. 'Learning for MPC with stability and safety guarantees'. In: *Automatica* 146 (Dec. 2022), p. 110598 (cit. on p. 63).
- [161] Kelley Ruehl and Diana Bull. 'Wave Energy Development Roadmap: Design to commercialization'. In: *OCEANS 2012 MTS/IEEE: Harnessing the Power of the Ocean* (2012) (cit. on p. 64).



# Appendices



---

# Model Predictive Control for Wave Energy Converters: A Moving Window Blocking Approach

The content of this manuscript has been presented at 21<sup>st</sup> *IFAC World Congress (2020)*, and the version of record of this manuscript has been published and is freely available in the Journal *IFAC-PapersOnLine*:

<https://doi.org/10.1016/j.ifacol.2020.12.1960>.

# Model Predictive Control for Wave Energy Converters: A Moving Window Blocking Approach

Juan Guerrero-Fernández\* Oscar J. González-Villarreal\*  
John Anthony Rossiter\* Bryn Jones\*

\* *Department of Automatic Control and Systems Engineering,  
University of Sheffield, UK (e-mail: [j.guerrero@sheffield.ac.uk](mailto:j.guerrero@sheffield.ac.uk);  
[ojgonzalezvillarreal1@sheffield.ac.uk](mailto:ojgonzalezvillarreal1@sheffield.ac.uk); [j.a.rossiter@sheffield.ac.uk](mailto:j.a.rossiter@sheffield.ac.uk);  
[b.l.jones@sheffield.ac.uk](mailto:b.l.jones@sheffield.ac.uk))*

**Abstract:** Ocean wave energy is one of the most concentrated sources of renewable energy. However, until now it has not reached the economic feasibility required to be commercialised. To improve the efficiency of wave energy converters, several advanced control strategies have been proposed, including Model Predictive Control (MPC). Nevertheless, the computational burden of the underlying optimisation problem is a drawback of conventional (Full-Degree of Freedom, F-DoF) MPC, which typically limits its application for real-time control of systems. In this paper, a Moving Window Blocking (MWB) approach is proposed to speed-up the time required for each optimisation problem by reducing the number of decision variables using input parameterised solutions. Numerical simulation of a generic single device point absorber wave energy converter controlled by this scheme confirms the potential of this approach.

Copyright © 2020 The Authors. This is an open access article under the CC BY-NC-ND license (<http://creativecommons.org/licenses/by-nc-nd/4.0>)

*Keywords:* Wave energy converters, Model predictive controller, Moving window blocking.

## 1. INTRODUCTION

Ocean wave energy is one of the most concentrated renewable energy sources, and its resources are vast in many countries around the globe (Sheng, 2019). The estimated worldwide potential of ocean wave power is 32 000 TW h (Mørk et al., 2010), which is more than the worldwide electricity consumption of about 25 721 TW h (International Energy Agency, 2019).

The development and implementation of wave energy converters (WEC) may have several benefits. Examples of the benefits range from individual benefits for the country such as increasing of their renewable energy matrix and guaranteeing energy supply diversity (Sheng, 2019), to global benefits by confronting the problems of climate change and the difficult challenge of reducing the dependency on conventional energy resources such as fossils or nuclear energy.

To date, wave energy technologies are technically immature for reliable and economical energy generation (Sheng, 2019). One of the biggest challenges is how to improve the efficiency of wave energy converters. To address this issue, several control strategies have been proposed to alter the dynamic behaviour of the device in order to maximise the extracted energy. *Model Predictive Control* (MPC) is a well-developed control strategy within academic and industry communities which takes into account constraints whilst optimising a given cost function (Faedo et al., 2017). Although MPC can have explicit offline solutions (H.J.Ferreau, H.G. Bock, 2008), this is not tractable for the WEC problem given the large amount

of variation present in the wave excitation forces which are external disturbances to the optimisation. Thus, for this application, MPC requires an online solution where at each sampling time, solves an Optimal Control Problem (OCP) to produce an optimal control sequence, the first of which is applied to the plant as the control action (Li and Belmont, 2014). However, one of the drawbacks of MPC is the computational burden required to solve the OCP.

To reduce the computational burden of the optimisation, a popular approach is to use input-parameterisation techniques which allow to reduce the number of degrees of freedom of the optimisation. Several input-parameterisation have been proposed such as Laguerre Polynomials (Wang, 2004), as well as orthonormal parameterisations based on collocation points, typically referred as pseudospectral methods (Garcia-Violini and Ringwood, 2019).

In this paper, a *Moving Window Blocking* (MWB) MPC approach is proposed with the idea of reducing the computational time required to solve the OCP at each sampling time. The results of the simulations show a performance comparable with the performance when implementing the Full-Degree of Freedom (F-DoF) MPC strategy, and offer a better performance than the Generalised Predictive Control (GPC) strategy.

The remaining part of this paper is organised as follows: Section 2 presents the mathematical model for a generic WEC. F-DoF Model Predictive Control and a detailed description of the proposed Moving Window Blocking MPC approach is given in Section 3. The results of the simulations are presented in Section 4. Finally, the conclusions and future work are set out in Section 5.

## 2. WEC MODELLING

For the development of the mathematical model of a wave energy converter (WEC), a heaving semi-submerged sphere is considered as in Figure 1. The hydrodynamic model is developed from first principles. Applying Newton's second law to the partially submerged sphere, the dynamics of the sphere are described by:

$$m \ddot{z}(t) = F_g - \iint_{S(t)} P(t) \mathbf{n} dS + F_{PTO}(t) \quad (1)$$

Where  $m$  is the floater mass,  $z$  is the vertical displacement of the body relative to its hydrostatic equilibrium position,  $F_g$  is the force due to gravity,  $F_{PTO}(t)$  is the force exerted by the Power Take-Off systems (PTO) (controller input  $u(t)$ ),  $P(t)$  is the pressure on an element  $dS$  on the buoy wetted surface,  $\mathbf{n}$  is a vector normal to the surface element,  $dS$  and  $S$  is the submerged wetted surface.

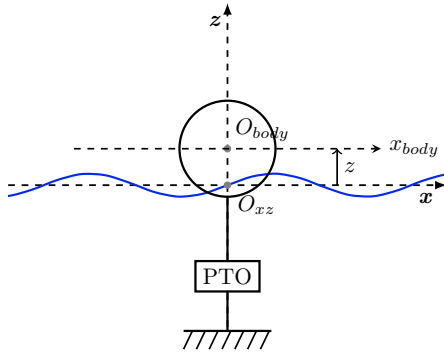


Fig. 1. A general wave energy converter with 1-DoF: heave

From (1), several models can be derived, depending on the complexity, computational time and accuracy desired. In this study, a linear hydrodynamic model is considered. For linear models, assuming the fluid is in-compressible, in-viscid and irrotational<sup>1</sup>, (1) is typically solved using potential flow theory, in which the potential problem is linearised and computed around the position of equilibrium. Considering small displacements, and seabed as reference system, (1) is rewritten as follows:

$$m \ddot{z}(t) = F_{res}(t) + F_{rad}(t) + F_{exc}(t) + F_{PTO}(t), \quad (2)$$

where  $F_{res}(t)$  is hydrostatic restoring force,  $F_{rad}(t)$  is the radiation force, and  $F_{exc}(t)$  the excitation force due to the incoming wave. The hydrostatic restoring force  $F_{res}(t)$  represent the spring-like effect of the surrounding ocean water into the buoy, and is determined by  $k_h$  hydrostatic stiffness and  $z(t)$  absorber position:

$$F_{res}(t) = -k_h z(t) \quad (3)$$

The excitation force  $F_{exc}(t)$  describes the interactions between the incident waves and the body at its place of equilibrium, and is represented by the convolution of the excitation impulse response  $k_{exc}$  with the otherwise undisturbed free-surface elevation  $\eta$  at the centre of the body:

$$F_{exc}(t) = \int_{-\infty}^t k_{exc}(t - \tau) \eta(\tau) d\tau \quad (4)$$

<sup>1</sup> This is a standard assumption in the wave energy literature (Faedo et al., 2017).

Similarly, the radiation force  $F_{rad}(t)$  is a damping/inertial force associated with waves radiated by the absorber oscillating in calm water scenario, and is expressed by the added mass  $\mu_\infty$  and the convolution product between the radiation impulse response  $k_{rad}$  and the absorber velocity  $\dot{z}(t)$ :

$$F_{rad}(t) = -\mu_\infty \ddot{z}(t) - \int_{-\infty}^t k_{rad}(t - \tau) \dot{z}(\tau) d\tau \quad (5)$$

The convolution kernels  $k_{exc}$ ,  $k_{rad}$  and the frequency-independent added mass  $\mu_\infty$  are computed numerically using boundary element methods (BEMs). In this study the open source *NEMOH* (Penalba et al., 2017) was employed. Combining (3)-(5) with (2) gives the widely used equation (in WEC studies) Cummins' equation (Cummins, 1962):

$$m \ddot{z}(t) = -k_h z(t) - \mu_\infty \ddot{z}(t) - \int_{-\infty}^t k_{rad}(t - \tau) \dot{z}(\tau) d\tau + \int_{-\infty}^t k_{exc}(t - \tau) \eta(\tau) d\tau + F_{PTO}(t) \quad (6)$$

At this point, a few statements can be made from (6). First, since the excitation force  $F_{exc}(t)$  depends on the undisturbed free-surface elevation  $\eta(t)$ , it can be considered as an independent input to the system. Second, (6) is represented in state-space form for control strategy implementation and third, the direct computation of the convolution integral in (5) in time-domain simulation is computationally expensive and cumbersome (Roessling and Ringwood, 2015). To avoid the direct computation of the convolution integral at every time step, several methods to approximate the integral have been proposed (Yu and Falnes, 1995; Roessling and Ringwood, 2015; Pérez and Fossen, 2008). Approximating the convolution integral in (5) by a state-space system with the state vector  $\underline{x}_r(t) \in \mathbb{R}^n$  is a common approach, where the input to the system is the velocity of the absorber ( $v = \dot{z}$ ) and the approximation of the convolution integral term of the radiation force is the output:

$$\begin{aligned} \dot{\underline{x}}_r(t) &= A_r \underline{x}_r(t) + B_r \dot{z}(t) \\ \int_{-\infty}^t k_{rad}(t - \tau) \dot{z}(\tau) d\tau &\approx C_r \underline{x}_r(t) \end{aligned} \quad (7)$$

This system is later included as a part of the overall model that describes the motion of the absorber. It is important to clarify that the system states in (7) have no physical meaning, but still contain information on the condition of the surrounding fluid (Cretel et al., 2011). In this study, the state space matrices  $A_r$ ,  $B_r$ , and  $C_r$  were computed by the open source toolbox *FOAMM* (Finite Order Approximation by Moment-Matching, based on the theoretical foundations presented in Faedo et al. (2018)) Defining the state and output vectors,  $\underline{x}_c \in \mathbb{R}^{n+2}$  and  $\underline{y}_c \in \mathbb{R}^2$ , for the linear time-invariant state-space system:

$$\underline{x}_c = \begin{bmatrix} z \\ \dot{z} \\ \underline{x}_r \end{bmatrix} \quad \underline{y}_c = \begin{bmatrix} z \\ \dot{z} \end{bmatrix} \quad (8)$$

the whole dynamics of the WEC is given by:

$$\begin{aligned} \dot{\underline{x}}_c(t) &= A_c \underline{x}_c(t) + B_c F_{pto}(t) + B_c F_{exc}(t) \\ \underline{y}_c(t) &= C_c \underline{x}_c(t) \end{aligned} \quad (9)$$

in which  $A_c \in \mathbb{R}^{(n+2) \times (n+2)}$ ,  $B_c \in \mathbb{R}^{(n+2) \times 1}$ ,  $C_c \in \mathbb{R}^{2 \times (n+2)}$ , are defined as:

$$A_c = \begin{bmatrix} 0 & 1 & \mathbf{0} \\ \frac{-k_h}{m+\mu_\infty} & 0 & \frac{-C_r}{m+\mu_\infty} \\ \mathbf{0} & B_r & A_r \end{bmatrix}; B_c = \begin{bmatrix} 0 \\ \frac{1}{m+\mu_\infty} \\ \mathbf{0} \end{bmatrix}; C_c = \begin{bmatrix} 1 & 0 & \mathbf{0} \\ 0 & 1 & \mathbf{0} \end{bmatrix}$$

where  $\mathbf{0}$  denotes a zero matrix of required dimensions.

By discretising system (9), and replacing  $F_{pto}$  and  $F_{exc}$  for  $u$  and  $u_{exc}$ , respectively, to use standard nomenclature, results in a general discrete state-space of the form.

$$\underline{x}_{k+1} = A_d \underline{x}_k + B_d \underline{u}_k + B_d \underline{u}_{exc_k} \quad (10a)$$

$$\underline{y}_k = C_d \underline{x}_k \quad (10b)$$

For this study, a discretisation of a zero-order hold was considered using a sampling time of  $T_s = 0.1s$ . The resulting state space matrices are given in section 4.

### 3. MODEL PREDICTIVE CONTROL

#### 3.1 General Objective

In this paper, Model Predictive Control was used as general optimal control methodology with the general purpose of maximising the mechanical energy  $E_{abs}$  absorbed by the PTO system over a time horizon  $T$ , defined as:

$$E_{abs} = - \int_t^{t+T} u(\tau) \dot{z}(\tau) d\tau \quad (11)$$

Furthermore, real WEC systems will typically present position, input and input increments (slew rates) constraints related to physical limits which can be handled naturally by the MPC formulation. To benefit from the moving window blocking approach presented in subsection 3.4, this paper focuses particularly on the case where the WEC is within a “safe” operating region (i.e., operating within the position constraints, without making contact with the end-stops). Indeed, the device should be locked in a survival mode when exposed to extreme sea conditions (Sheng, 2019); this is reasonable given it is generally not possible to guarantee output feasibility (such as the buoy positions) for dynamics systems under significant disturbances. In simple terms, if a big enough wave is applied to the system, it would not even be possible to prevent it from reaching the limits, regardless of the input selection. An alternative might be to use soft-constraints for some output violations, however, this is out of the scope of this paper.

The discrete-time optimisation problem is thus chosen as:

$$\text{minimise } J_k = \sum_{i=1}^{N_p} u_{k+i-1} \dot{z}_{k+i} \quad (12a)$$

$$\text{s.t. } u_{min} \leq u_{k+i-1} \leq u_{max} \quad (12b)$$

$$\Delta u_{min} \leq \Delta u_{k+i-1} \leq \Delta u_{max} \quad (12c)$$

where  $N_p$  is the prediction horizon. Note that this cost considers the force  $u$  and velocity  $\dot{z}$  at different time steps ( $k+i-1$  and  $k+i$ ). This is chosen to ensure causality of the solution as discussed in Li and Belmont (2014).

#### 3.2 Predictions

Following the methodology described in Cretel et al. (2010), the state space model (10) is augmented with the

previous input  $u_{k-1}$  to use the input increment  $\Delta u_k$  as the decision variable resulting in:

$$x_{k+1} = Ax_k + B\Delta u_k + B_w u_{exc_k} \quad (13a)$$

$$y_k = Cx_k \quad (13b)$$

where the state is now  $x_k = [\underline{x}_k^T u_{k-1}]^T \in \mathbb{R}^{n+3}$ , the output is  $y_k = [\underline{y}_k^T u_{k-1}]^T \in \mathbb{R}^3$ , and

$$A = \begin{bmatrix} A_d & B_d \\ \mathbf{0} & 1 \end{bmatrix} \quad B = \begin{bmatrix} B_d \\ 1 \end{bmatrix} \quad B_w = \begin{bmatrix} B_d \\ 0 \end{bmatrix} \quad C = \begin{bmatrix} C_d & \mathbf{0} \\ \mathbf{0} & 1 \end{bmatrix}$$

This change will allow simple expressions for input and input rate constraints, as well as the computation of the product  $(u_{k+i-1} \dot{z}_k)$  through an appropriate matrix  $Q$  as discussed in Cretel et al. (2010, 2011). By propagating the model (13a)  $N_p$  times forward, all future outputs  $\hat{Y} = [y_{k+1}^T, y_{k+2}^T, \dots, y_{k+N_p}^T]^T \in \mathbb{R}^{3N_p}$  are given by:

$$\hat{Y} = Gx_k + H\Delta\hat{U} + H_w\hat{U}_w \quad (14)$$

where  $\Delta\hat{U} = [\Delta\hat{u}_k, \Delta\hat{u}_{k+1}, \dots, \Delta\hat{u}_{k+N_p}]^T \in \mathbb{R}^{N_p}$  are the future input increments;  $\hat{U}_w = [\hat{u}_{w_k}, \hat{u}_{w_{k+1}}, \dots, \hat{u}_{w_{k+N_p}}]^T \in \mathbb{R}^{N_p}$  are the future wave excitation forces; and matrices  $G \in \mathbb{R}^{3N_p \times (n+3)}$  and  $H \in \mathbb{R}^{3N_p \times N_p}$  are defined as:

$$G = \begin{bmatrix} CA \\ CA^2 \\ \vdots \\ CA^{N_p} \end{bmatrix}^T \quad H = \begin{bmatrix} CB & \mathbf{0} & \dots & \mathbf{0} \\ CAB & CB & \ddots & \vdots \\ \vdots & \ddots & \ddots & \mathbf{0} \\ CA^{N_p-1}B & \dots & CAB & CB \end{bmatrix}$$

where  $\mathbf{0}$  are zeros matrices with the same dimensions of  $CB$ , and  $H_w$  is defined as  $H$  using  $B_w$  instead.

#### 3.3 Standard Optimisation

Having defined the prediction models, a standard quadratic cost function can be formulated as,

$$J = \frac{1}{2} \hat{Y}^T Q \hat{Y} \quad (15)$$

To compute the product  $(u_{k-1} \dot{z}_k)$ , the penalisation matrix  $Q \in \mathbb{R}^{3N_p \times 3N_p}$  is selected as a block diagonal matrix with the inner matrices  $q_{k+i}$  defined as (Cretel et al., 2010),

$$Q = \begin{bmatrix} q_{k+1} & \mathbf{0} & \dots & \mathbf{0} \\ \mathbf{0} & q_{k+2} & \ddots & \vdots \\ \vdots & \ddots & \ddots & \mathbf{0} \\ \mathbf{0} & \dots & \mathbf{0} & q_{k+N_p} \end{bmatrix} \quad q_{k+i} = \begin{bmatrix} 0 & 0 & 0 \\ 0 & 0 & 1 \\ 0 & 1 & 0 \end{bmatrix} \quad \forall i = [1, N_p] \quad (16)$$

By substituting the output predictions (14) in (15), rearranging in terms of the decision variables  $(\Delta\hat{U})$ , and including input and input rate constraints, the standard quadratic program (17) is obtained.

$$J = \frac{1}{2} \Delta\hat{U}^T E \Delta\hat{U} + \Delta\hat{U}^T f \quad \text{s.t.} \quad M \Delta\hat{U} \leq b \quad (17a)$$

$$E = H^T Q H \quad f = H^T Q (Gx_k + H_w \hat{U}_w) \quad (17b)$$

$$M = \begin{bmatrix} I \\ -I \\ D \\ -D \end{bmatrix} \quad b = \begin{bmatrix} \Delta u_{max} \mathbf{1} \\ -\Delta u_{min} \mathbf{1} \\ (u_{max} - u_{k-1}) \mathbf{1} \\ (-u_{min} + u_{k-1}) \mathbf{1} \end{bmatrix} \quad (17c)$$

where  $E \in \mathbb{R}^{N_p \times N_p}$  is a matrix known as the Hessian, here assumed to be positive definite;  $f \in \mathbb{R}^{N_p}$  is a column-vector;  $M \in \mathbb{R}^{4N_p \times N_p}$  is the constraint matrix;  $b \in \mathbb{R}^{4N_p}$  is the constraint vector;  $I \in \mathbb{R}^{N_p \times N_p}$  is an identity matrix;





$D \in \mathbb{R}^{N_p \times N_p}$  is a lower triangular matrix; and  $\mathbf{1} \in \mathbb{R}^{N_p}$  column-vector is a column vector of ones.

Having defined  $E, f, M, b$ , the optimisation can then be solved using any QP solver such as quadprog function of Matlab, QP OASES (H.J.Ferreau, H.G. Bock, 2008), etc. At each sampling time, only the first input is applied to the system and the process is repeated at the next sampling time, which is the well known receding horizon control strategy.

### 3.4 Moving Window Blocking

In this paper, we used a blocking approach where the input is parameterised in blocks of size  $N_b$  having equal values, e.g.  $u_k = u_{k+1} = \dots = u_{k+N_b-1}$  for the first block,  $u_{k+N_b} = u_{k+N_b+1} = \dots = u_{k+2N_b-1}$  for the second block, etc., thus allowing the decision variables to be spread over the prediction horizon, as opposed to the standard Generalized Predictive Control (GPC) approach where the decision variables are "congested" at the beginning, and left constant after a "control horizon" (Rossiter, 2018). An example comparison of this is visualised in Fig. 2 for the WEC system defined in section 2, and is further discussed in the results section 4. This distinctive feature of the blocking approach is important for this application for two main reasons: firstly, the solution obtained from the original problem using full degrees of freedom applied to the WEC system is constantly saturated as seen in Fig. 2, thus can be accurately represented by blocks; and secondly, depending on the wave future values, it might be more important to have decisions available at the future, example when the wave reaches its crest and trough (maximum/minimum values).

The aforementioned blocking parameterisation can be achieved by defining a blocking matrix ( $\mathbb{N}$ ) for the decision variables ( $\Delta\hat{U}$ ) of the form:

$$\Delta\hat{U} = \mathbb{N}\Delta\hat{U} \quad (18a)$$

$$\mathbb{N} = \begin{bmatrix} \mathbf{n} & \mathbf{0}_{N_b} & \dots & \mathbf{0}_{N_b} \\ \mathbf{0}_{N_b} & \mathbf{n} & \ddots & \vdots \\ \vdots & \ddots & \ddots & \mathbf{0}_{N_b} \\ \mathbf{0}_{N_b} & \dots & \mathbf{0}_{N_b} & \mathbf{n} \end{bmatrix} \quad \mathbf{n} = \begin{bmatrix} 1 \\ \mathbf{0}_{N_b-1} \end{bmatrix} \quad (18b)$$

where  $\hat{U} \in \mathbb{R}^{N_u}$  are the blocked decision variables which have reduced dimensions of  $N_u = \lceil \frac{N_p}{N_b} \rceil$   $\mathbf{n} \in \mathbb{R}^{N_b}$ , and  $\mathbf{0}_v \in \mathbb{R}^v$  is a column-vector of  $v$  zeros. For simplicity,  $N_p$  should be selected as a multiple integer of the block size  $N_b$ , otherwise the last  $\mathbf{n}$  in the diagonal might be different.

Moreover, as discussed in Cagienard et al. (2007), the application of standard blocking approaches has an inconsistent nature, and suffers from recursive feasibility problems given the decision in the previous time step cannot be replicated which is detrimental to the performance. To address this, the Moving Window Blocking (MWB) approach developed in Cagienard et al. (2007) proposed to shift the set of  $N_b$  admissible blocking matrices  $\mathbb{N}_i$  along with the moving horizon resulting in an input parameterisation of the form.

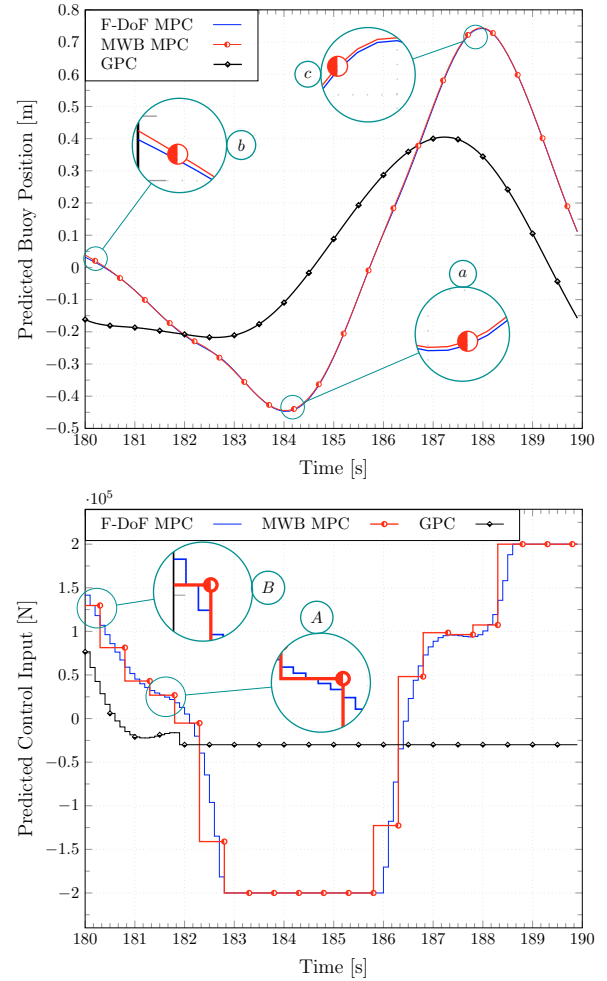


Fig. 2. Predicted Trajectories for Buoy Position  $z$  (upper plot) and Input  $u$  (lower plot).

$$\Delta\hat{U} = \mathbb{N}_i\Delta\hat{U} \quad \forall i = [1, N_b] \quad (19a)$$

$$\mathbb{N}_i = \begin{bmatrix} \mathbf{n}_1 & \mathbf{0}_{N_b-i} & \dots & \mathbf{0}_{N_b-i} \\ \mathbf{0}_{N_b} & \mathbf{n} & \ddots & \vdots \\ \vdots & \ddots & \ddots & \mathbf{0}_{N_b} \\ \mathbf{0}_{N_b-2+i} & \dots & \mathbf{0}_{N_b-2+i} & \mathbf{n}_f \end{bmatrix} \quad \mathbf{n}_1 = \begin{bmatrix} 1 \\ \mathbf{0}_{N_b-i} \end{bmatrix} \quad \mathbf{n}_f = \begin{bmatrix} 1 \\ \mathbf{0}_{N_b-2+i} \end{bmatrix} \quad (19b)$$

where  $\mathbf{n}$  and  $\mathbf{0}_v$  are defined as in (18). Notice the first and final block ( $\mathbf{n}_1, \mathbf{n}_f$ ) are shrinking and expanding, respectively. This parameterisation is then applied sequentially  $i = 1 \rightarrow N_b$  until the first block reaches its limit, and resets to its original size ( $i = 1$ ).

By substituting the MWB input parameterisation in the standard quadratic program (17), the application of the MWB approach then leads to formulating and solving  $N_b$  different quadratic programs sequentially and repeating infinitely  $i = 1 \rightarrow N_b, 1 \rightarrow N_b, 1 \rightarrow \dots$  as the horizon moves forward defined as:

$$J = \frac{1}{2} \Delta \hat{U}^T E_{\mathbb{N}}^{[i]} \Delta \hat{U} + \Delta \hat{U}^T f_{\mathbb{N}}^{[i]} \quad \text{s.t.} \quad M_{\mathbb{N}}^{[i]} \Delta \hat{U} \leq b \quad (20a)$$

$$E_{\mathbb{N}}^{[i]} = \mathbb{N}_i^T H^T Q H \mathbb{N}_i = \mathbb{N}_i^T E \mathbb{N}_i \quad (20b)$$

$$f_{\mathbb{N}}^{[i]} = \mathbb{N}_i^T H^T Q (G x_k + H_w \hat{U}_w) = \mathbb{N}_i^T f \quad (20c)$$

$$M_{\mathbb{N}}^{[i]} = \begin{bmatrix} \mathbb{N}_i \\ -\mathbb{N}_i \\ D_{\mathbb{N}_i} \\ -D_{\mathbb{N}_i} \end{bmatrix} \quad b = \begin{bmatrix} \Delta u_{max} \mathbf{1} \\ -\Delta u_{min} \mathbf{1} \\ (u_{max} - u_{k-1}) \mathbf{1} \\ (-u_{min} + u_{k-1}) \mathbf{1} \end{bmatrix} \quad (20d)$$

where  $E_{\mathbb{N}}^{[i]} \in \mathbb{R}^{N_u \times N_u}$  is the ‘‘compressed’’ Hessian, which can be pre-stored for faster computations. On the other hand, the ‘‘compressed’’ linear term  $f_{\mathbb{N}}^{[i]} \in \mathbb{R}^{N_u}$  can also be pre-stored by separating the values in  $f_{\mathbb{N}}^{[i]} = f_{1_{\mathbb{N}}}^{[i]} x_k + f_{2_{\mathbb{N}}}^{[i]} \hat{U}_w$  with  $f_{1_{\mathbb{N}}}^{[i]} = \mathbb{N}_i^T H^T Q G$  and  $f_{2_{\mathbb{N}}}^{[i]} = \mathbb{N}_i^T H^T Q H_w$ . Moreover, it is trivial to derive that when using the blocking matrix  $\mathbb{N}_i$  as defined in (19), the constraint matrix have redundant zero rows  $\forall i$ , and can be reduced to,

$$M_{\mathbb{N}}^{[i]} = M_{\mathbb{N}} = \begin{bmatrix} I_{\mathbb{N}} \\ -I_{\mathbb{N}} \\ D_{\mathbb{N}} \\ -D_{\mathbb{N}} \end{bmatrix} \quad b_{\mathbb{N}} = \begin{bmatrix} \Delta u_{max} \mathbf{1}_{\mathbb{N}} \\ -\Delta u_{min} \mathbf{1}_{\mathbb{N}} \\ (u_{max} - u_{k-1}) \mathbf{1}_{\mathbb{N}} \\ (-u_{min} + u_{k-1}) \mathbf{1}_{\mathbb{N}} \end{bmatrix} \quad (21)$$

where  $M_{\mathbb{N}} \in \mathbb{R}^{4N_u \times N_u}$  is the ‘‘reduced’’ constraint matrix,  $b_{\mathbb{N}} \in \mathbb{R}^{4N_u}$  is the ‘‘reduced’’ constraint vector,  $I_{\mathbb{N}} \in \mathbb{R}^{N_u \times N_u}$  is an identity matrix,  $D_{\mathbb{N}} \in \mathbb{R}^{N_u \times N_u}$  is a lower triangular matrix, and  $\mathbf{1}_{\mathbb{N}} \in \mathbb{R}^{N_u}$  is column-vector of ones, all of which have reduced dimensions  $N_u = \lceil \frac{N_p}{N_b} \rceil$  when compared to the original constraint terms (17c), thus can lead to significant computational benefits as discussed in the results section 4. Once the optimisation is solved, the original decision vector can be recovered using (19).

#### 4. RESULTS

In this section, we present the simulation results of the control of a point-absorber WEC using F-DoF MPC, GPC and the proposed Moving Window Blocking (MWB) MPC approach. The WEC model considered is a heaving semi-submerged sphere reacting against a fixed reference (see Fig. 1), with a radius of 5 m and draft of 5 m, mass  $m = 2.6831 \times 10^5$  kg placed in deep water. A sampling time of  $T_s = 0.1$  s was used. The hydrodynamic coefficients were computed using the open source *NEMOH* (Penalba et al., 2017). The convolution integral in the radiation force (5) is approximated by a state-space model of order 6 (See (7)). Here, the state-space matrices  $A_r$ ,  $B_r$ , and  $C_r$  are computed using the toolbox *FOAMM*, which is based in the moment-matching method (Faedo et al., 2018). The resulting state space matrices for the discretised model of (10) are given by (22). The Matlab code and results presented in this paper are available through a Code Ocean compute capsule <https://doi.org/10.24433/CO.0481002.v1> (Guerrero-Fernandez and Gonzalez Villarreal, 2019).

To focus on the comparison of the control strategies, which is the main driver of this study, perfect knowledge of the future wave forces  $\hat{U}_w$  and state  $x_k$  is considered during the simulation time. The wave elevation of the irregular sea wave was built using the JONSWAP (Joint North Sea Wave Project) spectrum discretised in frequency between

0.02 Hz to 0.80 Hz, corresponding to 1.25 s to 50 s periods respectively, with a frequency step of  $\Delta f = 5.2 \times 10^{-3}$  Hz. Considering a significant wave height  $H_0 = 2.0$  m and wave peak period  $T_p = 10.0$  s. Fig. 3 shows the resulting excitation force on the buoy, with a force range from  $8.7119 \times 10^5$  N to  $-8.5133 \times 10^5$  N.

Here, for comparison purpose, Full-Degrees Of Freedom (F-DoF) MPC strategy is considered as the control strategy which delivers the maximum possible extracted energy (100% efficiency). For the optimisation setup, a prediction horizon of 10 s ( $N_p = 100$ ) was used with a block size of  $N_b = 5$  for the MWB approach which resulted in  $N_u = 20$  decision variables. To perform a fair comparison, the GPC approach used the same amount of decision variables compressed at the beginning of the prediction horizon. Moreover, matrix  $B_d$  of (22) was re-scaled/normalized to avoid numeric conditioning problems of the optimisation. Finally, constraints on the input and input increment were considered as  $\|u_{k+i}\| \leq 200kN$  and  $\|\Delta u_{k+i}\| \leq 200kN \forall i = [0, N_p - 1]$ , respectively.

Fig. 4 shows the energy extracted for the different controllers studied in this paper, and the final value of the energy extracted at the end of the 600 s simulation is shown in Table 1. The results show that the proposed MWB approach offers almost the same amount of energy compared to the maximum feasible (F-DoF MPC), with an efficiency of 98.79%. On the other side GPC is ranked third in the amount of energy extracted, with an efficiency of 92.84%. Moreover, Zoom A in Fig. 4, shows the bidirectional reactive power flowing between the PTO and the absorber, condition required for the active control strategies to maximise the extracted energy (Pecher and Kofoed, 2017).

On an interesting note, it can be seen that F-DoF unconstrained MPC with input saturation failed to extract energy altogether as seen in Table 1. Similar results were obtained in Li and Belmont (2014). An alternative is to add an extra quadratic penalization term on the input of the form ( $J_{\lambda} = J + \lambda \sum u_{k+i-1}^2 \forall i = [1, N_p]$ ) to the cost function (12a) as discussed in Li and Belmont (2014), however, this causes disagreements between the optimisation terms, inevitable leading to suboptimalities. To perform a fair comparison, a brute-force search was performed to select the value of  $\lambda = 1.12$  which achieved the highest energy absorption for the unconstrained penalised ( $\lambda$ ) F-DoF MPC solution with an efficiency of 88.71, thus still resulting in worse performance than both, GPC and MWB.

Table 1. Energy Extracted for 600 s simulation using F-DoF MPC, MWB MPC, GPC and F-DoF Unconstrained MPC (with and without additional  $\lambda$  penalization terms)

Method	Energy extracted [MJ]	Efficiency [%]
F-DoF MPC	306.974	100
F-DoF Unc. MPC	-328.738	LOSS
F-DoF Unc. MPC ( $\lambda$ )	272.318	88.71
MWB MPC	303.274	98.79
GPC	285.000	92.84



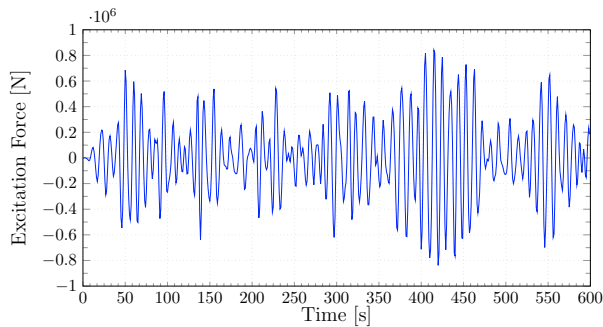


Fig. 3. Excitation force  $u_{exc}$  for a irregular sea condition built using the JONSWAP spectrum, with wave height  $H_0 = 2.0$  m and wave peak period  $T_p = 10.0$  s

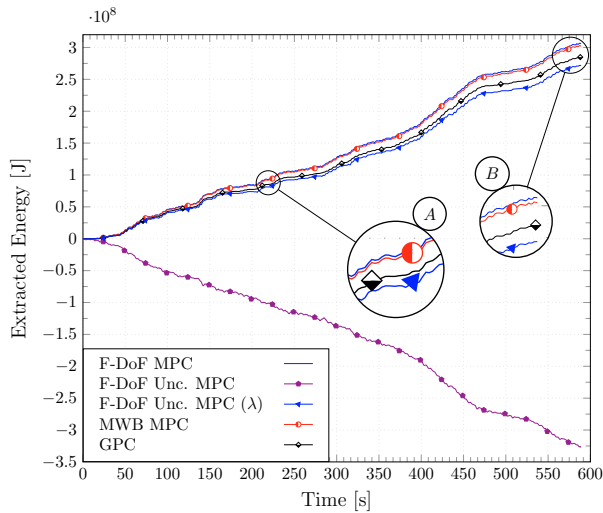


Fig. 4. Energy Extracted tendency for 600s simulation using F-DoF MPC, MWB MPC, GPC and F-DoF Unconstrained MPC (with/without  $\lambda$  terms)

Fig. 2 shows the predicted trajectories of the buoy position and the control input  $u$  for the three MPC solutions, namely: the F-DoF MPC, the MWB and the GPC. From the lower plot of Fig. 2, it can clearly be seen how the MWB approach embeds the blocked parameterisation, distributing the decision variables along the prediction horizon with the sequential shrinking approach (first block size of  $4 \rightarrow i = 2$ ) visible in the zooms A and B, respectively. In contrast, in the GPC approach, all the decision variables are calculated for the beginning of the prediction horizon and kept constant after a certain time which leads to a significant difference in the predicted trajectory of the control action.

$$A_d = \begin{bmatrix} 0.9905 & 0.0997 & -0.0003 & -0.0002 & 0.0003 & 0.0004 & -0.0005 & 0.0015 \\ -0.1896 & 0.9899 & -0.0048 & -0.0049 & 0.0057 & 0.0084 & -0.0096 & 0.0297 \\ -0.0253 & 0.2166 & 0.7789 & 0.2342 & -0.2682 & 0.1451 & -0.2394 & 0.1985 \\ -0.0021 & 0.0171 & -0.0373 & 1.0167 & -0.0214 & 0.0111 & -0.0190 & 0.0156 \\ -0.0361 & 0.3052 & -0.3113 & 0.3019 & 0.5081 & 0.6650 & -0.3376 & 0.2792 \\ 0.0013 & -0.0474 & 0.0476 & -0.0472 & -0.4112 & 0.8425 & 0.0486 & -0.0465 \\ -0.0217 & 0.1850 & -0.1887 & 0.1830 & -0.2292 & 0.1236 & 0.7820 & 0.3332 \\ 0.0015 & -0.0201 & 0.0203 & -0.0199 & 0.0232 & -0.0160 & -0.1424 & 0.9675 \end{bmatrix} \quad B_d = \begin{bmatrix} 0.0123 \\ 0.2465 \\ 0.0329 \\ 0.0028 \\ 0.0469 \\ -0.0017 \\ 0.0282 \\ -0.0019 \end{bmatrix} \cdot 10^{-6} \quad C_d = \begin{bmatrix} 1 & 0 \\ 0 & 1 \\ 0 & 0 \\ 0 & 0 \\ 0 & 0 \\ 0 & 0 \\ 0 & 0 \\ 0 & 0 \end{bmatrix}^T \quad (22)$$

On the other hand, the predicted trajectories of the buoy position can be seen in the upper plot of Fig. 2 where the solutions for both, F-DoF MPC and MWB MPC, are practically indistinguishable, with negligible differences visible in zooms *a*, *b* and *c*. This visual agreement is supported by the efficiency given in Table 1. In contrast, this can not be said about the GPC solution, where one can see the significant differences in the predicted trajectories, most likely related to the differences in the available control action trajectories. In simple terms, the GPC strategy is unable to replicate the position trajectory when using the same number of decision variables compressed in the beginning of the prediction horizon.

With regard to the computation times used to solve the optimal problem at each time step, Table 2 summarises relevant optimisation statistics of each method employed in this study when using the interior point method of Matlab R2018b “quadprog” function in a normal PC with an Intel i5-7500 @ 3.4 GHz CPU, and 8 GB @ 2.4 GHz DDR4 RAM. On average, the proposed MWB approach makes it possible to solve the optimal problem 12.6 times faster compared to the F-DoF MPC. The reason for this gain in the computation time is due to the fact that, in this case, the number of decision variables and constraints are reduced by 5 times ( $N_b = 5$ ), i.e., from  $N_p = 100$  to  $N_u = 20$  decision variables, and from  $4N_p = 400$  to  $4N_u = 80$  constraints, which ultimately leads to faster and lower amount of iterations required by the QP to solve the problem. Similar comments of the timing statistics can be made for the GPC strategy, with the main drawback being a performance degradation (efficiency of 92.84%). Also, it can be seen that the MWB provides the smallest standard deviation for both average timing statistics, thus leading to an optimisation with more consistent/repeatable behaviour.

Table 2. Statistics of the Optimisation

Method	Avg. opt. time [ms]	Avg. num. of QP iterations	Avg. opt. time per iter. [ms]	Gain
F-DoF MPC	$19.78 \pm 2.75$	$8.19 \pm 0.79$	$2.42 \pm 0.27$	-
MWB MPC	$1.58 \pm 0.23$	$6.75 \pm 0.98$	$2.37 \pm 0.04$	12.6
GPC	$1.39 \pm 0.51$	$7.37 \pm 1.17$	$1.93 \pm 0.10$	14.2

Finally, it should be pointed out that the main contribution of the MWB approach is not merely the reduction in the computation time required to solve the OCP at each sampling time, but the ability to retain almost the same performance than that of F-DoF via the shifting input parameterisation, a property that GPC does not deliver. Results provided in Tables 1 and 2 support this.

## 5. CONCLUSION

The control strategies presented in this study are intended to maximise the energy production of a generic point-absorber wave energy converter subject to input and input rate constraints related to physical limits. The system benefits from the ability of Model Predictive Control to include future information of both wave forces and physical constraints. Moreover, to reduce the computational burden, it uses Moving Window Blocking approach where the decision variables are parameterised through a set of input-blocking matrices which result in a sequence of Quadratic Programs of reduced size to be solved sequentially and repeating infinitely. This allows solutions up to 12.52 times faster with efficiency as low as 98.8% when compared to the Full Degrees of Freedom MPC optimal solution. Although both, the F-DoF MPC and the proposed MWB MPC approach are computationally feasible for this particular single WEC device model, the proposed control strategy could be a key methodology for implementing Centralised Model Predictive Control for wave farms. The solution of the proposed approach was further compared with GPC, as well as with two versions of Unconstrained F-DoF MPC, one of which was shown to result in a complete loss of energy extraction.

Future work will include the assessment of the solution using real-time embedded hardware such as FPGAs, as well as faster QP solvers such as QP OASES. Moreover, the application will be extended to wave farms using a centralised optimisation framework, and compared with decentralised/distributed approaches as well as with other parameterisation such as collocation points based on pseudospectral methods. Finally, the mathematical models and MPC formulation will be extended to the nonlinear case, and will include further modeling such as actuator dynamics and future wave force predictions.

Ultimately, enhancing peer collaboration and transparency, the findings provided in this paper and the Matlab code used in the simulation are accessible through a Code Ocean capsule (<https://doi.org/10.24433/CO.0481002.v1>) (Guerrero-Fernandez and Gonzalez Villarreal, 2019).

## ACKNOWLEDGEMENTS

The first author would like to acknowledge the support of MICITT (Ministerio de Ciencia, Tecnología y Telecomunicaciones) of Costa Rica, who funded this work through a scholarship under the contract MICITT-PINN-CON-2-14-17-1-027. The second author would like to acknowledge the support of CONACyT, Mexico.

## REFERENCES

- Cagienard, R., Grieder, P., Kerrigan, E.C., and Morari, M. (2007). Move blocking strategies in receding horizon control. *Journal of Process Control*, 17(6), 563–570.
- Cretel, J., Lewis, A.W., Lightbody, G., and Thomas, G.P. (2010). An application of Model Predictive Control to a wave energy point absorber. *IFAC Proceedings Volumes (IFAC-PapersOnline)*, 1, 267–272.
- Cretel, J.A., Lightbody, G., Thomas, G.P., and Lewis, A.W. (2011). Maximisation of energy capture by a wave-energy point absorber using model predictive control. In *Proceedings of the 18th World Congress The International Federation of Automatic Control*, 3714–3721. IFAC, Milano, Italy.
- Cummins, W. (1962). The impulse response fitting and ship motions. Technical report, Institut fuer Schiffbau der Universitaet, Hamburg, Hamburg.
- Faedo, N., Olaya, S., and Ringwood, J.V. (2017). Optimal Control, MPC and MPC-Like Algorithms for Wave Energy Systems: An Overview. *IFAC Journal of Systems and Control*.
- Faedo, N., Peña-Sanchez, Y., and Ringwood, J.V. (2018). Finite-order hydrodynamic model determination for wave energy applications using moment-matching. *Ocean Engineering*, 163, 251–263.
- Garcia-Violini, D. and Ringwood, J.V. (2019). Energy maximising robust control for spectral and pseudospectral methods with application to wave energy systems. *International Journal of Control*, 1–12.
- Guerrero-Fernandez, J. and Gonzalez Villarreal, O.J. (2019). Model Predictive Control for Wave Energy Converters: A Moving Window Blocking Approach. Code Ocean. Available in <https://doi.org/10.24433/CO.0481002.v1>.
- H.J.Ferreau, H.G. Bock, M.D. (2008). An online active set strategy to overcome the limitations of Explicit MPC. *International Journal of Robust and Nonlinear Control*, 18(October 2014), 816–830.
- International Energy Agency (2019). Electricity Information: Overview. Technical report, International Energy Agency. URL <https://webstore.iea.org/>.
- Li, G. and Belmont, M.R. (2014). Model predictive control of sea wave energy converters - Part I: A convex approach for the case of a single device. *Renewable Energy*, 69, 453–463.
- Mørk, G., Barstow, S., Kabuth, A., and Pontes, M.T. (2010). Assessing the global wave energy potential. In *Proceedings of the International Conference on Offshore Mechanics and Arctic Engineering - OMAE*, volume 3, 447–454. ASME.
- Pecher, A. and Kofoed, J.P. (2017). *Handbook of Ocean Wave Energy*. Springer.
- Penalba, M., Cortajarena, J.A., and Ringwood, J. (2017). Validating a Wave-to-Wire Model for a Wave Energy Converter—Part II: The Electrical System. *Energies*, 10(7), 1002.
- Pérez, T. and Fossen, T.I. (2008). Time-vs. frequency-domain Identification of parametric radiation force models for marine structures at zero speed. *Modeling, Identification and Control*, 29(1), 1–19.
- Roessling, A. and Ringwood, J.V. (2015). Finite order approximations to radiation forces for wave energy applications. *Renewable Energies Offshore*, 359–366.
- Rossiter, J. (2018). *A first course in predictive control*. CRC Press.
- Sheng, W. (2019). Wave energy conversion and hydrodynamics modelling technologies: A review. *Renewable and Sustainable Energy Reviews*, 482–498.
- Wang, L. (2004). Discrete model predictive controller design using Laguerre functions. *Journal of Process Control*, 14(2), 131–142.
- Yu, Z. and Falmes, J. (1995). State-space modelling of a vertical cylinder in heave. *Applied Ocean Research*, 17(5), 265–275.



## Efficiency-aware non-linear model-predictive control with real-time iteration scheme for wave energy converters

The version of record of this manuscript has been published and is freely available in the *International Journal of Control*, Published online: 26 May 2022:

<https://www.tandfonline.com/doi/full/10.1080/00207179.2022.2078424>.





## Efficiency-aware nonlinear model-predictive control with real-time iteration scheme for wave energy converters

Juan L. Guerrero-Fernandez, Oscar J. González-Villarreal & John Anthony Rossiter

To cite this article: Juan L. Guerrero-Fernandez, Oscar J. González-Villarreal & John Anthony Rossiter (2022): Efficiency-aware nonlinear model-predictive control with real-time iteration scheme for wave energy converters, International Journal of Control, DOI: [10.1080/00207179.2022.2078424](https://doi.org/10.1080/00207179.2022.2078424)

To link to this article: <https://doi.org/10.1080/00207179.2022.2078424>



© 2022 The Author(s). Published by Informa UK Limited, trading as Taylor & Francis Group.



Published online: 26 May 2022.



Submit your article to this journal [↗](#)



Article views: 472



View related articles [↗](#)



View Crossmark data [↗](#)

Full Terms & Conditions of access and use can be found at  
<https://www.tandfonline.com/action/journalInformation?journalCode=tcon20>



## Efficiency-aware nonlinear model-predictive control with real-time iteration scheme for wave energy converters

Juan L. Guerrero-Fernandez <sup>a</sup>, Oscar J. González-Villarreal <sup>b</sup> and John Anthony Rossiter <sup>a</sup>

<sup>a</sup>Department of Automatic Control and Systems Engineering, University of Sheffield, Sheffield, UK; <sup>b</sup>Centre for Autonomous and Cyber-Physical Systems, Cranfield University, Cranfield, UK

### ABSTRACT

Several solutions have been proposed in the literature to maximise the harvested ocean energy, but only a few consider the overall efficiency of the power take-off system. The fundamental problem of incorporating the power take-off system efficiency is that it leads to a nonlinear and non-convex optimal control problem. The main disadvantage of the available solutions is that none solve the optimal control problem in real-time. This paper presents a nonlinear model predictive control (NMPC) approach based on the real-time iteration (RTI) scheme to incorporate the power take-off system's efficiency when solving the optimal control problem at each time step in a control law aimed at maximising the energy extracted. The second contribution of this paper is the derivation of a condensing algorithm  $O(N^2)$  for 'output-only' cost functions required to improve computational efficiency. Finally, the RTI-NMPC approach is tested using a scaled model of the Wavestar design, demonstrating the benefit of this new control formulation.

### ARTICLE HISTORY

Received 24 September 2021  
Accepted 9 May 2022

### KEYWORDS

Wave energy converters; nonlinear model predictive controller; real-time iteration; power take-off-system efficiency; condensing algorithm  $O(N^2)$

## 1. Introduction

One of several challenges that wave energy technologies confront is their inability to produce electricity at a cost comparable with other grid-scale generation technologies like natural gas and wind (Coe et al., 2021, may). Several studies have identified the refining of advanced control strategies as a way to improve energy capture efficiency significantly and, as a result, give a clear path to increase the economic viability for wave energy converters (WEC) (Bull et al., 2016; Chang et al., 2018; Cordonnier et al., 2015; Neary et al., 2014).


Control strategies for wave energy converters can be divided into two groups based on the type of power take-off (PTO) utilised. Suppose the PTO only allows unidirectional energy flow from the ocean to the grid. In that case, the only control option is passive control, which produces a force that opposes the movement of the point absorber. Resistive control (Maria-Arenas et al., 2019; Sanchez et al., 2015; Wang et al., 2018) belongs to this group. Conversely, suppose the PTO allows bidirectional energy flow from the ocean to the grid and vice versa. In that case, active control is possible, for which reactive control (Maria-Arenas et al., 2019; Wang et al., 2018) can be mentioned as an example.

In theory, reactive control may be optimal by bringing the system to resonance, allowing for the theoretical maximum wave energy capture predicted by linear wave theory in unconstrained amplitude conditions (Falnes, 2002). However, it has many challenges and disadvantages: the optimal reactive control is anti-causal (requiring future prediction of the incident wave and wave excitation force (Falnes, 2002)), but also it involves dealing with large reactive power flux (as bringing the system to

resonance requires cancelling the reactive terms in the equation of motion) (Genest et al., 2014). On the other hand, reactive power consists of a back-and-forth energy exchange between the PTO and the oscillation system that contributes nothing to the average delivered power. The energy loss due to dissipative processes inherent in back-and-forth energy exchange is a crucial disadvantage of reactive control (Falcão & Henriques, 2015, august). This paper offers an advanced control strategy to significantly improve energy capture efficiency of the system.

In Strager et al. (2014, june), the performance of a reactively controlled single point-absorber WEC with a nonideally efficient PTO was studied for regular waves and the performance of regular and irregular waves was studied in Sanchez et al. (2015). For regular and irregular waves, partial reactive control was suggested (Genest et al., 2014) as a causal suboptimal control approach for a heaving single-body wave energy converter, along with studies of the impact of the actuators' efficiency in the annual mean absorbed power.

In Tona et al. (2015), a model predictive control (MPC) approach was described that explicitly considers the efficiency of the PTO system, with the control objective being to harvest the maximum amount of energy/mean power from the WEC. However this optimal control scenario, similarly to the one presented by the same author in Tona et al. (2019, 2020, august), can not be used for real-time implementation with small sampling times ( $T_p \leq 50$  ms) since they are based on an offline solution (Tona et al., 2020, august). Similarly, the MPC algorithm presented in Tona et al. (2019, 2020, august) uses a discrete objective function that weights the instantaneous power

**CONTACT** Juan L. Guerrero-Fernandez  j.guerrero@sheffield.ac.uk

© 2022 The Author(s). Published by Informa UK Limited, trading as Taylor & Francis Group.  
This is an Open Access article distributed under the terms of the Creative Commons Attribution-NonCommercial-NoDerivatives License (<http://creativecommons.org/licenses/by-nc-nd/4.0/>), which permits non-commercial re-use, distribution, and reproduction in any medium, provided the original work is properly cited, and is not altered, transformed, or built upon in any way.

value over the prediction horizon. The weightings are determined offline using an iterative optimisation approach based on repeated simulations of the state space model over a set of sea states (a Nelder-Mead optimisation algorithm is used).

The fundamental problem of incorporating the PTO system efficiency is that it leads to a nonlinear and non-convex optimal control problem. The main disadvantage of the available solutions is that none solve the optimal control problem in real-time. This paper presents a nonlinear model predictive control (NMPC) approach based on the real-time iteration (RTI) (Diehl et al., 2005) scheme. The proposed controller incorporates the PTO system's efficiency when solving the optimal control problem at each time step, in a control law aimed to maximise the energy extracted from the ocean waves.

The controller proposed in this study differentiates from others in that it does not require offline computations to address the nonlinear programming problem that arises from incorporating the PTO's efficiency into the optimal control problem. Our controller technique is unique in that it can adapt to changes in the sea condition to provide the best possible solution.

The control strategy proposed in this study is based on the assumption that the incident wave force (or incident wave moment in this case) for the current time step and a defined prediction horizon window is known at each sampling step. Another assumption is that the PTO system's efficiency  $\eta$  remains constant during the simulation time. That is, it does not vary as the actuator heats up. The dynamics of actuators are not considered in this work. It is considered much faster than WEC dynamics, and these do not appear to have a significant impact on electrical power production (Tona et al., 2020, august). Finally, it is assumed that the float motion can be described using a simple model derived from linear wave theory. Nonetheless, a critical nonlinearity in the OCP arises from the inclusion of the PTO system's efficiency of the instantaneous power at each time step of the prediction horizon window.

The second contribution of this paper is the derivation of the condensing algorithm  $O(N^2)$  (Andersson, 2013) for 'output-only' cost functions which allow some important computational efficiency gains required for real-time implementation. The overall RTI-NMPC strategy is presented and exemplified through computer simulations. The code and results presented in this paper are available through a Code Ocean capsule (Guerrero-Fernández & González-Villarreal, 2021).

The remainder of this paper is organised as follows: Section 2 presents the time-domain modelling of the wave energy converter used in this work. Section 3 formulates the general objective of any energy maximising control strategy. A detailed description of the modelling, prediction, optimisation and RTI to implement the proposed RTI-NMPC scheme is presented in Section 4. The results of the simulations are presented in Section 5. Finally, the Section 6 contains conclusions, summarises the paper's contribution, and describes future work.

## 2. Wave energy converter modelling

The WEC selected for testing the control algorithm proposed in the present paper is a scaled model of the Wavestar device used in the WEC control competition (Ringwood et al., 2017). The development of the model is kept to a minimum in this Section

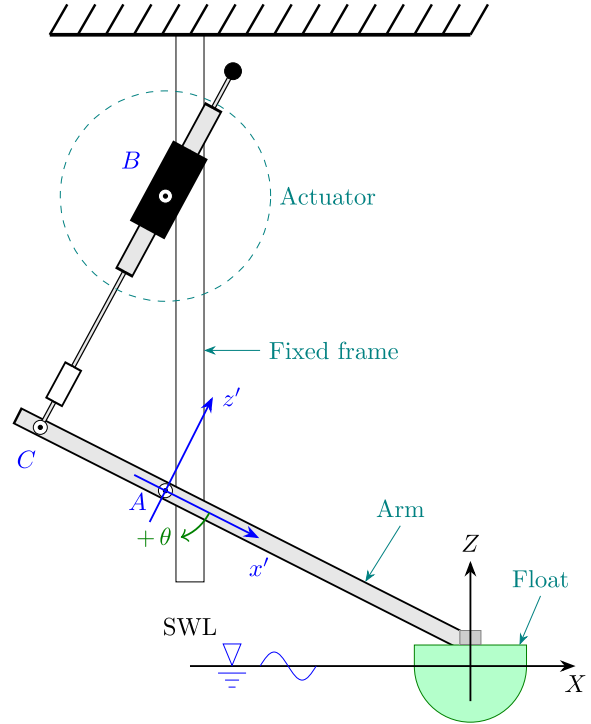


Figure 1. Diagram of the Wavestar WEC system.

for brevity. A semi-sphere serves as a floater in this model, and it is attached to a rotating arm, which is hinged at a fixed reference point A (Figure 1). For the float and linkage arm about point A, the device's dynamics can be reduced to an analogous equation-of-motion:

$$(J + J_{\infty})\ddot{\theta}(t) = -K_{hs}\theta(t) - b_v\dot{\theta}(t) - M_r(t) - M_{exc}(t) + M_{pto}(t) \quad (1a)$$

$$\dot{\underline{r}}(t) = A_r\underline{r}(t) + B_r\dot{\theta}(t) \quad (1b)$$

$$M_r(t) = C_r\underline{r}(t) + D_r\dot{\theta}(t) \quad (1c)$$

where:

- $\theta$  represents the angular displacement of the arm with respect to the equilibrium position,  $\dot{\theta}$  and  $\ddot{\theta}$  represent the angular velocity and angular acceleration of the arm.
- $J$  is the total mass moment of inertia of the float and pivot arm.
- $J_{\infty}$  is the added mass moment of the inertia.
- $K_{hs}$  is the hydrostatic coefficient,
- $b_v$  is a linear damping coefficient (Tom et al., 2018).
- $M_r$  is the radiation moment.
- $M_{exc}$  is the excitation moment due to the incident wave.
- $M_{pto}$  is the PTO moment (input to the system).
- $(A_r, B_r, C_r, D_r)$  are the state space matrices used to approximate the radiation moment  $M_r$  avoiding the direct computation of the convolution integral in time-domain simulation. The state vector  $\underline{r}(t)$  have no physical meaning, but still contain information on the condition of the surrounding fluid (Cretel et al., 2010).





**Remark 2.1:** It is crucial to recall that all of the parameters and variables in Equation (1a) are specified w.r.t. the rotating point A. For more details of the model development, the interested reader is referred to Tom, Ruehl, and Ferri (2018) and Tona et al. (2020, august).

### 3. Problem formulation

#### 3.1 General objective

The main objective of a PTO system controller is to transfer as much energy as possible from the waves to the grid for a broad range of sea states. The electrical energy  $E_e$  absorbed by the grid over a time horizon  $T$ , is defined as:

$$E_e = - \int_t^{t+T} P_e(\tau) d\tau = - \int_t^{t+T} \Gamma(\tau) P_m(\tau) d\tau \quad (2)$$

where  $P_e$  denotes the electrical power delivered to the grid,  $P_m$  the instantaneous hydromechanical power absorbed by the PTO system,  $\Gamma$  the overall efficiency of the PTO system, and  $\tau$  is the variable of integration.

The negative sign in Equation (2) is because the energy is drawn from the WEC and thus, the maximisation of the energy absorbed corresponds to a minimisation of the control objective (Nguyen et al., 2016, june).

The instantaneous hydromechanical absorbed power is given by:

$$P_m(t) = M_{pto}(t)\dot{\theta}(t) \quad (3)$$

where  $M_{pto}$  is the PTO moment and  $\dot{\theta}$  represents the angular velocity of the arm. To use standard nomenclature,  $M_{pto}(t_k)$  is replaced by  $u_k$ .

Substituting (3) in (2) the optimal control problem can be formulated as:

$$\min_u -E_e = \int_t^{t+T} \Gamma(\tau) u(\tau) \dot{\theta}(\tau) d\tau \quad (4a)$$

$$\text{s.t. } \dot{\mathbf{x}}(t) = f(\mathbf{x}, u, w, t) \quad (4b)$$

$$U_{min} \leq u(t) \leq U_{max} \quad (4c)$$

The equivalent discrete-time optimisation problem is given by:

$$\min_{u_i} J = \sum_{i=1}^{N_p} \gamma_{k+i} u_{k+i-1} \dot{\theta}_{k+i} \quad (5a)$$

$$\text{s.t. } \mathbf{x}_{k+1} = f(\mathbf{x}_k, u_k, w_k) \quad (5b)$$

$$U_{min} \leq u_k \leq U_{max} \quad (5c)$$

where  $N_p$  is the prediction horizon, Equation (5b) represents the WEC dynamics, with the states  $\mathbf{x} = [\theta \ \dot{\theta} \ \mathbf{r}]^T$ ,  $u_k$  the control input,  $w_k$  the discrete-time value for the excitation moment  $M_{exc}$ , and  $\gamma_k$  the specific value for the PTO efficiency at time instant  $t_k$ ; that is,  $\Gamma(t_k) = \gamma_k$ .

**Remark 3.1:** Equation (5a) considers the velocity  $\dot{\theta}$  and the control input  $u$  at different time steps ( $k+i$  and  $k+i-1$ ). This is chosen to ensure causality of the solution as discussed in Li and Belmont (2014).

#### 3.2 Power take-off efficiency

One of the common control policies proposed to increase the amount of energy extracted from the ocean waves is reactive control. The main idea of this strategy is to match the intrinsic impedance of the system by supplying power to the PTO system for some parts of the sinusoidal cycle (Ringwood et al., 2014). One of the main limitations of reactive control is that it creates a particular demand on PTO systems to allow for bi-directional power flow. Still, it can yield energy losses if it is not tuned correctly (Li & Belmont, 2014; Mériçaud & Tona, 2020; Ringwood et al., 2014).

PTO systems are not perfect in real-world applications, which means that the electrical power  $P_e$  is never equal to the absorbed mechanical power  $P_m$ . In other words, because of the losses that occur throughout the conversion stage, the electrical power available at the end of the mechanical-to-electrical conversion stage is less than the absorbed mechanical power, i.e.  $0 \leq P_e \leq P_m$ . If a reactive control strategy is adopted, at certain times, the PTO system must return some electric power from the grid back into the ocean ( $P_m \leq 0$ ). In those instants, and because of the losses in the conversion stages, the electrical power provided by the grid to the PTO system must be larger than  $|P_m|$ , i.e.  $P_e \leq P_m \leq 0$  (Mériçaud & Tona, 2020).

Given that the efficiency of the PTO system varies depending on the direction of the energy flow (float-to-grid or grid-to-float directions), the energy-maximising control strategy must consider the efficiency when solving the OCP (Andersen et al., 2015). Other studies have discussed the impact of nonideal PTO efficiency on WEC control (Bacelli et al., 2015; Falcão & Henriques, 2015, august; Genest et al., 2014; Mériçaud & Tona, 2020; Sanchez et al., 2015; Tedeschi et al., 2011; Tom et al., 2019; Tona et al., 2015, 2019), with the main drawback that none of them solves the OCP related to the nonlinear output equation of the model in real-time (see Section 4.1, Equation (8)), which is the main contribution of this paper.

The PTO system efficiency can be modelled by a modification of a step function, having two different values for the efficiency depending if the PTO system is working as motoring (grid-to-float) or as generator (float-to-grid). Using this modified-step function model, the instantaneous power extracted is given by:

$$P_e(t) = \Gamma(t) P_m(t), \begin{cases} \Gamma(t) = \mu_{gen} & \text{if } P_m(t) \geq 0 \\ \Gamma(t) = \mu_{mot} & \text{if } P_m(t) < 0 \end{cases} \quad (6)$$

where  $\mu_{gen}$  is the global efficiency of the PTO system when it delivers energy to the grid and  $\mu_{mot}$  is the global efficiency when the PTO system consumes energy from the grid.

### 4. Nonlinear model predictive control

Because of its ability to explicitly handle constraints and nonlinear dynamics that define the system of interest, NMPC is becoming increasingly popular for real-time optimal control solutions (Diehl et al., 2005). The following subsections are intended to offer a quick overview of each of the steps/phases involved in developing NMPC.

Let us first define some notations used in the following subsections. The upper bar ( $\bar{x}$ ) represents a nominal-guessed point

which is considered a ‘desirable-optimal’ trajectory to be used by the NMPC framework to optimise and improve the solution iteratively. Similarly, the hat ( $\hat{x}$ ) represents the predicted, whilst the variable without any additional notation will be reserved for the real/simulated value. Also, the underbar notation for vectors ( $\bar{x}$ ) will be dropped for the sake of readability and to simplify the notation of the following equations.

#### 4.1 Modelling

In this paper, we consider a general ordinary differential equation describing the system evolution in continuous time of a generic wave energy converter on a time interval  $[0, T]$  of the form:

$$\dot{x}(t) = f(x(t), u(t), w(t), t), \quad t \in [0, T] \quad (7a)$$

$$y(t) = g(x(t), u(t), w(t), t) \quad (7b)$$

where  $t \in \mathbb{R}$  is the time,  $u(t) \in \mathbb{R}^{n_u}$  are the control input,  $x(t) \in \mathbb{R}^{n_x}$  is the state,  $w(t) \in \mathbb{R}^{n_w}$  is wave excitation input, and  $y(t) \in \mathbb{R}^{n_y}$ . The function  $f$  is a map from states, control input, wave input, and time to the rate of change of the state, i.e.  $f: \mathbb{R}^{n_x} \times \mathbb{R}^{n_u} \times \mathbb{R}^{n_w} \times [0, T] \mapsto \mathbb{R}^{n_x}$ . Similar definition for  $g$ . Also it is assume that  $f$  and  $g$  are continuous with respect to  $x$  and  $t$ .

The prediction and optimisation presented in Sections 4.2 and 4.3 respectively, are formulated in discrete time, therefore to translate the continuous-time model into the discrete-time model, a discretisation by integration is implemented (González-Villarreal, 2021). For this study, we decided to use the explicit 4th order Runge-Kutta method.

In the present study, the output function  $g(x_k, u_k, w_k)$  is selected as follows:

$$y_k = g_k = \begin{bmatrix} \dot{\theta}_k \\ \gamma_k u_{k-1} \end{bmatrix} \quad (8)$$

On the other hand, the PTO efficiency model presented in Equation (6) suffers from a discontinuity between the two cases  $P_m(t) \geq 0$  and  $P_m(t) < 0$ . In gradient-based optimisation approaches, such a discontinuous function is undesirable. Therefore, a smoothed approximation to Equation (6), continuous in  $P_m(t) = 0$ , must be implemented to prevent problems with the optimisation technique.

A modified-hyperbolic tangent function is used to approximate Equation (6) in Mérigaud and Tona (2020) and Tona et al. (2015). Although a *sigmoid function* or another comparable activation function may be used to approximate this sort of discontinuous function, the approximation using *tanh* is preserved in this study and is given by:

$$\Gamma_{approx}(t) = \alpha + \beta \tanh(\varphi P_m(t)) \quad (9)$$

where  $\alpha$  is an offset,  $\beta$  is a scaling factor, and  $\varphi$  is a real positive parameter that determines the accuracy of the approximation. Defined as  $\alpha = (\mu_{mot} + \mu_{gent})/2$ , and  $\beta = (\mu_{mot} - \mu_{gent})/2$ .

#### 4.2 Prediction

The derivation of the prediction model discussed in this Section follows a similar pattern to that presented in González-Villarreal

and Rossiter (2020b) and is presented here to allow the contents of this paper to be self-contained. Using a first order multivariable Taylor series expansion, the linearised model for Equation (7a) at time step  $k$ , is given by:

$$\hat{x}_{k+1} = \bar{x}_{k+1} + A_k \delta \hat{x}_k + B_k \delta \hat{u}_k + B_{w,k} \delta \hat{w}_k \quad (10)$$

where  $\delta \hat{x}_k = \hat{x}_k - \bar{x}_k$ ,  $\delta \hat{u}_k = \hat{u}_k - \bar{u}_k$ , and  $\delta \hat{w}_k = \hat{w}_k - \bar{w}_k$  are the deviations of the state, control input and wave excitation moment from their nominal points  $(\bar{x}_k, \bar{u}_k, \bar{w}_k)$  at time step  $t = k$  respectively, and  $A_k$ ,  $B_k$ , and  $B_{w,k}$  are the partial derivatives w.r.t. the states, control input, and wave excitation input moment, which will be defined shortly.

The wave excitation moment deviation  $\delta \hat{w}_k$  requires special consideration at this stage. The approach used in this work assumes that the wave excitation moment at the current time and for a specific time horizon is known at each time step. Therefore, the nominal and predicted trajectory for the wave excitation moment is the same at each time step, i.e.  $\delta \hat{w}_k = 0$  for all  $k$ , and thus the following derivation does not take this term into account. But practical implementation could take deviations into account, which could emerge considering a correction-estimation of the predicted wave during the feedback phase.

$$A_k = \left. \frac{\partial f(x,u,w)}{\partial x} \right|_{\substack{\bar{x}_k \\ \bar{u}_k \\ \bar{w}_k}} \quad B_k = \left. \frac{\partial f(x,u,w)}{\partial u} \right|_{\substack{\bar{x}_k \\ \bar{u}_k \\ \bar{w}_k}} \\ \bar{x}_{k+1} = f(\bar{x}_k, \bar{u}_k, \bar{w}_k)$$

The deviation  $\delta x_{k+1} = x_{k+1} - \bar{x}_{k+1}$  at time step  $t = k + 1$  can be approximated by:

$$\delta \hat{x}_{k+1} = A_k \delta \hat{x}_k + B_k \delta \hat{u}_k \quad (11)$$

Given that the nominal point  $\bar{x}_{k+1}$  and the linearisation matrices  $A_k, B_k$  are parametrically dependent on  $\bar{x}_k, \bar{u}_k, \bar{w}_k$ , and that the value for  $x_k$  and  $w_k$  are already known at a given sampling time  $t = k$  (either by measurements or by state estimation), the value for  $\bar{x}_{k+1}$  can only be computed if the value for the optimal control input  $\bar{u}_k$  is known. Similar for  $\bar{x}_{k+2}$ , for which the value of  $\bar{u}_{k+1}$  is needed.

If values for the future optimal-nominal input trajectory  $\bar{U} = [\bar{u}_k^T, \bar{u}_{k+1}^T, \dots, \bar{u}_{k+N_p-1}^T]^T$  are assumed or guessed, the projected nominal state trajectory  $\bar{X} = [\bar{x}_{k+1}^T, \bar{x}_{k+2}^T, \dots, \bar{x}_{k+N_p}^T]^T$  and the linearisation matrices  $A_k, B_k$  can be computed for future time steps  $t = k + 1, k + 2, \dots, k + N_p$ , where  $N_p$  is known as the prediction horizon. A typical strategy to guess the nominal input trajectory  $\bar{U}$  (no necessarily the optimum) is to simulate the system in free response, i.e.  $\bar{U} = [0_0, \dots, 0_{N_p-1}]$  for  $k = 0$ , the system is linearised around the resulting state trajectory, and the optimisation improves the initial guess at every iteration using a Newton-type framework (Diehl et al., 2005; Gros et al., 2016). This technique is often referred as *single-shooting*. Other techniques such as *multiple shooting* and *collocation points* can also be used with the proposed approach (Quirynen et al., 2015).



After obtaining  $\bar{X}$  with  $\bar{U}$ , Equation (11) can be shifted forward:

$$\delta\hat{x}_{k+2} = A_{k+1}\delta\hat{x}_{k+1} + B_{k+1}\delta\hat{u}_{k+1} \quad (12)$$

Substituting Equation (11) into Equation (12) yields:

$$\delta\hat{x}_{k+2} = A_{k+1}(A_k\delta\hat{x}_k + B_k\delta\hat{u}_k) + B_{k+1}\delta\hat{u}_{k+1} \quad (13)$$

By recursively repeating the preceding procedure for  $N_p$  steps and considering just the system output (Equation (8)), the predicted deviations from the nominal output trajectory may be expressed in a matrix form by:

$$\delta\hat{Y} = G_y\delta x_k + H_y\delta\hat{U} \quad (14)$$

where  $\delta\hat{Y} = \hat{Y} - \bar{Y} = [\delta y_{k+1}^T, \delta y_{k+2}^T, \dots, \delta y_{k+N_p}^T]^T$  are the output deviations,  $\delta\hat{U} = \hat{U} - \bar{U} = [\delta\hat{u}_k^T, \delta\hat{u}_{k+1}^T, \dots, \delta\hat{u}_{k+N_p-1}^T]^T$  are the control input deviations. The matrices  $G_y$  and  $H_y$  are given by:

$$G_y = \begin{bmatrix} C_1A_0 \\ C_2A_1A_0 \\ \vdots \\ C_{N_p}A_{N_p-1} \cdots A_1A_0 \end{bmatrix} \quad (15)$$

$$H_y = \begin{bmatrix} C_1B_0 & \mathbf{0} & \cdots & \mathbf{0} \\ C_2A_1B_0 & C_2B_1 & \cdots & \vdots \\ C_3A_2A_1B_0 & C_3A_2B_1 & \ddots & \mathbf{0} \\ \vdots & \vdots & \ddots & \vdots \\ C_{N_p}A_{N_p-1} \cdots A_1B_0 & C_{N_p}A_{N_p-1} \cdots A_2B_1 & \cdots & C_{N_p}B_{N_p-1} \end{bmatrix} \quad (16)$$

The dimensions for these matrices are  $G_y = [N_p n_y \times n_x]$ ,  $H_y = [N_p n_y \times N_p n_u]$ , and  $C_k$  is the partial derivative of Equation (8) w.r.t. nominal state, evaluated at the specific time step  $t = k$ , and is given by:

$$C_k = \left. \frac{\partial g(x, u, w)}{\partial x} \right|_{\substack{\bar{x}_k \\ \bar{u}_k \\ \bar{w}_k}}$$

In addition, the matrix  $\mathbf{0}$  represents a matrix of zeros with the same dimensions as the matrix  $C_k B_k$ .

### 4.3 Optimisation

Following the definition of the prediction models, the cost function described in Equation (5a) can be recast as follows:

$$J = \frac{1}{2}\hat{Y}^T Q \hat{Y} + \frac{1}{2}\delta\hat{U}^T R \delta\hat{U} \quad (17)$$

where the matrix  $R$  is a positive definite matrix with dimensions  $[N_p n_u \times N_p n_u]$  and constant elements over its diagonal.  $Q$  is selected as a block diagonal matrix with dimensions  $[N_p n_u \times N_p n_u]$  and inner matrices  $q_i$  used to compute the product  $\hat{\theta}_k \times$

$\gamma_k u_{k-1}$  as defined in Guerrero-Fernández et al. (2020).

$$Q = \begin{bmatrix} q_1 & \mathbf{0} & \cdots & \mathbf{0} \\ \mathbf{0} & q_2 & \ddots & \vdots \\ \vdots & \ddots & \ddots & \mathbf{0} \\ \mathbf{0} & \cdots & \mathbf{0} & q_{N_p} \end{bmatrix} \quad q_i = \begin{bmatrix} 0 & 1 \\ 1 & 0 \end{bmatrix} \quad \forall i = [1, N_p] \quad (18)$$

The reader may have observed that, in addition to the condensed format of (17), the cost differs from (5a) in that it includes an additional term that penalises the input deviation. The input deviation term is included for two reasons: first, it smooths the control signal, making the requirement for the actuator's response limit less stringent, and second, according to Ringwood et al. (2014), Li and Belmont (2014), Mériçaud and Tona (2020) and Bacelli and Coe (2021), a reactive control strategy with a cost function based solely on maximising the extracted energy can result in overall negative energy absorbed, implying that the system is losing energy rather than absorbing energy from the waves.

Finally, the standard quadratic programming (QP) formulation is obtained by substituting the linearised output prediction Equation (14) in Equation (17), grouping similar terms w.r.t. the decision variable  $\delta\hat{U}$ , and omitting any constant terms in the cost function:

$$J = \frac{1}{2}\delta\hat{U}^T E \delta\hat{U} + \delta\hat{U}^T f \quad \text{s.t.} \quad M\delta\hat{U} \leq \rho \quad (19a)$$

$$E = H_y^T Q H_y + R \quad (19b)$$

$$f = H_y^T Q [\bar{Y} + G_y \delta x_k] \quad (19c)$$

where  $E \in \mathbb{R}^{N_p n_u \times N_p n_u}$  is a symmetric matrix known as the hessian and  $f \in \mathbb{R}^{N_p n_u}$  is a column vector usually referred as the linear term;  $M \in \mathbb{R}^{2N_p n_u \times N_p n_u}$  is the constraints matrix and  $\rho \in \mathbb{R}^{2N_p n_u}$  is the constraints vector, defined as:

$$M = \begin{bmatrix} I \\ -I \end{bmatrix} \quad \rho = \begin{bmatrix} U_{max} - \bar{U} \\ -(U_{min} - \bar{U}) \end{bmatrix} \quad (20)$$

Here, the matrix  $M$  and the vector  $\rho$  are defined considering only constraints in the control input. If constraints for any states are required,  $M$  and  $\rho$  must be slightly reformulated. The reader may have also noticed that  $G_y$  and  $H_y$ , therefore  $E$  and  $f$ , are time-dependent, which is one of the main reasons why NMPC is computationally expensive.

After defining  $E, f, M$ , and  $\rho$ , the OCP can be solved using any QP solver, such as Matlab's `quadprog` function, `qpOASES` (Ferreau et al., 2008), and so on. In this study, `qpOASES` was used. Once the QP problem has been solved, the new control input sequence is computed, recalling that  $\hat{U} = \bar{U} + \delta U$ . Only the first input is applied to the system, and the procedure is repeated at the next time step, which is known as the *receding horizon* scheme (González-Villarreal & Rossiter, 2020a).

### 4.4 Real-time iterations scheme

In this Section, we recall the RTI scheme first introduced by Diehl et al. (2005). A fully converged NMPC should ideally re-linearise the predictions and thus cost function Equation (19a) until no deviations are necessary, i.e.  $\delta\hat{U} =$

0 (González-Villarreal & Rossiter, 2020a). is not computationally tractable in real-time applications since one must provide a solution at each time step under strict time constraints and avoid solving a problem that is just ‘getting older’ (Gros et al., 2016).

The RTI exploits the fact that NMPC is required to solve optimisations closely related from one-time step to the next, which has proven to be a very successful and popular method of tackling the problem at hand. The RTI scheme is summarised in the following subsections.

#### 4.4.1 Initial value embedding

Choosing an appropriate initial estimate for  $\hat{U}$  optimal, denoted as  $\hat{U}^*$ , is critical for fast and reliable convergence of the sequential quadratic programming (SQP) approach. It can help avoid a premature exit from the SQP algorithm with an infeasible solution, but also it allows for complete Newton steps in the SQP, which yields a fast convergence rate (Gros et al., 2016). To facilitate the estimation, the previous optimal input trajectory is utilised in a shifted version to hot-start the solution at the following sampling time, generally by duplicating the last value. In the case of active-set-based SQP, the Lagrange multipliers  $\lambda$ , linked to the optimisation constraints, may also be used to hot-start the QP in a shifted version (González-Villarreal & Rossiter, 2020b).

#### 4.4.2 Single sequential quadratic programming iteration

One of the most efficient approaches to handle nonlinear programming (NLP) problems is sequential quadratic programming (SQP) ( Nocedal, 2006). In the SQP approach, the NLP is sequentially approximated by QPs, delivering Newton directions for performing steps towards the solution starting from the available guess. Iterations are performed until convergence is reached, taking (not necessarily full) Newton steps (Gros et al., 2016). However, within the RTI scheme, only one iteration of SQP is performed, given that the optimisation is ‘warm-started’ from the prior solution (González-Villarreal & Rossiter, 2020b).

#### 4.4.3 Computation separation

The separation of the computation is perhaps the essential aspect of the RTI scheme. It divides the calculations into preparation and feedback phases. A timing diagram that illustrates this can be seen in Gros et al. (2016).

- *Preparation phase*: It uses the last applied input trajectory  $u_{k-1}$  to predict the state  $\hat{x}_{k|k-1}$ , which is then used to linearise and prepare a QP to be later solved in the feedback phase.
- *Feedback phase*: as soon as the state  $x_k$  becomes available, the state deviation  $\delta x_k = x_k - \hat{x}_{k|k-1}$  is used to complete the calculation of  $f, \rho$  and the optimal correction  $\delta \hat{U}^*$  to the current trajectory  $\hat{U}$ .

#### 4.5 Efficient algorithm $O(N^2)$ to compute the hessian $E$

Because of its dimensions and time-varying nature, the hessian  $E$  is one of the most computationally expensive operations of the OCP mentioned above. Fortunately, the underlying structure of the matrix  $H_y$  allows the implementation of the so-called  $O(N^2)$

condensing algorithm, initially presented in Andersson (2013) and re-derived in González-Villarreal (2021). It provides an efficient calculation of the hessian term  $H_y^T Q H_y$  via a recursive-like operation that takes advantage of the block triangular structure of matrix  $H_y$  to avoid the zero terms computations, as well as any repeated terms that may result from the direct calculation. However, the condensing algorithm  $O(N^2)$  presented in the preceding studies was derived for quadratic optimisations considering states/inputs and state-input costs, whereas, for the formulation presented in this paper, an algorithm for ‘output-only’ cost functions is required.

For the sake of simplicity, the algorithm is derived here considering the resulting hessian with a short horizon of  $N_p = 3$ .

$$E = \underbrace{\begin{bmatrix} C_1 B_0 & 0 & 0 \\ C_2 A_1 B_0 & C_2 B_1 & 0 \\ C_3 A_2 A_1 B_0 & C_3 A_2 B_1 & C_3 B_2 \end{bmatrix}}_{H_y} \underbrace{\begin{bmatrix} q_1 & 0 & 0 \\ 0 & q_2 & 0 \\ 0 & 0 & q_3 \end{bmatrix}}_Q$$

$$E = \underbrace{\begin{bmatrix} C_1 B_0 & 0 & 0 \\ C_2 A_1 B_0 & C_2 B_1 & 0 \\ C_3 A_2 A_1 B_0 & C_3 A_2 B_1 & C_3 B_2 \end{bmatrix}}_{H_y}$$

$$E = \begin{bmatrix} E_{1,1} & E_{1,2} & E_{1,3} \\ E_{2,1} & E_{2,2} & E_{2,3} \\ E_{3,1} & E_{3,2} & E_{3,3} \end{bmatrix}$$

One can see that a good starting point towards computing the hessian is the multiplication of  $Q H_y$ . The resulting matrix  $S$  is given by:

$$S = \begin{bmatrix} s_{1,1} & 0 & 0 \\ s_{2,1} & s_{2,2} & 0 \\ s_{3,1} & s_{3,2} & s_{3,3} \end{bmatrix} = \begin{bmatrix} q_1 C_1 B_0 & 0 & 0 \\ q_2 C_2 A_1 B_0 & q_2 C_2 B_1 & 0 \\ q_3 C_3 A_2 A_1 B_0 & q_3 C_3 A_2 B_1 & q_3 C_3 B_2 \end{bmatrix} \quad (21)$$

Separating the hessian column-wise, the first column of it is computed as follows:

$$\begin{bmatrix} E_{1,1} \\ E_{2,1} \\ E_{3,1} \end{bmatrix} = \begin{bmatrix} B_0^T C_1^T & B_0^T A_1^T C_2^T & B_0^T A_1^T A_2^T C_3^T \\ 0 & B_1^T C_2^T & B_1^T A_2^T C_3^T \\ 0 & 0 & B_2^T C_3^T \end{bmatrix} \begin{bmatrix} s_{1,1} \\ s_{2,1} \\ s_{3,1} \end{bmatrix} \quad (22)$$

The algorithm is based on iteratively reusing terms that were computed previously. Starting from the last term  $E_{3,1}$ :

$$E_{3,1} = B_2^T C_3^T s_{3,1} \quad \mapsto \quad Z_{3,1} = C_3^T s_{3,1}$$

$$E_{3,1} = B_2^T Z_{3,1}$$

The next term  $E_{2,1}$  is computed as:

$$E_{2,1} = B_1^T C_2^T s_{2,1} + B_1^T A_2^T C_3^T s_{3,1}$$

Reusing the term  $Z_{3,1}$  computed previously:

$$E_{2,1} = B_1^T (C_2^T s_{2,1} + A_2^T Z_{3,1}) \quad \mapsto \quad Z_{2,1} = C_2^T s_{2,1} + A_2^T Z_{3,1}$$

$$E_{2,1} = B_1^T Z_{2,1}$$



Using the same logic, the last term  $E_{1,1}$  can be calculated as function of  $Z_{2,1}$ , and hence of  $Z_{3,1}$ :

$$E_{1,1} = B_0^T (C_1^T s_{1,1} + A_1^T Z_{2,1}) \quad \mapsto \quad Z_{1,1} = C_1^T s_{1,1} + A_1^T Z_{2,1}$$

$$E_{1,1} = B_0^T Z_{1,1}$$

Thus, an obvious pattern can be seen where the hessian can be calculated by recursively computing the terms with an expression like  $Z_{k,j} = C_k^T s_{k,j} + A_j^T Z_{k+1,j}$  for  $k, j \in [1, \dots, N_p \times n_u]$ , and then calculating the hessian term  $E_{k,j} = B_{k-1}^T Z_{k,j}$ . Keeping in mind that in the case where  $k = j$ , the term  $R(k, j)$  needs to be added to  $E_{k,j}$ , i.e. to the diagonal of the hessian, see Equation (19b).

Because the hessian is symmetric (Nocedal, 2006), the final algorithm only calculates the lower triangular terms and duplicates the rest of the terms.

Finally, this approach can also be used to re-derive the algorithm  $O(N)$  (Andersson, 2013), which can be used to calculate the linear term  $f$ , see Equation (19c), for 'output-only' cost functions.

## 5. Numerical results

In this section, numerical results of the proposed control strategy implemented on the benchmark scale model of the Wavestar (Ringwood et al., 2017) are presented.

### 5.1 Model parameters

The model parameters used in this study are summarised in Table 1.

### 5.2 Wave conditions

The wave climate is characterised by the significant wave height  $H_{m0}$ , the peak wave period  $T_p$  and the wave direction. A series of three unidirectional sea states, generated using the JONSWAP spectrum, are used for this study. The spectrum parameters are given in Table 2, based on the sea states used in the WECCOMP (Tona et al., 2019).

### 5.3 Simulation and control parameters

Given that the main goal of this work is to evaluate the RTI-NMPC proposed for WECs, all simulation trials were done in the nominal case, i.e. no noise or uncertainty was included. It

**Table 1.** Model parameters for the scale model of the Wavestar device, taken from Tona et al. (2019) and Ringwood et al. (2017).

Hydrodynamic parameters		
Inertia of arm and float	$J$	1.04 kg m <sup>2</sup>
Added inertia	$J_\infty$	0.4805 kg m <sup>2</sup>
Hydrostatic stiffness coefficient	$K_{hs}$	92.33 N m rad <sup>-1</sup>
Rotational linear damping	$b_v$	1.80 N m rad <sup>-1</sup> s <sup>-1</sup>
Radiation moment impulse response realisation		
$A_r = \begin{bmatrix} -13.59 & -13.35 \\ 8.00 & 0.00 \end{bmatrix}$	$B_r = \begin{bmatrix} 8.0 \\ 0.0 \end{bmatrix}$	
$C_r = \begin{bmatrix} 4.739 & 0.5 \end{bmatrix}$	$D_r = -0.1586$	

**Table 2.** Parameters for wave generation using JONSWAP spectrum. Significant wave height  $H_{m0}$ , peak period  $T_p$  and peak enhancement factor  $\gamma$ .

Name <sup>a</sup>	$H_{m0}$ [m]	$T_p$ [s]	$\gamma$ [-]	Duration [s]
SS4	0.0208	0.988	3.3	98.8
SS5	0.0625	1.412	3.3	141.2
SS6	0.1042	1.836	3.3	183.6

<sup>a</sup>Names are given to have consistency with the names given in the WECCOMP (Tona et al., 2019).

**Table 3.** Simulation and control tuning parameters

Parameter	Value
Simulation time [s]	$100 \times T_p$
Control sampling time [ms]	10
Prediction horizon [samples] <sup>⊗</sup>	Round( $2 \times T_p/dt, 5$ )
$\mu_{gen}^*$	0.7
$\mu_{mot}^*$	$0.7^{-1}$
$\varphi^\dagger$	1000
Control limit [Nm]	$\pm 12$

\*Suggested by Ringwood et al. (2017).

†Used in PTO efficiency function approximation.

⊗Operator Round(number, multiple) returns a number rounded to the desired multiple.

was also assumed that the vector containing the future wave excitation moment is known throughout the prediction horizon.

Regarding the prediction horizon, research on wave excitation force prediction suggests that prediction strategies can predict wave excitation force for swell waves extremely accurately up to two peak wave periods in the future (Fusco & Ringwood, 2010). In light of the foregoing, a prediction horizon equivalent to two peak wave periods ( $N_p = 2 \times T_p/dt$ ) was chosen for each sea state. Other relevant control tuning parameters are summarised in Table 3.

### 5.4 Results on the amount of energy absorbed

With the idea to have a reference point for each sea state, simulations were carried out using NMPC with an efficiency of 100%. This will give us an estimate of how much energy can be harvested in the case of an ideal bi-directional PTO system.

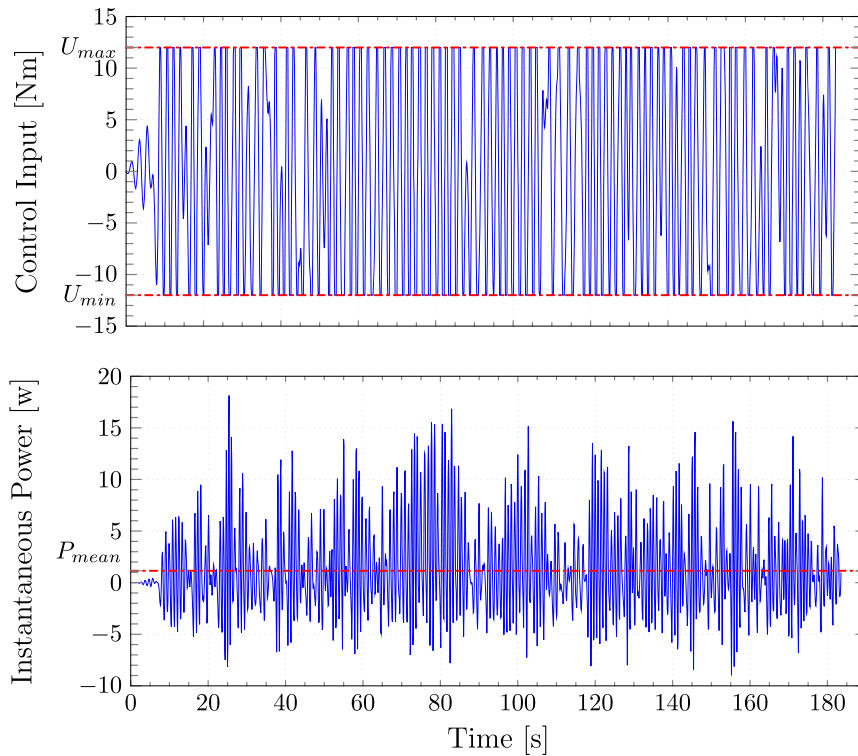
Figure 2 shows the absorbed power over the simulation time for the sea state SS6. For this simulation, the absorbed energy was 249.75 J with a mean power of 1.4988 W.

Figure 2 also shows how the control input takes the form of a bang-bang type of control, mostly assigning the values of  $u_k = \pm 12$ . Similar results were obtained for sea states SS4 and SS5, summarised in Table 4.

After establishing a reference point for each sea state, further simulations were run with the specified value for PTO system efficiency (see Table 3).

Figure 3 depicts the absorbed power by the WEC model across the simulation time with a cost function without the matrix  $R$  (See Equation (19a)), which penalises the input deviation. Figure 3 and Table 5 complement prior studies (Bacelli & Coe, 2021; Li & Belmont, 2014; Mériçaud & Tona, 2020; Ringwood et al., 2014) where energy loss was reported. Even when considering the PTO system efficiency in the OCP at each sample time, a reactive control strategy can result in overall negative energy absorbed if not correctly tuned.





**Figure 2.** Control input and absorbed power by the Wavestar model under sea state SS6 with an ideal bidirectional PTO system. The red dashed line represents the mean absorbed power.

**Table 4.** Energy absorbed and mean power for the sea states considering an ideal bidirectional PTO System.

Sea State	Energy Absorbed [J]	Mean Power [W]
SS4	2.90	0.0366
SS5	71.78	0.5820
SS6	249.75	1.4988

Another insight we can get from Figure 3 is that, even when the control input constraints are met, the input trajectory does not appear acceptable due to the fast change in its value, resulting in severe mechanical wear of the actuator, shortening its life cycle. Hence, there needs to be a trade-off between energy capture and actuator activity in practice.

On the other hand, Figure 4 depicts the control input and the absorbed power for sea state SS6 across the simulation time after simulating the system with a cost function as described in Equation (19a).

From the data depicted in Figure 4 we can make the following remarks. First, it is clear that the proposed control strategy is successful in absorbing a net positive power from the ocean waves; second, in contrast to the findings in Figure 3, RTI-NMPC with the added weighting matrix  $R$  strives to avoid consuming energy from the grid; and third, one can see how the control input is smoother for RTI-NMPC with the added weighting matrix  $R$  compared with the one presented in Figure 3 (the reader may consider the resolution for the time length

shown in both figures). For sea states SS4 and SS5, similar findings are obtained with cost function (19a), these are presented in Table 6.

Now, to compare the control strategy proposed around RTI-NMPC with the added weighting matrix  $R$ , two additional sets of simulations were performed using a linear model predictive controller (MPC) and a proportional controller, also known as resistive control in the ocean wave energy community (Maria-Arenas et al., 2019; Sanchez et al., 2015; Wang et al., 2018).

The advantage of employing a resistive control is that it is computationally cheap, i.e. speedy and physically simple to implement, for example, with electronic components. Still, the disadvantage is that it is suboptimal, and the proportional gain must be adjusted for each specific sea state. MPC, on the other hand, even though it attempts to provide an optimal solution at each sample time, the absence of the PTO system efficiency in the OCP renders its solution meaningless at the current time step, resulting in a suboptimal control law, or even in a net negative absorbed energy, depending on the sea state and tuning parameters used in the simulation. For comparative purposes, Figure 5 shows the control input and absorbed power by the Wavestar model for sea state SS6. Figure 6 shows the energy absorbed by the WEC for each control strategy.

The reader may also see in Figure 6 the percentage of energy absorbed in comparison to the ideal scenario with an efficiency of 100%. From there, we can observe that, while the proportion of energy collected by RTI-NMPC is low in general, 58.9% of

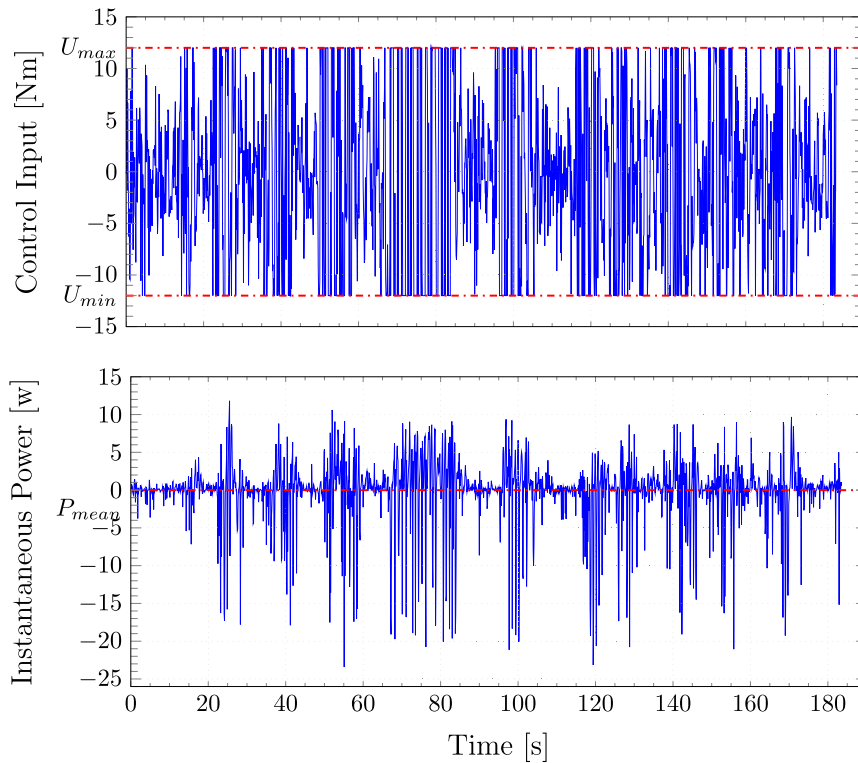


**Figure 3.** Control input and absorbed energy by the PTO system with an efficiency value as presented in Table 3 and a cost function without the matrix  $R$  for sea state SS6. The mean delivered power is  $-0.0087$  W and absorbed energy of  $-7.8038$  J, which represent a loss of energy.

**Table 5.** Energy absorbed and mean power for the sea states for a nonideal bidirectional PTO System using a cost function inside RTI-NMPC control strategy without the matrix  $R$ .

Sea State	Energy Absorbed [J]	Mean Power [W]
SS4	-65.3	-0.6234
SS5	-46.4	-0.3252
SS6	-7.8038	-0.0087

249.5 J, it is significantly higher when compared to the other two control laws considered, 20.4% for MPC and 23.6% for the resistive controller. Between them, RTI-NMPC can absorb roughly three times more than the MPC and two and a half times more than the resistive controller.

Another interesting fact we can extract from these results is that standard MPC, which is well understood and highly praised for linear systems, could not extract more energy than a simple resistive controller. So, linear MPC is not worth the effort, especially considering the extra costs when designing/buying a PTO system that can offer a bidirectional energy flow.

Finally, an intriguing finding is that, as indicated in Table 6, linear MPC cannot extract energy for sea state 5. The total amount of energy absorbed is negative, implying that the system loses energy rather than absorbing it from the waves. This energy loss is because MPC's forecasts are invalid since it does not incorporate the PTO system's efficiency into each OCP. To put it another way, the MPC controller borrows energy from the grid with the 'promise' of returning it with interest in the

not-too-distant future. Yet, the controller fails due to inaccurate predictions and thus cannot meet this promise.

### 5.5 Computational efficiency of the proposed NMPC algorithm

Before evaluating the computational performance of the proposed RTI-NMPC strategy for each of the sea states, we are interested in highlighting how much time may be saved when computing the hessian using the proposed algorithm  $O(N^2)$  against standard matrix-vector operations. The average time required to calculate the hessian for both approaches mentioned above is summarised in Table 7 for different prediction horizons.

To determine the average execution time of the hessian and the proposed RTI-NMPC strategy, a customised C++ code was written using the Eigen3 C++ library and tested on a PC running Ubuntu 20.04 LTS terminal for Windows 10 with an Intel i5-7400 CPU @ 3.4 GHz with 8 GB of RAM. For each prediction horizon, the average execution time was calculated using 10000 simulations.

Table 7 shows how the time saving from computing the hessian increases as the number of points in the prediction horizon increases. Even though we know that the time it takes to compute the hessian is not the only factor to consider when trying to solve an OCP, it is undoubtedly the most important.

For example, using normal matrix-vector operations, we can observe that computing the hessian for 300 steps ahead takes

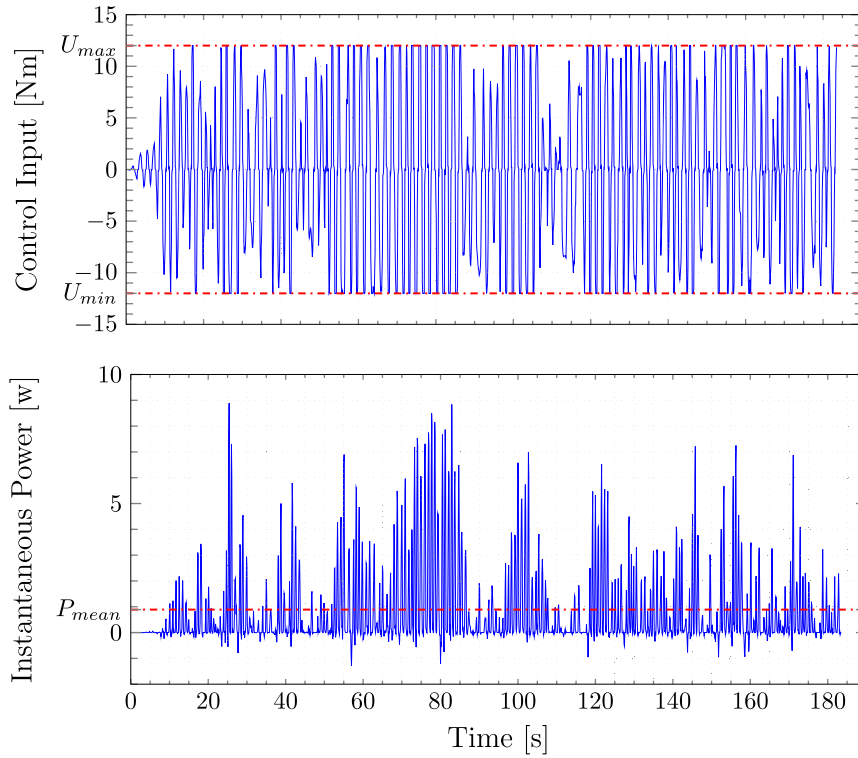


**Figure 4.** Control input and absorbed power by the Wavestar model undersea state SS6 using a cost function without considering the matrix  $R$  that penalises the input slew rate.

**Table 6.** Energy absorbed and mean power for resistive control, MPC, and RTI-NMPC for each sea state.

Sea State	Resistive		MPC		RTI – NMPC	
	Absorbed Energy [J]	Mean Power [W]	Absorbed Energy [J]	Mean Power [W]	Absorbed Energy [J]	Mean Power [W]
SS4	1.4974	0.01899	1.1914	0.01537	1.9499	0.02458
SS5	18.2770	0.1468	-13.1914	-0.1083	40.875	0.3210
SS6	59.0760	0.3566	51.0505	0.3532	147.092	0.8897

longer than the 10 ms sampling time used in this study. This indicates that the controller would not deliver a solution in the allotted time if typical matrix-vector operations are applied. In general, we can attain saving times of 1.5 times to 4.8 times for prediction horizons within the typical range that we can encounter in wave energy applications (between  $1 T_p$  to  $2 T_p$  of the dominant wave).

After studying the computing performance of algorithm  $O(N^2)$ , Table 8 gathers the average execution times with its respective standard deviation for the proposed RTI-NMPC using the algorithm  $O(N^2)$  to compute the hessian  $E$  and the algorithm  $O(N)$  for the linear term  $f$  for different prediction horizons for the three sea states. Recall that for this paper, the QP solver qpOASES was used.

Here, it is essential to note that the timings are determined by the number of points ahead used for the prediction horizon in each simulation, not the actual sea state characteristics.

Two prediction horizons were chosen for each sea state, corresponding to one peak period ( $1 \times T_p$ ) and two peak periods ( $2 \times T_p$ ) of the dominant wave. For example, that would be 185

and 365 steps ahead in the case for sea state SS6 (see Table 8 for the prediction horizon for the other sea states).

Let us now turn our attention to the execution times. For sea state SS6 we can see that for 185 steps ahead, the entire RTI-NMPC implementation would take around 1.581 ms (i.e.  $T_{exc} + \sigma_{exc}$ ) to solve the OCP at each time step, which is within the sampling time used in this study (10 ms). However, in the case of 365 steps ahead, the implementation would take around 11.840 ms in the worst-case scenario. If this is the case, the controller will not provide an optimal solution within the 10 ms sampling time frame.

One quick and straightforward solution to this problem could be to reduce the prediction horizon for something in between one peak period ( $1 \times T_p$ ) and two peak periods ( $2 \times T_p$ ) of the dominant wave. Moving blocking strategies, such as the one presented in González-Villarreal and Rossiter (2020b), could also be used as a possible solution but are not discussed here. The main takeaway from this Section is that the proposed algorithm would allow faster computation required to achieve real-time performance.



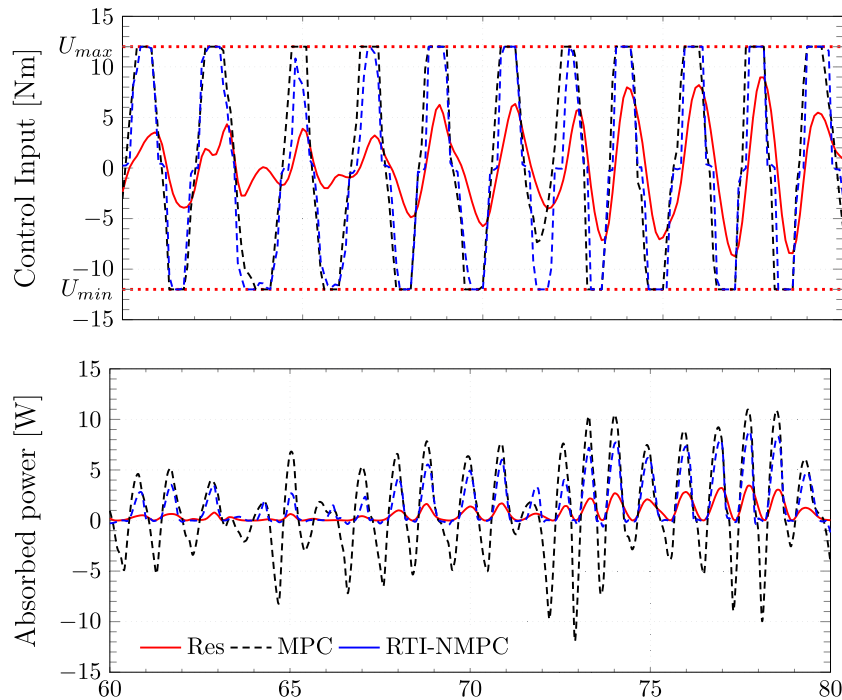


**Figure 5.** Control input and absorbed power by the Wavestar model undersea state SS6 with different control strategies. In blue NMPC using the modified cost function Equation (17), in black MPC and red resistive control proportional.

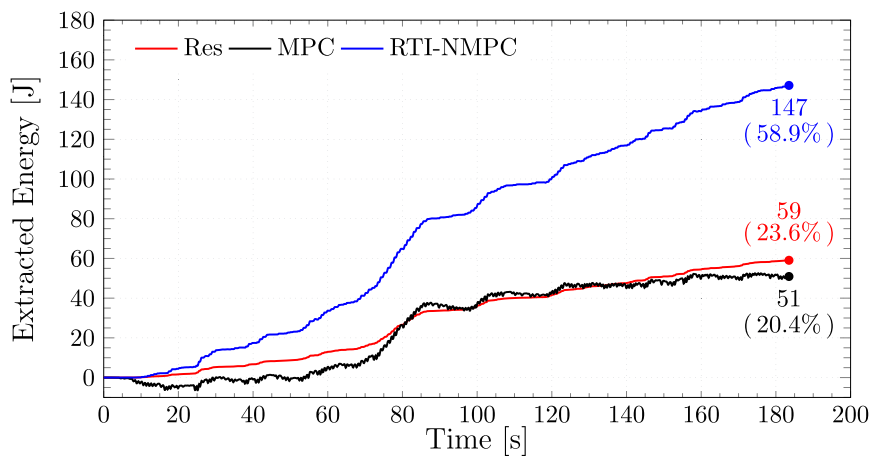


**Figure 6.** Energy absorbed by the Wavestar model undersea state SS6 with different control strategies. In blue RTI-NMPC using the modified cost function Equation (17), in black MPC and red resistive control. The value in parenthesis represents the percentage of energy absorbed concerning the maximum theoretical amount, 249.5 J.

## 6. Conclusions

This paper presents a nonlinear model predictive control strategy based on the real-time iteration scheme (NMPC-RTI). The controller can take into account the efficiency of the PTO system when solving the OCP at each time step. This is a key feature in a control policy that maximises the energy extracted from the ocean waves.

Computer simulations of a reactive controller for a single point absorber of a Wavestar-scale model wave energy converter with a nonideal PTO system efficiency indicate that the

RTI-NMPC approach can significantly improve wave energy converter performance.

The RTI-NMPC approach outperforms the other two control policies tested for the specific case in Section 5. The proposed approach harvests roughly two and a half times the amount of energy extracted by a resistive controller and nearly three times that of linear MPC while keeping the amount of power 'borrowed' from the grid to a bare minimum.

On the other hand, with linear MPC, despite attempting to provide an optimal solution at each sample time, the overall optimisation procedure becomes meaningless at the current

**Table 7.** Average time for computing the hessian  $E$  using algorithm  $O(N^2)$  and standard matrix-vector operations.

Np	Avg. Time using algorithm $O(N^2)$ [ms]	Avg. using standard matrix-vector operations [ms]	Gain [-]
100	0.318 ± 0.039	0.547 ± 0.141	1.720
200	1.236 ± 0.126	3.766 ± 0.245	3.047
300	2.848 ± 0.212	10.179 ± 0.583	3.574
365	4.500 ± 0.441	17.892 ± 1.040	3.976
400	5.426 ± 0.274	22.795 ± 0.497	4.201
500	8.803 ± 0.331	42.671 ± 0.789	4.847

**Table 8.** Average execution times for the proposed RTI-NMPC using the algorithm  $O(N^2)$  to compute the hessian  $E$  and the algorithm  $O(N)$  for the linear term  $f$  for different prediction horizons.

Np [Points ahead]	Avg. Exc. Time $T_{exc}$ [ms]	Avg. Standard Deviation $\sigma_{exc}$ [ $\pm$ ms]
		<b>SS6</b>
185	1.139	0.422
365	8.707	3.133
		<b>SS5</b>
140	0.607	0.199
280	3.971	0.746
		<b>SS4</b>
100	0.260	0.074
200	1.607	0.089

time step due to the absence of the PTO system efficiency in the OCP, which causes significant differences in the predictions of the generated energy resulting in an ill-posed optimisation (Rossiter, 2018). This ultimately leads to suboptimal control law, or even a net negative absorbed energy, depending on the sea state and tuning parameters used in the simulation.

Another interesting finding of this study, related to the previous point, is that in some cases, linear MPC cannot harvest more energy than a simple resistive controller, which makes it a very interesting feat that many previous studies have otherwise ignored. This may also be seen in the reactive power that MPC ‘consumes’ at specific points during the simulation, as opposed to the resistive controller, which consumes no power from the grid at all.

Finally, this study also derived a computationally efficient algorithm  $O(N^2)$  for ‘only-output’ cost functions, which offers significant time savings for computing the hessian for large prediction horizons. The computational time savings achieved by implementing the  $O(N^2)$  condensing procedure could allow for the use of larger prediction horizons and/or faster sample rates, as long as more precise prediction algorithms are available. Here, a sample rate of 10 ms was shown to be feasible with realistic horizons and without excessive computing power.

Future work on the proposed strategy will be concerning the robustness of the controller design in the face of unmodelled system dynamics and the performance of the control law with imperfect wave force/torque prediction.

To summarise, the controller presented in this paper: non-linear model predictive control based on the real-time iteration scheme can significantly improve wave energy converter performance, reducing at the same time the amount of energy temporally borrowed from the grid.

Ultimately, enhancing peer collaboration and transparency, the findings provided in this paper and the code used in the simulation are accessible through a Code Ocean capsule available at Guerrero-Fernández and González-Villarreal (2021).

## Acknowledgments

The first author would like to acknowledge the support of MICITT (Ministerio de Ciencia, Tecnología y Telecomunicaciones) of Costa Rica, who funded this work through a scholarship under the contract MICITT-PINN-CON-2-1-4-17-1-027.

## Disclosure statement

No potential conflict of interest was reported by the author(s).

## ORCID

Juan L. Guerrero-Fernandez  <http://orcid.org/0000-0002-4652-3005>

Oscar J. González-Villarreal  <http://orcid.org/0000-0003-1975-3582>

John Anthony Rossiter  <http://orcid.org/0000-0002-1336-0633>

## References

- Andersen, P., Pedersen, T. S., Nielsen, K. M., & Vidal, E. (2015). *Model predictive control of a wave energy converter*. 2015 IEEE Conference on Control Applications (CCA), Sidney, NSW, Australia, Sept. 21–23. <http://doi.org/10.1109/CCA.2015.7320829>.
- Andersson, J. (2013). A General-Purpose Software Framework for Dynamic Optimization (Doctoral dissertation, University of Sheffield) <https://lirias.kuleuven.be/retrieve/243411>.
- Bacelli, G., & Coe, R. G. (2021). Comments on control of wave energy converters. *IEEE Transactions on Control Systems Technology*, 29(1), 478–481. <https://doi.org/10.1109/TCST.2020.2965916>.
- Bacelli, G., Genest, R., & Ringwood, J. V. (2015). Nonlinear control of flap-type wave energy converter with a non-ideal power take-off system. *Annual Reviews in Control*, 40(2), 116–126. <https://doi.org/10.1016/j.jarcontrol.2015.09.006>.
- Bull, D., Jenne, D. S., Smith, C. S., Copping, A. E., & Copeland, G. (2016). Levelized cost of energy for a backward bent duct buoy. *International Journal of Marine Energy*, 16(3), 220–234. <https://doi.org/10.1016/j.ijome.2016.07.002>.
- Chang, G., Jones, C. A., Roberts, J. D., & Neary, V. S. (2018). A comprehensive evaluation of factors affecting the levelized cost of wave energy conversion projects. *Renewable Energy*, 127(11), 344–354. <https://doi.org/10.1016/j.renene.2018.04.071>.
- Coe, R. G., Bacelli, G., & Forbush, D. (2021, May). A practical approach to wave energy modeling and control. *Renewable and Sustainable Energy Reviews*, 142, 110791. <https://doi.org/10.1016/j.rser.2021.110791>.
- Cordonnier, J., Gorintin, F., De Cagny, A., Clément, A. H., & Babarit, A. (2015). SEAREV: Case study of the development of a wave energy converter. *Renewable Energy*, 80(10), 40–52. <https://doi.org/10.1016/j.renene.2015.01.061>.
- Creteil, J., Lewis, A. W., Lightbody, G., & Thomas, G. P. (2010). An application of model predictive control to a wave energy point absorber. *IFAC Proceedings Volumes*, 43(1), 267–272. <https://doi.org/10.3182/2010.329-3-PT-3006.00049>.
- Diehl, M., Bock, H. G., & Schlöder, J. P. (2005). A real-time iteration scheme for nonlinear optimization in optimal feedback control. *SIAM Journal on Control and Optimization*, 43(5), 1714–1736. <https://doi.org/10.1137/S0363012902400713>.
- Falcão, A. F., & Henriques, J. C. (2015, August). Effect of non-ideal power take-off efficiency on performance of single- and two-body reactively controlled wave energy converters. *Journal of Ocean Engineering and Marine Energy*, 1(3), 273–286. <https://doi.org/10.1007/s40722-015-0023-5>.
- Falnes, J. (2002). *Ocean waves and oscillating systems: Linear interactions including wave-energy extraction*. Cambridge: Cambridge University Press. <https://doi.org/10.1017/CBO9780511754630>.

- Ferreau, H. J., Bock, H. G., & Diehl, M. (2008). An online active set strategy to overcome the limitations of explicit MPC. *International Journal of Robust and Nonlinear Control*, 18(8), 816–830. <https://doi.org/10.1002/rnc.1251>.
- Fusco, F., & Ringwood, J. V. (2010). Short-term wave forecasting for real-time control of wave energy converters. *IEEE Transactions on Sustainable Energy*, 1(2), 99–106. <https://doi.org/10.1109/TSTE.2010.2047414>.
- Genest, R., Bonnefoy, F., Clément, A. H., & Babarit, A. (2014). Effect of non-ideal power take-off on the energy absorption of a reactively controlled one degree of freedom wave energy converter. *Applied Ocean Research*, 48(10), 236–243. <https://doi.org/10.1016/j.apor.2014.09.001>.
- González-Villarreal, O. J. (2021). Efficient Real-Time Solutions for Nonlinear Model Predictive Control with Applications. (Doctoral dissertation, University of Sheffield). <https://theses.whiterose.ac.uk/29336/>
- González-Villarreal, O. J., & Rossiter, A. (2020a). Fast hybrid dual mode NMPC for a parallel double inverted pendulum with experimental validation. *IET Control Theory and Applications*, 14(16), 2329–2338. <https://doi.org/10.1049/iet-cta.2020.0130>.
- González-Villarreal, O. J., & Rossiter, A. (2020b). Shifting strategy for efficient block-based non-linear model predictive control using real-time iterations. *IET Control Theory and Applications*, 14(6), 865–877. <https://doi.org/10.1049/iet-cta.2019.0369>.
- Gros, S., Zanon, M., Quirynen, R., Bemporad, A., & Diehl, M. (2016). From linear to nonlinear MPC: bridging the gap via the real-time iteration. *International Journal of Control*, 93(1), 62–80. <https://doi.org/10.1080/00207179.2016.1222553>.
- Guerrero-Fernández, J., & González-Villarreal, O. J. (2021). Code Ocean Capsule for paper: Efficiency-aware non-linear model-predictive control with real-time iteration scheme for wave energy converters <https://codeocean.com/capsule/6928248/tree>
- Guerrero-Fernández, J., González-Villarreal, O. J., Rossiter, A., & Jones, B. (2020). Model predictive control for wave energy converters: A moving window blocking approach. *IFAC-PapersOnLine*, 53(2), 12815–12821. 21st IFAC World Congress. <https://doi.org/10.1016/j.ifacol.2020.12.1960>.
- Li, G., & Belmont, M. R. (2014). Model predictive control of sea wave energy converters – Part I: A convex approach for the case of a single device. *Renewable Energy*, 69(09), 453–463. <https://doi.org/10.1016/j.renene.2014.03.070>
- Maria-Arenas, A., Garrido, A. J., Rusu, E., & Garrido, I. (2019). Control strategies applied to wave energy converters: State of the art. *Energies*, 12(16), 1–19. <https://doi.org/10.3390/en12163115>.
- Mérigaud, A., & Tona, P. (2020). Spectral control of wave energy converters with non-ideal power take-off systems. *Journal of Marine Science and Engineering*, 8(11), 1–15 <https://doi.org/10.3390/jmse8110851>.
- Neary, V. S., Lawson, M., Previsic, M., Copping, A., Hallett, K. C., Labonte, A., Rieks, J., & Murray, D. (2014). Methodology for Design and Economic Analysis of Marine Energy Conversion (MEC) Technologies. In *Marine Energy Technology Symposium*. Sandia National Laboratories. Technical Report
- Nguyen, H. N. N., Sabiron, G., Tona, P., Kramer, M. M., & Vidal Sanchez, E. (2016, June). Experimental validation of a nonlinear mpc strategy for a wave energy converter prototype. In *Proceedings of the International Conference on Offshore Mechanics and Arctic Engineering – OMAE* (Vol. 6, pp. 1–10). American Society of Mechanical Engineers (ASME). <https://doi.org/10.1115/OMAE2016-54455>.
- Nocedal, J., & Wright, Stephen J. (2006). *Numerical optimization* (2nd ed.). Springer Series in Operations Research and Financial Engineering. Springer New York, NY. <https://doi.org/10.1007/978-0-387-40065-5>.
- Quirynen, R., Vukov, M., & Diehl, M. (2015). Multiple shooting in a microsecond. In Thomas Carraro, Michael Geiger, Rolf Rannacher, & Stefan Körkel (Eds.), *Multiple shooting and time domain decomposition methods* (pp. 183–201). Springer Cham. [https://doi.org/10.1007/978-3-319-23321-5\\_7](https://doi.org/10.1007/978-3-319-23321-5_7).
- Ringwood, J. V., Bacelli, G., & Fusco, F. (2014). Energy-maximizing control of wave-energy converters: The development of control system technology to optimize their operation. *IEEE Control Systems Magazine*, 34(5), 30–55. <https://doi.org/10.1109/MCS.2014.2333253>.
- Ringwood, J. V., Ferri, F., Ruehl, K. M., Yu, Y. H., Coe, R. G., Bacelli, G., Weber, J., & Kramer, M. M. (2017). *A competition for WEC control systems*. Proceedings of the 12th European Wave and Tidal Energy Conference, Ireland, 27th Aug-1st Sept.
- Rossiter, J. A. (2018). *A first course in predictive control* (2nd ed.). Boca Raton: CRC Press. ISBN 9781032339160.
- Sanchez, E. V., Hansen, R. H., & Kramer, M. M. (2015). Control performance assessment and design of optimal control to harvest ocean energy. *IEEE Journal of Oceanic Engineering*, 40(1), 15–26. <https://doi.org/10.1109/JOE.2013.2294386>.
- Strager, T., Martin dit Neuville, A., Fernández López, P., Giorgio, G., Mureşan, T., & Andersen, P. (2014, June). *Optimising Reactive Control in Non-Ideal Efficiency Wave Energy Converters*. International Conference on Offshore Mechanics and Arctic Engineering, San Francisco, California, USA, June 8-13. <https://doi.org/10.1115/OMAE2014-23005>.
- Tedeschi, E., Carraro, M., Molinas, M., & Mattavelli, P. (2011). Effect of control strategies and power take-off efficiency on the power capture from sea waves. *IEEE Transactions on Energy Conversion*, 26(4), 1088–1098. <http://doi.org/10.1109/TEC.2011.2164798>.
- Tom, N., Ruehl, K., & Ferri, F. (2018). *Numerical Model Development and Validation for the WECCOMP Control Competition*. ASME 2018 37th International Conference on Ocean, Offshore and Arctic Engineering, Madrid, Spain, June 17-22. <https://doi.org/10.1115/OMAE2018-78094>.
- Tom, N. M., Madhi, F., & Yeung, R. W. (2019). Power-to-load balancing for heaving asymmetric wave-energy converters with nonideal power take-off. *Renewable Energy*, 131(1), 1208–1225. <https://doi.org/10.1016/j.renene.2017.11.065>.
- Tona, P., Nguyen, H. N., Sabiron, G., & Creff, Y. (2015). *An efficiency-aware model predictive control strategy for a heaving buoy wave energy converter*. 11th European wave and tidal energy conference-EWTEC 2015, Nantes, France, September 6-11. <http://www.ewtec.org/conferences/ewtec-2015/>.
- Tona, P., Sabiron, G., & Nguyen, H. N. (2019). An Energy-Maximising MPC Solution to the WEC Control Competition. ASME 2019 38th International Conference on Ocean, Offshore and Arctic Engineering, Glasgow, Scotland, UK, June 9-14. <https://doi.org/10.1115/OMAE2019-95197>.
- Tona, P., Sabiron, G., Nguyen, H. N., Mérigaud, A., & Ngo, C. (2020, August). *Experimental Assessment of the IFPEN Solution to the WEC Control Competition*. ASME 2020 39th International Conference on Ocean, Offshore and Arctic Engineering, Online, August 3-7. <https://doi.org/10.1115/OMAE2020-18669>.
- Wang, L., Isberg, J., & Tedeschi, E. (2018). Review of control strategies for wave energy conversion systems and their validation: The wave-to-wire approach. *Renewable and Sustainable Energy Reviews*, 81(11), 366–379. <https://doi.org/10.1016/j.rser.2017.06.074>.



---

# Non-linear Model Predictive Control based on Real-Time Iteration Scheme for Wave Energy Converters using WEC-Sim

The content of this manuscript has been presented at the ASME 2022 41<sup>st</sup> *International Conference on Ocean, Offshore, and Arctic Engineering OMAE2022*, Hamburg Germany (2022), and the version of record is published in the Proceedings of the Conference. It is included in this dissertation with the corresponding permission from ASME Publications.



# Nonlinear Model Predictive Control Using Real-Time Iteration Scheme for Wave Energy Converters Using WEC-Sim Platform

## Preprint

Juan Luis Guerrero-Fernández,<sup>1</sup> Nathan Michael Tom,<sup>2</sup> and John Anthony Rossiter<sup>1</sup>

*1 University of Sheffield*

*2 National Renewable Energy Laboratory*

*Presented at ASME 2022 41<sup>st</sup> International Conference on Ocean, Offshore and Arctic Engineering (OMAE2022)*

*Hamburg, Germany*

*June 5–10, 2022*

**NREL is a national laboratory of the U.S. Department of Energy  
Office of Energy Efficiency & Renewable Energy  
Operated by the Alliance for Sustainable Energy, LLC**

This report is available at no cost from the National Renewable Energy Laboratory (NREL) at [www.nrel.gov/publications](http://www.nrel.gov/publications).

Contract No. DE-AC36-08GO28308

**Conference Paper**  
NREL/CP-5700-81943  
June 2022





# Nonlinear Model Predictive Control Using Real-Time Iteration Scheme for Wave Energy Converters Using WEC-Sim Platform

## Preprint

Juan Luis Guerrero-Fernández,<sup>1</sup> Nathan Michael Tom,<sup>2</sup> and John Anthony Rossiter<sup>1</sup>

*1 University of Sheffield*

*2 National Renewable Energy Laboratory*

### Suggested Citation

Guerrero-Fernandez, Juan Luis, Nathan Tom, and John Rossiter. 2022. *Nonlinear Model Predictive Control Using Real-Time Iteration Scheme for Wave Energy Converters Using WEC-Sim Platform: Preprint*. Golden, CO: National Renewable Energy Laboratory. NREL/CP-5700-81943. <https://www.nrel.gov/docs/fy22osti/81943.pdf>.

**NREL is a national laboratory of the U.S. Department of Energy  
Office of Energy Efficiency & Renewable Energy  
Operated by the Alliance for Sustainable Energy, LLC**

This report is available at no cost from the National Renewable Energy Laboratory (NREL) at [www.nrel.gov/publications](http://www.nrel.gov/publications).

Contract No. DE-AC36-08GO28308

**Conference Paper**  
NREL/CP-5700-81943  
June 2022

National Renewable Energy Laboratory  
15013 Denver West Parkway  
Golden, CO 80401  
303-275-3000 • [www.nrel.gov](http://www.nrel.gov)

## NOTICE

This work was authored in part by the National Renewable Energy Laboratory, operated by Alliance for Sustainable Energy, LLC, for the U.S. Department of Energy (DOE) under Contract No. DE-AC36-08GO28308. Funding provided by the U.S. Department of Energy Office of Energy Efficiency and Renewable Energy Water Power Technologies Office. The views expressed herein do not necessarily represent the views of the DOE or the U.S. Government. The U.S. Government retains and the publisher, by accepting the article for publication, acknowledges that the U.S. Government retains a nonexclusive, paid-up, irrevocable, worldwide license to publish or reproduce the published form of this work, or allow others to do so, for U.S. Government purposes.

This report is available at no cost from the National Renewable Energy Laboratory (NREL) at [www.nrel.gov/publications](http://www.nrel.gov/publications).

U.S. Department of Energy (DOE) reports produced after 1991 and a growing number of pre-1991 documents are available free via [www.OSTI.gov](http://www.OSTI.gov).

*Cover Photos by Dennis Schroeder: (clockwise, left to right) NREL 51934, NREL 45897, NREL 42160, NREL 45891, NREL 48097, NREL 46526.*

NREL prints on paper that contains recycled content.





# NONLINEAR MODEL PREDICTIVE CONTROL BASED ON REAL-TIME ITERATION SCHEME FOR WAVE ENERGY CONVERTERS USING WEC-SIM

**Juan Luis Guerrero-Fernández\***  
Department of Automatic Control  
and System Engineering  
University of Sheffield  
Sheffield, United Kingdom  
Email: j.guerrero@sheffield.ac.uk

**Nathan Michael Tom**  
National Renewable  
Energy Laboratory  
Golden, CO, USA  
Email: nathan.tom@nrel.gov

**John Anthony Rossiter**  
Department of Automatic Control  
and System Engineering  
University of Sheffield  
Sheffield, United Kingdom  
Email: j.a.rossiter@sheffield.ac.uk

## ABSTRACT

*One of several challenges that wave energy technologies face is their inability to generate electricity cost-competitively with other grid-scale energy generation sources. Several studies have identified two approaches to lower the levelised cost of electricity: reduce the cost over the device's lifetime or increase its overall electrical energy production. Several advanced control strategies have been developed to address the latter. However, only a few take into account the overall efficiency of the power take-off (PTO) system, and none of them solve the optimisation problem that arises at each sampling time on real-time. In this paper, a detailed Nonlinear model predictive control (NMPC) approach based on the real-time iteration (RTI) scheme is presented, and the controller performance is evaluated using a time-domain hydrodynamics model (WEC-Sim). The proposed control law incorporates the PTO system's efficiency in a control law to maximise the energy extracted. The study also revealed that RTI-NMPC clearly outperforms a simple resistive controller.*

---

\*Address all correspondence to this author.

## 1 INTRODUCTION

A wave energy converter (WEC) is a device that converts the energy carried by the ocean waves into electrical energy through a power take-off (PTO). WECs can be classified into oscillating bodies or oscillating water columns based on their primary operating principle [1]. Today, a broad spectrum of concepts for wave energy conversion have been proposed and investigated.

One of several challenges that wave energy technologies face is their inability to generate electricity cost-competitively with other grid-scale energy generation sources, such as natural gas and wind [2]. The levelised cost of electricity (LCOE) is defined as the ratio of the total cost to total electrical energy produced over the lifetime of a wave energy converter, which is commonly reported in U.S. dollars per kilowatt-hour units [3]. Several studies have identified two ways to reduce the LCOE for ocean wave energy: reduce the cost over the device's lifetime or increase the device's overall electrical energy production [4–7].

Several control strategies for wave energy converters can be found in literature [8–10] and can be divided into two groups: passive control and active control. A passive

controller implements a force that opposes the movement of the point absorber, and the energy flow is unidirectional, from the ocean to the grid. Resistive control [8, 11–13] is an example of this type. On the other side, active controllers involve a bidirectional energy flow from the sea to the grid and vice versa. Model predictive control (MPC) and spectral and pseudospectral methods [9, 12, 13] belong to this category. This paper offers a solution for the latter: an advanced control strategy to significantly improve energy capture efficiency.

In [14], the performance of a reactively controlled single point absorber of a Wavestar WEC with a nonideally efficient PTO was studied for regular waves, and the performance of regular and irregular waves was studied in [11]. For regular and irregular waves, partial reactive control was suggested in [15] as a causal suboptimal control approach for a heaving single-body wave energy converter, along with studies of the impact of the actuators' efficiency in the annual mean absorbed power.

In [16], an MPC approach was described that explicitly considers the efficiency of the PTO system. However, this controller, similarly to the one presented by the same authors in [17, 18], cannot be used for real-time implementation with small sampling times ( $T_p \leq 50$  ms) since they are based on an offline solution [18]. Similar, the MPC algorithm presented in [17, 18] uses a discrete objective function that weights the instantaneous power value over the prediction horizon. The weightings are determined offline using an iterative optimisation approach based on repeated simulations of the WEC model over a set of sea states (a Nelder-Mead optimisation algorithm is used).

The major contribution of this paper is the implementation of a nonlinear model predictive control (NMPC) approach based on the real-time iteration (RTI) scheme [19] to incorporate the PTO system's efficiency when solving the optimal control problem (OCP) at each time step in a control policy that aims to maximise the amount of energy extracted from the ocean waves.

This research builds on previous work in [20]. A key extension is that the assumptions about the incident wave moment at the current time step and for a prediction horizon window are removed in this paper. Here, wave excitation moment is estimated using a Kalman filter, and the vector of future wave excitation moment is predicted using an autoregressive (AR) model. A further important novelty is that the simulation is performed on WEC-Sim to provide

a more realistic/accurate simulation.

The structure of this paper is outlined as follows. Section 3 presents the time-domain modelling of the wave energy converter used in this work. Section 2 formulates the general objective of any energy-maximising control strategy. A detailed description of the modelling, prediction, optimisation and real-time iteration to implement the proposed RTI-NMPC scheme are presented in Section 4. The results of the simulations are presented in Section 5. Finally, Section 6 contains conclusions, summarises the paper's contribution and describes future work.

## 2 PROBLEM FORMULATION

The main objective of a wave energy converter controller is to transfer as much energy as possible from the ocean waves to the grid for a broad range of sea states. The electrical energy  $E_e$  absorbed by the grid over a time horizon  $T$ , is defined as:

$$E_e = - \int_t^{t+T} P_e(\tau) d\tau = - \int_t^{t+T} \Gamma(\tau) P_m(\tau) d\tau \quad (1)$$

where  $P_e$  denotes the electrical power delivered to the grid,  $P_m$  the raw hydromechanical power absorbed by the PTO system,  $\Gamma$  the overall efficiency of the PTO system and  $\tau$  is the variable of integration.

The negative sign in Eq. (1) is because the energy is drawn from the WEC and thus the maximisation of the energy absorbed corresponds to a minimisation of the control objective [21].

The instantaneous hydromechanical absorbed power is given by:

$$P_m(t) = M_{pto}(t) \dot{\theta}(t) \quad (2)$$

where  $M_{pto}$  is the PTO moment and  $\dot{\theta}$  represents the angular velocity of the arm.

Finally, to use standard nomenclature,  $M_{pto}(t_k)$  is replaced by  $u_k$ , and the discrete-time optimisation problem is



given by:

$$\text{minimise } J = \sum_{i=1}^{N_p} \gamma_{k+i} u_{k+i-1} \dot{\theta}_{k+i} \quad (3a)$$

$$\text{s.t. } \underline{x}_{k+1} = f(\underline{x}_k, u_k, w_k) \quad (3b)$$

$$U_{min} \leq u_k \leq U_{max} \quad (3c)$$

where  $N_p$  is the prediction horizon, Eq. (3b) represents the WEC dynamics with the states  $\underline{x} = [\theta \ \dot{\theta} \ \underline{r}]^T$ , the variables in  $\underline{x}$  are defined in Section 3,  $u_k$  the control input,  $w_k$  the discrete-time value for the excitation moment  $M_{exc}(t_k)$ , and  $\gamma_k$  the specific value for the PTO efficiency at time instant  $t_k$ ; that is,  $\Gamma(t_k) = \gamma_k$ .

*Remark 1:* equation (3a) considers the velocity  $\dot{\theta}$  and the control input  $u$  at different time steps ( $k+i$  and  $k+i-1$ ). This is chosen to ensure causality of the solution as discussed in [22].

### 3 WAVE ENERGY CONVERTER MODELLING

The WEC chosen for testing the nonlinear controller strategy is a scaled model of a single device based on the Wavestar concept [23] used in the WEC Control Competition (WECCOMP) [24]. In this point-absorber WEC, a hemisphere acts as a floater, and it is coupled to a rotating arm hinged at a fixed reference point A. (See Fig. 1.)

#### State space model

The dynamics of the WEC in the pitch degree of freedom, assuming that the system's oscillations are modest, can be written in the time domain as follows [25]:

$$(J + J_\infty) \ddot{\theta}(t) = -K_{hs} \theta(t) - b_v \dot{\theta}(t) - M_{rad}(t) - M_{exc}(t) + M_{pto}(t) \quad (4a)$$

$$\dot{\underline{r}}(t) = A_r \underline{r}(t) + B_r \dot{\theta}(t) \quad (4b)$$

$$M_{rad}(t) = C_r \underline{r}(t) + D_r \dot{\theta}(t) \quad (4c)$$

where:

- $\theta$  represents the angular displacement of the arm with respect to the equilibrium position,  $\dot{\theta}$  and  $\ddot{\theta}$  represent the angular velocity and angular acceleration of the arm.

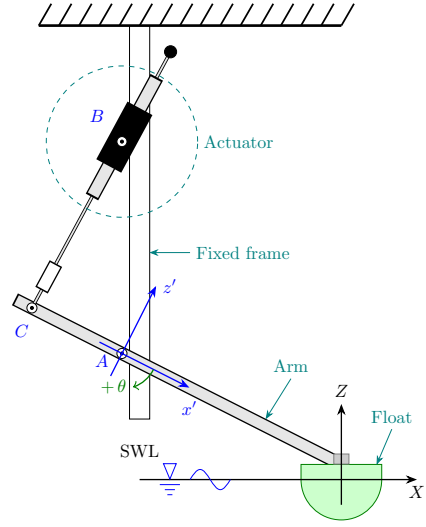


FIGURE 1. DIAGRAM OF THE WAVESTAR WEC SYSTEM

- $J$  is the total mass moment of inertia of the float and pivot arm.
- $J_\infty$  is the added mass moment of the inertia.
- $K_{hs}$  is the hydrostatic coefficient.
- $b_v$  is a linear damping coefficient.
- $M_{rad}$  is the radiation moment.
- $M_{exc}$  is the excitation moment due to the incident wave.
- $M_{pto}$  is the PTO moment (Input to the system).
- $A_r, B_r, C_r, D_r$ , are the state space matrices used to approximate the radiation moment  $M_{rad}$  avoiding the direct computation of the convolution integral in time-domain simulations. The state vector  $\underline{r}(t)$  have no physical meaning, but still contain information on the condition of the surrounding fluid [26].

For more details of the model development, the interested reader is referred to [3, 18].

*Remark:* Parameters and variables in Eq. (4) are specified with respect to the rotating point A.

#### Power take-off efficiency

PTO systems are not perfect in real-world applications, which means that the electrical power  $P_e$  is never equal to the absorbed mechanical power  $P_m$ , i.e.,  $0 \leq P_e \leq P_m$ . If a reactive control strategy is adopted, at certain times, the PTO system must return some electric power from the grid

back into the ocean ( $P_m \leq 0$ ). In those instants, and because of the losses in the conversion stages, the electrical power provided by the grid to the PTO system must be larger than  $|P_m|$ , i.e.,  $P_e \leq P_m \leq 0$ .

Given that the efficiency of the PTO system varies depending on the direction of the energy flow (float-to-grid or grid-to-float direction), the energy-maximising control strategy must consider the efficiency when solving for the optimal control input [27]. Other studies have discussed the impact of nonideal PTO efficiency on WEC control [11, 15–17, 28–32]. The main drawback of the cited studies is that none of them solves the optimal control problem related to the nonlinear output equation of the model in real time (see Eq. (9)), which is the main contribution of this paper.

The overall efficiency of a PTO system can be modelled using a modified-step function with two different values for the efficiency depending on whether the PTO system is working as a motor (grid-to-float) or as a generator (float-to-grid). Therefore, the instantaneous extracted power can be expressed as:

$$P_e(t) = \Gamma(t) P_m(t), \begin{cases} \Gamma(t) = \mu_{gen} & \text{if } P_m(t) \geq 0 \\ \Gamma(t) = \mu_{mot} & \text{if } P_m(t) < 0 \end{cases} \quad (5)$$

where  $\mu_{gen}$  is the global efficiency of the PTO system when it delivers energy to the grid and  $\mu_{mot}$  is the global efficiency when the PTO system consumes power from the grid.

### WEC-Sim numerical model

The work presented in this paper is based on a numerical simulation of the WEC device using the WEC-Sim code. WEC-Sim is a time-domain open-source code that solves the system dynamics of WECs consisting of rigid bodies, PTO systems, mooring systems, and control systems [3]. WEC-Sim calculates the dynamic response of the WEC device by solving the WEC's equation of motion for each rigid body about its centre of gravity  $C_g$  in the 6 degrees of freedom based on Cummins' equation [25]. The reader is referred to [3] for a detailed description of the code implementation and validation of the numerical model for the scaled Wavestar model against wave tank experiments.

### Wave excitation moment estimation

Many of the optimal control strategies for wave energy converters studied in the literature rely on the availability of measurements of the wave elevation and/or the exciting forces caused by the incoming waves [33–36]. This requirement is often difficult, if not impossible, to meet due to the limited number of sensors available and time. To that end, wave excitation force/moment has to be estimated via measuring other quantities, such as the position or velocity of the float.

The approach followed here, which was first proposed in [34] and implemented in [17], is based on a Kalman filter coupled with a random-walk model for the wave excitation moment. The main features of this solution are [17]: (1) only standard WEC measurements (position, velocity), (2) there is no significant lag compared to “true” values, and (3) no (implicit) unrealistic assumption about the time-invariant nature of the sea state is made; therefore it can be implemented in any sea state. The algorithm is fully described in [34].

### Wave excitation moment prediction

This study used a linear AR model to predict the wave excitation moment. The AR model, which was first introduced in [37], implies that the wave excitation moment  $M_{exc,k}$  at any given time  $t_k$  is linearly dependent on its past values via the parameters  $a_i$  (in [37] a concept was proposed for sea surface elevation, but the analogy to excitation moment is immediate):

$$M_{exc,k} = \sum_{i=1}^N a_i \cdot M_{exc,k-i} + \zeta_k \quad (6)$$

where  $N$  is the AR model order and  $\zeta$  is a disturbance term considered in the prediction.

If an estimate of the parameters  $\hat{a}_{i,k}$  at time instant  $t_k$  is computed and the noise is assumed to be Gaussian and white, the best prediction for the wave excitation moment  $M_{exc,k+p|k}$  at instant  $t_k$  can be derived from Eq. (6) as:

$$\hat{M}_{exc,k+p|k} = \sum_{i=1}^N \hat{a}_{i,k} \cdot \hat{M}_{exc,k+p-i|k} \quad (7)$$



where,  $\hat{M}_{exc,k+p-i|k} \equiv \hat{M}_{exc,k}$  if  $k+p-i \leq k$  (i.e., information already acquired, no need of prediction).

For brevity, the reader is invited to extract in-depth descriptions of AR models from [37–39].

#### 4 NONLINEAR MODEL PREDICTIVE CONTROL

NMPC is becoming increasingly popular for real-time optimal control solutions due to its ability to explicitly handle constraints and nonlinear dynamics that define the system of interest [40]. The following subsections are meant to provide a quick overview of each of the steps involved in RTI-NMPC.

Let us first define some notations used in the following sections. The upper-bar ( $\bar{\cdot}$ ) represents a nominally guessed point that is considered a “desirable-optimal” trajectory that the NMPC framework will use to optimise and improve the solution iteratively. Similarly, the hat ( $\hat{\cdot}$ ) represents the predicted trajectory value, whereas the variable with no additional notation will be reserved for the real/simulated value. In addition, for readability and to simplify the notation of the following equations, the underbar notation for vectors ( $\underline{\cdot}$ ) will be dropped.

##### Modelling

In this paper, a discrete-time nonlinear dynamic model describing the dynamics of a generic wave energy converter of the following form is considered:

$$x_{k+1} = f(x_k, u_k, w_k) \quad (8a)$$

$$y_k = g(x_k, u_k, w_k) \quad (8b)$$

where  $x_{k+1}$ ,  $u_k$  and  $y_k$  are vectors containing the  $n_x$  states,  $n_u$  inputs and  $n_y$  the outputs of the system, respectively.

The output function  $g(x_k, u_k, w_k)$  is selected as follows:

$$y_k = g_k = \begin{bmatrix} \hat{\theta}_k \\ \gamma_k u_{k-1} \end{bmatrix} \quad (9)$$

Equation (5), on the other hand, which models PTO efficiency, has a discontinuity between the two cases:  $P_m(t) \geq 0$  and  $P_m(t) < 0$ . Such a discontinuous function is undesirable in gradient-based optimisation approaches. A

smoothed approximation to Eq. (5), at  $P_m(t) = 0$ , must be implemented to avoid problems with the efficient implementation of the optimisation algorithm.

In [32] and [16], a modified-hyperbolic tangent function is used to approximate Eq. (5). The approximation using  $\tanh$  is preserved in this study and is given by:

$$\Gamma_{approx}(t) = \alpha + \beta \tanh(\varphi P_m(t)) \quad (10)$$

where  $\alpha$  is an offset,  $\beta$  is a scaling factor, and  $\varphi$  is a real positive parameter that determines the accuracy of the approximation.

##### Prediction

The prediction model discussed in this section is derived similarly to that presented in [41] and is presented here to allow the contents of this paper to be self-contained. Using a first order multivariable Taylor series expansion, the linearised model for Eq. (8a) at a given time step  $t_k$  is given by:

$$\hat{x}_{k+1} = \bar{x}_{k+1} + A_k \delta \hat{x}_k + B_k \delta \hat{u}_k + B_{w,k} \delta \hat{w}_k \quad (11)$$

where  $\delta \hat{x}_k = \hat{x}_k - \bar{x}_k$ ,  $\delta \hat{u}_k = \hat{u}_k - \bar{u}_k$ , and  $\delta \hat{w}_k = \hat{w}_k - \bar{w}_k$  are the deviations of the state, control input and wave excitation moment from their nominal points ( $\bar{x}_k, \bar{u}_k, \bar{w}_k$ ) at time step  $t_k$  respectively, and  $A_k$ ,  $B_k$ , and  $B_{w,k}$  are the partial derivatives with respect to the states, control input, and wave excitation input moment, which will be defined shortly.

The wave excitation moment deviation  $\delta \hat{w}_k$  requires special consideration at this stage. Because the approach described in this study is based on the prediction of future wave excitation moment, the nominal and predicted trajectory for the wave excitation moment is considered to be the same at each time step, i.e.,  $\delta \hat{w}_k = 0$  for all  $k$ , and thus the following derivation ignores this term.

$$A_k = \left. \frac{\partial f(x,u,w)}{\partial x} \right|_{\substack{\bar{x}_k \\ \bar{u}_k \\ \bar{w}_k}} \quad B_k = \left. \frac{\partial f(x,u,w)}{\partial u} \right|_{\substack{\bar{x}_k \\ \bar{u}_k \\ \bar{w}_k}}$$

$$\bar{x}_{k+1} = f(\bar{x}_k, \bar{u}_k, \bar{w}_k)$$

The deviation  $\delta \hat{x}_{k+1} = \hat{x}_{k+1} - \bar{x}_{k+1}$  at time step  $t_{k+1}$

can be approximated by:

$$\delta \hat{x}_{k+1} = A_k \delta \hat{x}_k + B_k \delta \hat{u}_k \quad (12)$$

Given that the nominal point  $\bar{x}_{k+1}$  and the linearisation matrices  $A_k, B_k$  are parametrically dependent on  $\bar{x}_k, \bar{u}_k, \bar{w}_k$ , and that the value for  $x_k$  is already known at a given sampling time  $t_k$  (either by measurements or by state estimation), the value for  $\bar{x}_{k+1}$  can only be derived by guessing (or estimating) an optimal-nominal value for  $\bar{u}_k$  around which the trajectory will be linearised.

If values for the future optimal-nominal input trajectory  $\bar{U} = [\bar{u}_k^T, \bar{u}_{k+1}^T, \dots, \bar{u}_{k+N_p-1}^T]^T$  are guessed, the projected nominal state trajectory  $\bar{X} = [\bar{x}_{k+1}^T, \bar{x}_{k+2}^T, \dots, \bar{x}_{k+N_p}^T]^T$  and the linearisation matrices  $A_k, B_k$  can be computed for future time steps  $t = k+1, k+2, \dots, k+N_p$ , where  $N_p$  is known as the prediction horizon. This technique is often referred as *single-shooting*. Other techniques such as *multiple shooting* and *collocation points* can also be used with the proposed approach [40].

After obtaining  $\bar{X}$  with  $\bar{U}$ , Eq. (12) can be shifted forward:

$$\delta \hat{x}_{k+2} = A_{k+1} \delta \hat{x}_{k+1} + B_{k+1} \delta \hat{u}_{k+1} \quad (13)$$

Substituting Eq. (12) into Eq. (13) yields:

$$\delta \hat{x}_{k+2} = A_{k+1} (A_k \delta \hat{x}_k + B_k \delta \hat{u}_k) + B_{k+1} \delta \hat{u}_{k+1} \quad (14)$$

By recursively repeating the preceding procedure for  $N_p$  steps and considering just the system output (Eq. (9)), the predicted deviations from the nominal output trajectory may be expressed in a matrix form by:

$$\delta \hat{Y} = G_y \delta x_k + H_y \delta \hat{U} \quad (15)$$

where  $\delta \hat{Y} = \hat{Y} - \bar{Y} = [\delta y_{k+1}^T, \delta y_{k+2}^T, \dots, \delta y_{k+N_p}^T]^T$  are the output deviations,  $\delta \hat{U} = \hat{U} - \bar{U} = [\delta \hat{u}_k^T, \delta \hat{u}_{k+1}^T, \dots, \delta \hat{u}_{k+N_p-1}^T]^T$  are the control input deviations. The matrices  $G_y$  and  $H_y$  are given by:

$$G_y = \begin{bmatrix} C_1 A_0 \\ C_2 A_1 A_0 \\ \vdots \\ C_{N_p} A_{N_p-1} \cdots A_1 A_0 \end{bmatrix} \quad (16)$$

$$H_y = \begin{bmatrix} C_1 B_0 & \mathbf{0} & \dots & \mathbf{0} \\ C_2 A_1 B_0 & C_2 B_1 & \dots & \vdots \\ C_3 A_2 A_1 B_0 & C_3 A_2 B_1 & \ddots & \mathbf{0} \\ \vdots & \vdots & \ddots & \vdots \\ C_{N_p} A_{N_p-1} \cdots A_1 B_0 & C_{N_p} A_{N_p-1} \cdots A_2 B_1 & \dots & C_{N_p} B_{N_p-1} \end{bmatrix} \quad (17)$$

The dimensions for these matrices are  $G_y = [N_p n_y \times n_x]$ ,  $H_y = [N_p n_y \times N_p n_u]$ , and  $C_k$  is the partial derivative of Eq. (9) with respect to nominal state, evaluated at the specific time step  $t = k$ , and is given by:

$$C_k = \left. \frac{\partial g(x, u, w)}{\partial x} \right|_{\substack{\bar{x}_k \\ \bar{u}_k \\ \bar{w}_k}}$$

In addition, the matrix  $\mathbf{0}$  represents a matrix of zeros with the same dimensions as the matrix  $C_k B_k$ .

### Optimisation

Following the definition of the prediction models, the cost function described in Eq. (3a) can be recast as follows:

$$J = \frac{1}{2} \hat{Y}^T Q \hat{Y} + \frac{1}{2} \delta \hat{U}^T R \delta \hat{U} \quad (18)$$

where the matrix  $R$  is a positive definite matrix with dimensions  $[N_p n_u \times N_p n_u]$  and constant elements over its diagonal.  $Q$  is selected as a block diagonal matrix with dimensions  $[N_p n_y \times N_p n_y]$  and inner matrices  $q_i$  used to compute the product  $\hat{\theta}_k \times \gamma_k u_{k-1}$  as defined in [42].

$$Q = \begin{bmatrix} q_1 & \mathbf{0} & \dots & \mathbf{0} \\ \mathbf{0} & q_2 & \ddots & \vdots \\ \vdots & \ddots & \ddots & \mathbf{0} \\ \mathbf{0} & \dots & \mathbf{0} & q_{N_p} \end{bmatrix} \quad q_i = \begin{bmatrix} 0 & 1 \\ 1 & 0 \end{bmatrix} \quad \forall i = [1, N_p] \quad (19)$$

Equation (18) includes an additional term that penalises the input deviation. This term is included for two reasons: first, it smooths out the control signal, making the requirement for the actuator's response limit less stringent; and second, according to [10, 22, 32, 43], a reactive control strategy with a cost function solely based on maximising





the extracted energy can result in overall negative energy absorbed, implying that the system is losing energy rather than absorbing energy from the waves.

Finally, by inserting the linearised output prediction Eq. (15) in Eq. (18), grouping comparable terms with respect to the decision variable  $\delta\hat{U}$ , and excluding any constant terms in the cost function, the standard quadratic programming (QP) formulation is obtained:

$$J = \frac{1}{2} \delta\hat{U}^T E \delta\hat{U} + \delta\hat{U}^T f \quad \text{s.t.} \quad M \delta\hat{U} \leq \rho \quad (20a)$$

$$E = H_y^T Q H_y + R \quad (20b)$$

$$f = H_y^T Q [\bar{Y} + G_y \delta x_k] \quad (20c)$$

where  $E \in \mathbb{R}^{N_p n_u \times N_p n_u}$  is a symmetric matrix known as the Hessian and  $f \in \mathbb{R}^{N_p n_u}$  is a column vector usually referred as the linear term;  $M \in \mathbb{R}^{2N_p n_u \times N_p n_u}$  is the constraints matrix and  $\rho \in \mathbb{R}^{2N_p n_u}$  is the constraints vector, defined as:

$$M = \begin{bmatrix} I \\ -I \end{bmatrix} \quad \rho = \begin{bmatrix} U_{max} - \bar{U} \\ -(U_{min} - \bar{U}) \end{bmatrix} \quad (21)$$

In the present work, only constraints in the control input are considered. If any states' constraints are required,  $M$  and  $\rho$  must be slightly reformulated. It is worth noting that  $G_y$  and  $H_y$ , and hence  $E$  and  $f$ , are time-dependent, which is one of the main reasons why NMPC is computationally expensive.

Having defined  $E$ ,  $f$ ,  $M$ , and  $\rho$ , the OCP can be solved using any QP solver, such as Matlab's quadprog function and qpOASES [44], to mention two. In this paper, quadprog was used. The new control input sequence is computed once the QP problem is solved, recalling that  $\hat{U} = \bar{U} + \delta U$ . From the new control input sequences, only the first input is applied to the system, and the procedure is repeated at the next time step, which is known as the *receding horizon* scheme [45].

### Real-time iterations scheme

The RTI scheme was first introduced in [19] for non-linear optimisation in optimal feedback control. A fully converged NMPC should ideally re-linearise the predictions and thus cost function Eq. (20) until no deviations are necessary, i.e.,  $\delta\hat{U} = \mathbf{0}$  [45]. This is not computationally

tractable in real-time applications since one must provide a solution at each time step under strict time constraints and avoid solving a problem that is just “getting older” [46].

The RTI scheme is briefly commented on in the following subsections.

**Initial value embedding.** Choosing an appropriate initial estimate for  $\hat{U}$  optimal, denoted as  $\hat{U}^*$ , is critical for fast and reliable convergence of the SQP iteration. To facilitate the estimation, the previous optimal input trajectory is employed in a shifted version to *hot-start* the solution at the following sampling time, generally by duplicating the last value [46].

**Single SQP Iteration.** The computing burden can be further decreased by executing only a single SQP iteration at each time step, i.e., only linearising the OCP once instead of re-linearising it until convergence.

**Computation separation.** The separation of the computation is perhaps the essential aspect of the RTI scheme. It divides the calculations into preparation and feedback phases. A timing diagram that illustrates this can be seen in [46].

## 5 RESULTS

The numerical results of the proposed control strategy applied on the Wavestar benchmark scale model simulated on WEC-Sim are reported in this section.

### Model parameters

Table 1 summarises the parameters used in the equation of motion for the dynamics of the WEC, Eq. (4).

### Wave conditions

The performance of the proposed controller is evaluated in a series of three unidirectional sea states generated by the JONSWAP spectrum. In general, wave climate is characterised by the significant wave height  $H_{m0}$ , the peak wave period  $T_p$ , and wave direction. The spectrum parameters are shown in Table 2, based on the sea states utilised in the WECCOMP [24].

**TABLE 1.** MODEL PARAMETERS FOR THE SCALE MODEL OF THE WAVESTAR DEVICE [17, 47].

Hydrodynamic parameters				
Inertia of arm and float	$J$	1.04 kg m <sup>2</sup>		
Added inertia	$J_\infty$	0.4805 kg m <sup>2</sup>		
Hydrostatic stiffness coefficient	$K_{hs}$	92.33 N m rad <sup>-1</sup>		
Rotational linear damping	$b_v$	1.80 N m rad <sup>-1</sup> s <sup>-1</sup>		
Radiation moment impulse response realisation				
$A_r =$	$\begin{bmatrix} -13.59 & -13.35 \\ 8.00 & 0.00 \end{bmatrix}$		$B_r =$	$\begin{bmatrix} 8.0 \\ 0.0 \end{bmatrix}$
$C_r =$	$\begin{bmatrix} 4.739 & 0.5 \end{bmatrix}$		$D_r =$	-0.1586

**TABLE 2.** PARAMETERS FOR WAVE GENERATION USING JONSWAP SPECTRUM. SIGNIFICANT WAVE HEIGHT  $H_{m0}$ , PEAK PERIOD  $T_p$  AND PEAK ENHANCEMENT FACTOR  $\gamma$ .

Name <sup>‡</sup>	$H_{m0}$ [m]	$T_p$ [s]	$\gamma$ [-]	Duration [s]
SS4	0.0208	0.988		98.8
SS5	0.0625	1.412	3.3	141.2
SS6	0.1042	1.836		183.6

<sup>‡</sup> Names are given to have consistency with the names given in the WECCOMP [24].

### Simulation and control parameters

Regarding the prediction horizon, research on wave excitation force prediction suggests that prediction strategies can predict wave excitation force for swell waves extremely accurately up to two peak wave periods in the future [37]. However, the prediction horizon chosen in this study for each sea state is more conservative, i.e., one peak wave period ( $N_p = 1 \times T_p/dt$ ).

After studying the literature on wave prediction for WEC, specifically AR models, we found that there are

**TABLE 3.** SIMULATION AND CONTROL TUNING PARAMETERS.

Parameter	Value
Simulation time [ s ]	$100 \times T_p$
Control sampling time [ms]	50
AR Order [lags]	18
AR training set [-]	$10 \times \text{AR order}$
Prediction horizon [samples]	$\text{Ceil}(1 \times T_p/dt, 5)$
$\mu_{gen}$	0.7
$\mu_{mot}$	$0.7^{-1}$
$\varphi^*$	1000
Control limit [N m]	$\pm 12$

\* Used in PTO efficiency function approximation.

widely disparate claims regarding the model order required to predict wave excitation, ranging from 12 lags to 32 lags in [37] to 10 lags to 200 lags in [38].

Therefore, the following procedure was followed to determine the model order: first, the WEC system was simulated without a control law extracting the wave excitation moment from the simulation. Second, using this information, partial autocorrelation on the wave excitation moment signal was performed, and it was found that a model with 18 lags would be sufficient to predict the wave excitation moment. The AR model is updated every second during simulations independently of the sea state selected.

Other relevant control tuning parameters are summarised in Table 3.

The simulation for each sea state lasts at least 100 times the peak period, with the first 25 s used as a wave ramp and hence omitted in the power and energy computation. Also, the prediction algorithm started working after 10 s of simulation, whereas the controller started working after 15 s.

Let us now turn our attention to the extracted energy and power. Figure 2 shows the control input and absorbed power over the simulation time for sea state SS6 running under the RTI-NMPC controller. For this simulation, the absorbed energy was 127.43 J with a mean power





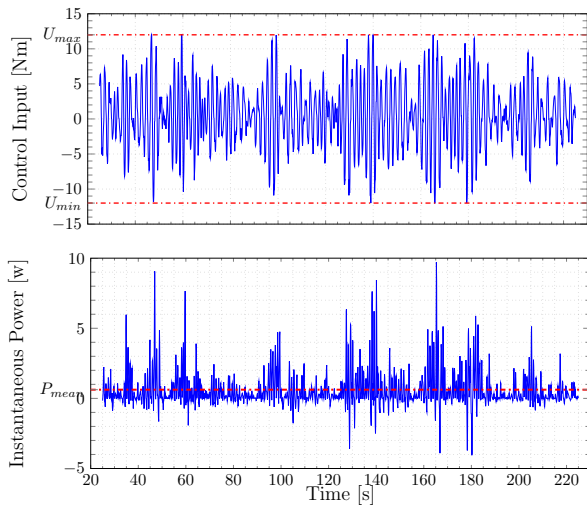


**FIGURE 2.** CONTROL INPUT AND ABSORBED POWER BY THE WAVESTAR SCALED MODEL FOR SEA STATE SS6 WITH REAL-TIME ITERATION NONLINEAR MODEL PREDICTIVE CONTROL. THE RED DASHED LINE REPRESENTS THE MEAN ABSORBED POWER.

of 0.6204W. Results obtained for sea states SS4 and SS5 are summarised in Table 4.

From the data depicted in Fig. 2 we can make the following remarks. First, it is clear that the proposed control strategy successfully absorbs a net positive power from the ocean waves; second, RTI-NMPC strives to avoid consuming energy from the grid.

To compare the control strategy proposed around RTI-NMPC, one additional set of simulations was performed using a proportional controller, proportional to the arm angular velocity of the WEC, also known as resistive control in the ocean wave energy community [8, 11–13].

For comparative purposes, Fig. 3 shows the control input and absorbed power by the Wavestar model for sea state SS6 running a resistive controller. For this case, the absorbed energy was 73.09J with a mean power of 0.3538W. Results obtained for sea states SS4 and SS5 are summarised in Table 4.

Finally, Fig. 4 shows the energy absorbed by the WEC for each control strategy. From there, we can observe that RTI-NMPC can absorb roughly 1.75 times more than the resistive controller.

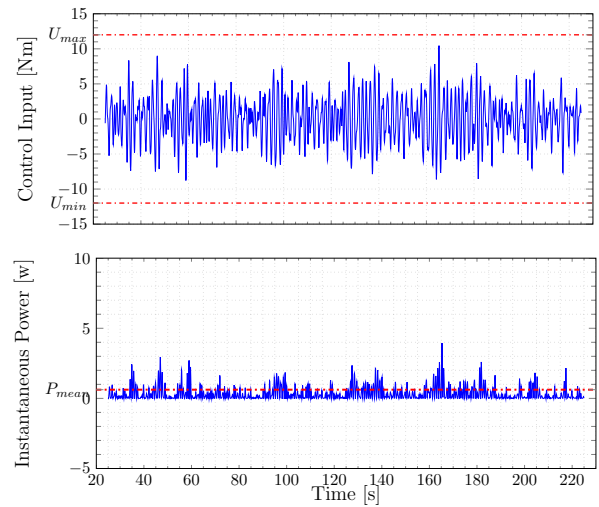


**FIGURE 3.** CONTROL INPUT AND ABSORBED POWER BY THE WAVESTAR SCALED MODEL FOR SEA STATE SS6 WITH RESISTIVE CONTROL. THE RED DASHED LINE REPRESENTS THE MEAN ABSORBED POWER.

**TABLE 4.** ENERGY ABSORBED AND MEAN POWER FOR RESISTIVE CONTROL AND RTI-NMPC FOR EACH SEA STATE.

Sea State	Resistive		RTI - NMPC	
	Absorbed Energy [J]	Mean Power [W]	Absorbed Energy [J]	Mean Power [W]
SS4	2.121	0.01968	3.103	0.02867
SS5	23.055	0.14807	42.855	0.27624
SS6	73.092	0.35385	127.434	0.62041

## 6 CONCLUSIONS

This work describes an NMPC approach based on the RTI scheme for including the PTO efficiency system when solving the OCP at each time step in a control policy that maximises the energy harvested from ocean waves.

WEC-Sim simulations of the Wavestar-scaled model wave energy converter demonstrate that RTI-NMPC is able to solve in real time a nonlinear optimal control problem

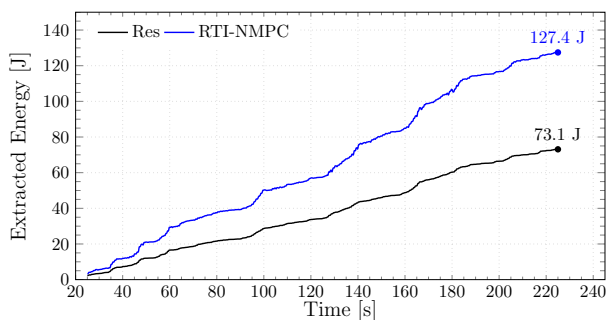


**FIGURE 4.** ENERGY ABSORBED BY THE WAVESTAR MODEL FOR SEA STATE SS6 WITH DIFFERENT CONTROL STRATEGIES. IN BLUE RTI-NMPC, IN BLACK RESISTIVE CONTROL.

that includes the nonideal efficiency of the PTO system. At the same time, the proposed RTI-NMPC approach can significantly improve wave energy converter performance.

Figures from Section 5 show the performance of the proposed RTI-NMPC approach for sea state SS6. Results show that RTI-NMPC clearly outperforms the resistive controller, harvesting roughly 1.75 times the amount of energy extracted by a resistive controller while keeping the amount of power “borrowed” from the grid to a bare minimum.

Future work on the proposed strategy will focus on the controller’s robustness in the face of unmodeled system dynamics, the incorporation of nonlinear hydrodynamics, and the controller’s performance with alternative lengths for the prediction horizon in the wave excitation moment algorithm.

To summarise, it appears that nonlinear model predictive control based on the real-time iteration method could be utilised to considerably enhance the absorbed energy from ocean waves, hence reducing the levelised cost of electricity.

Finally [48], to improve peer cooperation and openness, the findings presented in this paper and the code used in the simulations are available through a GitHub repository available at [49].

#### ACKNOWLEDGMENT

The first author would like to acknowledge the support of MICITT (Ministerio de Ciencia, Tecnología y Tele-

comunicaciones) of Costa Rica, who funded this work through a scholarship under the contract MICITT-PINN-CON-2-1-4-17-1-027.

This work was authored in part by the National Renewable Energy Laboratory, operated by Alliance for Sustainable Energy, LLC, for the U.S. Department of Energy (DOE) under Contract No. DE-AC36-08GO28308. Funding provided by the U.S. Department of Energy Office of Energy Efficiency and Renewable Energy Water Power Technologies Office. The views expressed in the article do not necessarily represent the views of the DOE or the U.S. Government. The U.S. Government retains and the publisher, by accepting the article for publication, acknowledges that the U.S. Government retains a nonexclusive, paid-up, irrevocable, worldwide license to publish or reproduce the published form of this work, or allow others to do so, for U.S. Government purposes.

#### REFERENCES

- [1] Falcão, A. F. O., 2010. “Wave energy utilization: A review of the technologies”. *Renewable and Sustainable Energy Reviews*, **14**(3), pp. 899–918.
- [2] Coe, R. G., Bacelli, G., and Forbush, D., 2021. “A practical approach to wave energy modeling and control”. *Renewable and Sustainable Energy Reviews*.
- [3] Tom, N., Ruehl, K., and Ferri, F., 2018. “Numerical Model Development and Validation for the WECC-COMP Control Competition”. In 37th Inter. Conference on Ocean, Offshore, and Arctic Engineering.
- [4] Bull, D., Jenne, D. S., Smith, C. S., Copping, A. E., and Copeland, G., 2016. “Levelized cost of energy for a backward bent duct buoy”. *International Journal of Marine Energy*, **16**, pp. 220–234.
- [5] Chang, G., Jones, C. A., Roberts, J. D., and Neary, V. S., 2018. “A comprehensive evaluation of factors affecting the levelized cost of wave energy conversion projects”. *Renewable Energy*, **127**, 11, pp. 344–354.
- [6] Neary, V. S., Lawson, M., Previsic, M., Copping, A., Hallett, K. C., Labonte, A., Rieks, J., and Murray, D., 2014. “Methodology for design and economic analysis of marine energy conversion (mec) technologies”. *Marine Energy Technology Symposium*.
- [7] Cordonnier, J., Gorintin, F., De Cagny, A., Clément, A. H., and Babarit, A., 2015. “SEAREV: Case study

- of the development of a wave energy converter”. *Renewable Energy*.
- [8] Maria-Arenas, A., Garrido, A. J., Rusu, E., and Garrido, I., 2019. “Control strategies applied to wave energy converters: State of the art”. *Energies*, **12**(16).
- [9] Faedo, N., Olaya, S., and Ringwood, J. V., 2017. “Optimal Control, MPC and MPC-Like Algorithms for Wave Energy Systems: An Overview”. *IFAC Journal of Systems and Control*.
- [10] Ringwood, J. V., Bacelli, G., and Fusco, F., 2014. “Energy-maximizing control of wave-energy converters: The development of control system technology to optimize their operation”. *IEEE Control Systems*.
- [11] Sanchez, E. V., Hansen, R. H., and Kramer, M. M., 2015. “Control performance assessment and design of optimal control to harvest ocean energy”. *IEEE Journal of Oceanic Engineering*.
- [12] Hals, J., Falnes, J., and Moan, T., 2011. “A Comparison of Selected Strategies for Adaptive Control of Wave Energy Converters”. *Journal of Offshore Mechanics and Arctic Engineering*.
- [13] Wang, L., Isberg, J., and Tedeschi, E., 2018. “Review of control strategies for wave energy conversion systems and their validation: the wave-to-wire approach”. *Renewable and Sustainable Energy Reviews*.
- [14] , 2014. *Optimising Reactive Control in Non-Ideal Efficiency Wave Energy Converters*, ASME.
- [15] Genest, R., Bonnefoy, F., Clément, A. H., and Babarit, A., 2014. “Effect of non-ideal power take-off on the energy absorption of a reactively controlled one degree of freedom wave energy converter”. *Applied Ocean Research*, **48**, oct, pp. 236–243.
- [16] Tona, P., Nguyen, H.-n., Sabiron, G., and Creff, Y., 2015. “An Efficiency-Aware Model Predictive Control Strategy for a Heaving Buoy Wave Energy Converter”. In *Ewtec*, pp. 1–10.
- [17] , 2019. An energy-maximising mpc solution to the wec control competition, Vol. 10, American Society of Mechanical Engineers.
- [18] , 2020. Experimental Assessment of the IFPEN Solution to the WEC Control Competition, Vol. Volume 9: Ocean Renewable Energy of *International Conference on Offshore Mechanics and Arctic Engineering*.
- [19] Diehl, M., Bock, H. G., and Schlöder, J. P., 2005. “A real-time iteration scheme for nonlinear optimization in optimal feedback control”. *SIAM Journal on Control and Optimization*, **43**(5), pp. 1714–1736.
- [20] Guerrero-Fernández, J., González-Villarreal, O. J., and Rossiter, J. A. Efficiency-aware non-linear model-predictive control with real-time iteration scheme for wave energy converters - [*Manuscript submitted for publication*].
- [21] Nguyen, H.-N. N., Sabiron, G., Tona, P., Kramer, M. M., and Vidal Sanchez, E., 2016. “Experimental validation of a nonlinear mpc strategy for a wave energy converter prototype”. In *Proceedings of the International Conference on Offshore Mechanics and Arctic Engineering - OMAE*, Vol. 6, American Society of Mechanical Engineers (ASME), pp. 1–10.
- [22] Li, G., and Belmont, M. R., 2014. “Model predictive control of sea wave energy converters - Part I: A convex approach for the case of a single device”. *Renewable Energy*.
- [23] Hansen, R. H., and Kramer, M. M., 2011. “Modelling and control of the wavestar prototype”. In *9th European Wave and Tidal Energy Conference (EWTEC)*.
- [24] Ringwood, J., Ferri, F., Tom, N., Ruehl, K., Faedo, N., Bacelli, G., Yu, Y. H., and Coe, R. G., 2019. “The wave energy converter control competition: Overview”. In *Proceedings of the International Conference on Offshore Mechanics and Arctic Engineering - OMAE*, Vol. 10.
- [25] Falnes, J., 2002. *Ocean Waves and Oscillating Systems: Linear Interactions Including Wave-Energy Extraction*. Cambridge University Press.
- [26] Cretel, J., Lewis, A. W., Lightbody, G., and Thomas, G. P., 2010. “An application of Model Predictive Control to a wave energy point absorber”. *IFAC Proceedings Volumes (IFAC-PapersOnline)*.
- [27] Andersen, P., Pedersen, T. S., Nielsen, K. M., and Vidal, E., 2015. “Model predictive control of a wave energy converter”. In *2015 IEEE Conference on Control and Applications*.
- [28] Tedeschi, E., Carraro, M., Molinas, M., and Mattavelli, P., 2011. “Effect of control strategies and power take-off efficiency on the power capture from sea waves”. *IEEE Transactions on Energy Conversion*, **26**(4), dec.
- [29] Bacelli, G., Genest, R., and Ringwood, J. V., 2015. “Nonlinear control of flap-type wave energy converter with a non-ideal power take-off system”. *Annual Reviews in Control*, **40**, jan, pp. 116–126.

- [30] Falcão, A. F., and Henriques, J. C., 2015. “Effect of non-ideal power take-off efficiency on performance of single- and two-body reactively controlled wave energy converters”. *Journal of Ocean Engineering and Marine Energy*, **1**(3), aug, pp. 273–286.
- [31] Tom, N. M., Madhi, F., and Yeung, R. W., 2019. “Power-to-load balancing for heaving asymmetric wave-energy converters with nonideal power take-off”. *Renewable Energy*, **131**, feb, pp. 1208–1225.
- [32] Mérigaud, A., and Tona, P., 2020. “Spectral control of wave energy converters with non-ideal power take-off systems”. *Journal of Marine Science and Engineering*.
- [33] Ling, B. A., and Batten, B. A., 2015. “Real Time Estimation and Prediction of Wave Excitation Forces on a Heaving Body”. In 34th International Conference on Ocean, Offshore and Arctic Engineering OMAE2015.
- [34] Nguyen, H. N., and Tona, P., 2017. “Wave Excitation Force Estimation for Wave Energy Converters of the Point-Absorber Type”. *IEEE Transactions on Control Systems Technology*, **26**(6), nov, pp. 2173–2181.
- [35] Abdelkhalik, O., Zou, S., Bacelli, G., Robinett, R. D., Wilson, D. G., and Coe, R. G., 2016. “Estimation of excitation force on wave energy converters using pressure measurements for feedback control”. In OCEANS 2016 MTS/IEEE Monterey, IEEE.
- [36] Davis, A. F., and Fabien, B. C., 2020. “Wave excitation force estimation of wave energy floats using extended Kalman filters”. *Ocean Engineering*.
- [37] Fusco, F., and Ringwood, J. V., 2010. “Short-Term Wave Forecasting for Real-Time Control of Wave Energy Converters”. *IEEE Transactions on Sustainable Energy*, **1**(2), pp. 99–106.
- [38] Pena-Sanchez, Y., Merigaud, A., and Ringwood, J. V., 2020. “Short-Term Forecasting of Sea Surface Elevation for Wave Energy Applications: The Autoregressive Model Revisited”. *IEEE Journal of Oceanic Engineering*, **45**(2), apr, pp. 462–471.
- [39] Nguyen, H. N., and Tona, P., 2018. “Short-term wave force prediction for wave energy converter control”. *Control Engineering Practice*, **75**, jun, pp. 26–37.
- [40] Quirynen, R., Vukov, M., and Diehl, M., 2015. “Multiple Shooting in a Microsecond”. In *Multiple Shooting and Time Domain Decomposition Methods*. Springer, Cham, pp. 183–201.
- [41] Gonzalez Villarreal, O. J., and Rossiter, A., 2020. “Shifting strategy for efficient block-based non-linear model predictive control using real-time iterations”. *IET Control Theory and Applications*.
- [42] Guerrero-Fernández, J., González-Villarreal, O. J., Rossiter, J. A., and Jones, B., 2020. “Model predictive control for wave energy converters: A moving window blocking approach”. *IFAC-PapersOnLine*, **53**(2), pp. 12815–12821. 21th IFAC World Congress.
- [43] Bacelli, G., and Coe, R. G., 2021. “Comments on Control of Wave Energy Converters”. *IEEE Transactions on Control Systems Technology*, **29**(1), jan.
- [44] Ferreau, H. J., Bock, H. G., and Diehl, M., 2008. “An online active set strategy to overcome the limitations of Explicit MPC”. *International Journal of Robust and Nonlinear Control*, **18**, pp. 816–830.
- [45] Gonzalez, O., and Rossiter, A., 2020. “Fast hybrid dual mode NMPC for a parallel double inverted pendulum with experimental validation”. *IET Control Theory and Applications*.
- [46] Gros, S., Zanon, M., Quirynen, R., Bemporad, A., and Diehl, M., 2016. “From linear to nonlinear MPC: bridging the gap via the real-time iteration”. *International Journal of Control*, sep, pp. 1–19.
- [47] Ringwood, J. V., Ferri, F., Ruehl, K. M., Yu, Y.-H., Coe, R. G., Bacelli, G., Weber, J., and Kramer, M. M., 2017. “A competition for WEC control systems”. In 12th European Wave and Tidal Energy Conference.
- [48] Åström, K. J., and Murray, R. M., 2008. *Feedback Systems: An Introduction for Scientists and Engineers*, 2nd editio ed. Princeton University Press Princeton, NJ, USA.
- [49] [https://github.com/WEC-Sim/WEC-Sim\\_Applications](https://github.com/WEC-Sim/WEC-Sim_Applications).



